# PERFORMANCE OF MUNICIPAL SOLID WASTE AS FUEL IN A BINARY DIRECT CARBON FUEL CELL

BY

ANTHONY, Richard Ajaw
MEng/SIPET/2018/9226

A THESIS SUBMITTED TO THE POSTGRADUATE SCHOOL FEDERAL UNIVERSITY OF TECHNOLOGY, MINNA, NIGERIA IN PARTIAL FULFILLMENT OF THE REQUIRMENTS FOR THE AWARD OF THE DEGREE OF MASTER OF ENGINEERING IN CHEMICAL ENGINEERING

NOVENBER, 2023

# DECLARATION

I hereby declare thet this thesis titled “Performance of Municipal Waste as Fuel in a Binary Direct Carbon Fuel Cell ” is a collection of my original research work and it has

not been presented for any other qualification anywhere. Information from other sources (published or unpublished) has been duly acknowledged.

ANTHONY, Richard Ajaw
MEng/SIPET/2018/9226
Federal University of Technology, Minna

_____
Signature/ Date

CERTIFICATION

The thesis titled: “Performance of Municipal Solid Waste as Fuel in a Binary Direct Carbon Fuel Cell.” By ANTHONY, Richard Ajaw (MEng/SIPET/2018/9226) meets the regulations governing the award of the degree of (MEng) of the Federal University of Technology, Minna and it is approved for its contribution to scientific knowledge and literary presentation.

| | |
|---|---|
| Eng. Prof. O. D Adeniyi | …… |
| Supervisor | Signature & Date |
| Eng. Prof. O. D Adeniyi | …… |
| Head of Department | Signature & Date |
| Eng. Prof. Z. D. Osunde | …….. |
| Dean School of Infrastructure, Process Engineering and Technology | Signature & Date |

Engr. Prof. O.K. Abubakre …….

Dean of Postgraduate School Signature & Date

## ACKNOWLEDGEMENT

Great thanks and praise is to the Almighty God for giving me the determination, opportunity and strength to be part of this great institution. I will like to acknowledge my supervisor Prof O. D. Adeniyi for his supervision and guidance throughout the course of this work. I would like to express my gratitude to my father, mother, brothers and sisters. Nothing would be possible without your prayers and support. I also appreciate the effort of Dr Saheed Mustapha. Chemistry Department, Federal University of Technology Minna, whom I always run to whenever I needed advice, many thanks to you . I sincerely want to appreciate all the lecturers who thought me during the course work. May Almighty God bless you all. I am no forgetting all the academic and non-academic staff of the chemical engineering, FUT, Minna. I pray that God will reward you abundantly. I

will like to also appreciate the effort, understanding and intelligence exhibited by my

colleagues in the course of this study. Not forgetting Mr Benjamin Peter, as well as others

whom God has used to add an energy to my growth, I acknowledge you.

.

## ABSTRACT

A variety of abundant carbonaceous fuels such as municipal solid waste (MSW) and biochar from biomass carbonization can be utilized to generate electricity in a direct carbon fuel cell (DCFC) system. The direct carbon fuel cell uses waste materials as its fuel source which is a renewable energy source in a DCFC, making it economically-viable for waste management and reduction of greenhouse effect. With a remarkable high efficiency yield. To investigate electrochemical performance in a DCFC, the municipal solid waste was (MSW) collected from a dump site. The solid waste was sorted into three samples of the saw dust, orange peel and sugarcane bagasse and its combination respectively. The samples were sun dried for 7 days to ensure homogeneity. Size reduction was carried out by hand mill and sieved with 500µm (0.5mm). The three solid waste samples each was subjected to thermochemical conversion by slow pyrolysis reaction at a temperature of 500$^{o}$C at 10$^{o}$C/min for 30 minutes. Each biochar samples and its combination as MSW were then characterized to determine the proximate and ultimate analysis. The proximate analysis was used to obtain the fixed carbon content of 20.77, 22.60, 27.30 and 29.97 (wt%) for the four biochar samples respectively, while the ultimate analysis was used to determine the calorific values of 7.0, 5.8, 9.78 and 7.9 (Mj/kg) for the corresponding biochar samples. The overall results obtained for peak electrochemical performance test recorded from the MHDCFC operations based on cell voltage, current density and power density for saw dust was 0.44 V, 17.6 mA/cm$^2$ and 7.74 at mW/cm$^2$ at 200$^0$C respectively, orange peel b was 0.41 V, 16.4 mA/cm$^2$ and 2.296 mW/cm$^2$ at 250$^0$C respectively, sugarcane

bagasse was 0.39 V, 15.6 mA/cm$^2$ and 6.084 mW/cm$^2$ respectively, MSW biochar 0.65 V, 26.0 mA/cm$^2$, 16.90 mW/cm$^2$ at 250$^0$C respectively. The peak percentage values obtained for saw dust, orange peel, sugarcane bagasse and MSW biochar was 65 %, 16.4 %, 27 % and 44% respectively at a resistance of 1.0 Ω based on fuel utilization coefficient and higher heating value (HHV). From the results obtained, all things being equal and probably at reduced or no decrease in the reaction site available to the reactant gasses due to polarisation losses, it can be deduced that more than 100% efficiency is attainable in MHDCFC operations at a very minimal cost.

TABLE OF CONTENTS

LIST OF TABLES

Table Page

LIST OF FIGURES

LIST OF PLATES

Plate Page

B12 MHDCFC Electrochemical Performance @ 250$^{o}$C Orange peel
B13 MHDCFC Electrochemical Performance @ 100$^{o}$C Sugarcane bagasse
B14 MDCFC Electrochemical Performance @ 150$^{o}$C Sugarcane bagasse
B15 MHDCFC Electrochemical Performance @ 200$^{o}$C Sugarcane bagasse

B16: MHDCFC Electrochemical Performance @ 250$^{o}$C Sugarcane bagasse

ABBREVIATIONS

AC= Ash content

C= Carbon

CV= Calorific value

DCFC= Direct carbon fuel cell

FC= Fixed carbon

H= Hydrogen

MC= Moisture content

MCDCFC= Molten carbonate direct carbon fuel cell

MHDCFC= Molten hydroxide direct carbon fuel cell

MSW= Municipal solid waste

N= Nitrogen

O =Oxygen

OCV= Open circuit voltage

S= Sulphur

SEM= Scanning Electron Microscopy

SODCFC= Solid oxide direct carbon fuel cell

SW= Solid waste

VM= Volatile matter

XRD=X-Ray diffractio

# CHAPTER ONE

# 1.0 INTRODUCTION

## 1.1 Background to the Study

There has been a rise in population growth, rural to urban migration, and industrial expansion. These factors have contributed to a substantial increase in waste generation, which has become a matter of global concern due to its socio-economic and environmental implications. (Omisore, 2018). There are two main categories for Municipal Solid Waste. Both are organic or inorganic. The waste materials are categorized based on their potential for resource recovery and their hazardous nature. The types of MSW include organic matter, such as food waste and yard waste, and batteries (Axon 2017). Due to their unique characteristics, each of these materials requires specific handling and disposal methods. (Hamad et al., 2014).

The discrepancy is caused by differences in consumption patterns, waste management infrastructure, and economic development levels. (Aleluia and Ferrão 2016). energy security have sparked interest in the utilization of biomass energy. The advantage of absorbing carbon dioxide during plant growth is that it makes a lesser contribution to global warming. There is a crucial challenge in finding ways to generate energy without compromising food production. DCFCs can use a wide range of carbon-rich materials as potential fuels. DCFCs have the flexibility to use readily available and abundant raw materials. (Elleuch et al., 2015).

The high energy content and easy availability of MSW make it a good choice as a fuel for DCFCs. The energy content of coals is greater than that of pyrolyzed MSW. The waste materials make up half of the total weight. Waste materials are very promising for DCFCs. It is important to study the feasibility of utilizing waste materials in DCFCs (Bishoge et al.,2019).

The Direct Carbon Fuel Cells (DCFCs) have attracted growing attention nowadays as an efficient generator of electrical power. It has the advantages of a near 100 % thermodynamic efficiency and a practical efficiency of about 80 % far higher than hydrogen fuel cell technologies and coal fired generator. The overall process of generating electricity by a DCFC system is relatively simple compared to other fuel cell technologies and does not require expensive preparation of any gaseous fuel, as well as accepts a variety of carbon-rich materials (coal, graphite, carbon black, coke, active carbon, etc.) as potential fuels. (Elleuch et al., 2015).

## 1.2 Statement of the Research Problem

Every nation depends on electricity for its socio-economic and technological progress. In Nigeria, the demand for electricity far exceeds the supply. The country's development is hampered by the electricity problem. There is a correlation between access to electricity and socio- economic development. Over the past four decades, Nigeria has employed various methods for electricity generation, including gas-fired, oil-fired, hydroelectric, and more recently, gas-fired systems. These methods have not been able to meet the demand (Sambo et al,2006). As a result, the adoption of fuel cells, which offer high efficiency and environmentally friendly power generation, has gained attention as a potential solution to bridge the electricity demand gap (Munnings et al,2014). One of the best solution is fuel

cell technology. Because it uses the same electrochemical principles as traditional feul cells but relies on a solid carbonaceous materials as fuel, direct carbon fuel cell (DCFC) technology has drawn a lot of interest. (Moya et al,2017)

## 1.3 Aim and Objectives

The aim of this research is to investigate performance of sorted Municipal Solid Waste (MSW) as fuel in a binary direct carbon fuel cell. This aim will be achieved with the following objectives.

1.To obtain Biochar from sorted Municipal Solid Waste and it's combination through pyrolysis.

2.To characterise the Biochar by conducting proximate analysis, ultimate analysis, calorific values, X-ray diffraction (XRD) and scanning electron microscope (SEM/EDX).

3.To prepare electrolyte and biomass carbon fuel with molten hydroxide mixtures.

4.To investigate the electrochemical performance of biomass (sawdust, orange peel, sugarcane bagasse) carbon fuel with molten hydroxide mixture in a binary direct carbon fuel cell.

## 1.4 Scope of Study

This research using pyrolysis, characterization of the biochar, Electrolyte preparation by heating the hydroxide salts at a high temperature then investigating the electrochemical performance of the sorted municipal solid waste in a molten hydroxide direct carbon fuel cell.

## 1.5 Justification of the Study

The abundant availability of solid waste in many parts of Nigeria is what motivates this research. Solid waste can be used to address the problem of electricity instability. Fuel cell technology provides high efficiency and low emissions in electricity production. A constant supply of fuel and oxygen for stable operation is ensured by fuel cells.

# CHAPTER TWO

# 2.0 LITERATURE REVIEW

## 2.1 Municipal Solid Waste MSW

### 2.1.1 Composition of MSW

Plastic, and some items are some of the materials collected from households. The composition of household pollutes the type of community, consumer incomes and lifestyles, degree of industrialization, institutional presence, and level of commercial

activity. Communities with higher incomes tend to generate more waste. The quantity and composition of waste can be influenced by a number of factors. During the summer, there is more food waste and less paper waste. A higher amount of waste is produced by larger communities., (Pichtel 2014, Czajczy'nska et al,2017)

### 2.1.2 Types of municipal solid waste.

Municipal solid waste (MSW) can be categorized into three main types:

1. Residential waste: This type of waste includes the waste produced by households in residential neighbourhoods, such as single-family homes or apartment complexes.
2. Commercial waste: It encompasses the waste generated as a result of business activities and operations.
3. Municipal services waste: This category includes waste generated from waste collected from, parks, and other public areas. It refers to the waste generated by the maintenance and cleaning activities carried out by the municipal authorities in the community.

## 2.2 Sources of Municipal Solid Waste

Municipal solid waste (MSW) is a diverse mixture of waste materials generated from various sources, including households, public places, commercial institutions, hospitals, industries, wastewater plants, electronic industries, and more. The composition of MSW can vary depending on the specific sources and the region. However, the majority of substances found in MSW typically include:

1. Paper: This includes newspapers, magazines, cardboard, packaging materials, office paper, and other paper-based products.
2. Vegetable matter: Organic waste such as food scraps, yard trimmings, leaves, branches, and other plant-based materials.
3. Plastics: Various types of plastic materials, including bottles, containers, packaging, bags, and other plastic products.
4. Metals: Ferrous and non-ferrous metals, such as steel, aluminum, tin, copper, and other metal objects.
5. Textiles: Clothing, fabrics, carpets, and other textile products that are discarded.
6. Rubber: Rubber materials from tires, footwear, and other rubber-based products.
7. Glass: Bottles, jars, and other glass containers.

These substances represent some of the common components found in MSW, but the exact composition can vary depending on local waste management practices and the specific waste generation patterns in a particular area. (Omari 2015).

### 2.2.1 Wood and garden waste

There is an inorganic fraction. Non-biodegradable materials found in garden waste include soil and stones. The inorganic fraction is not suitable for direct energy conversion, but it can be separated and recycled for other purposes. There is an opportunity for sustainable waste management practices to be promoted with the inclusion of garden waste. Communities can reduce the environmental impact of waste disposal by effectively managing and utilizing garden waste. (Boldrin, et al, 2010, Czajczy'nska et al,2017).

The organic fraction of household rubbish has the potential to be processed and recovered in a beneficial manner. This can involve various waste management techniques. Composting, anaerobic digestion, or thermal conversion can be used to process organic waste materials such as food scraps, garden waste, and wood. The organic matter can be broken down and converted into useful forms, such as compost or biochar. Valuable resources can be obtained, reduced waste and promoted a more sustainable approach to waste management by recovering the organic content of household rubbish. The practices contribute to the concept of the circular economy, where organic materials are recycled and reused. (Paradela,et al, 2009, Czajczy'nska et al,2017)

### 2.2.2 Food waste

Food waste is a good source of fuels. The components of food waste include fats, sugars, vitamins, and other carbon-based substances. Food waste can be categorized based on its origin. Fruit and vegetable peels, husks, and stems, are included in these groups. In the absence of oxygen, selected food waste materials can be degraded through the process of pyrolysis. Pyrolysis of food waste can yield biochar, which is a carbon-rich material, and syngas, which is a mixture of gases. The derived products can be used as renewable energy sources. The reduction of fossil fuel dependency can be achieved by the use of the biofuels produced. The biochar can be used as a soil amendment. Valuable resources can be recovered from selected food waste streams, which can be used to contribution to the circular economy. (Grycová,et al, 2016, Czajczyn´ska et al.2017).

### 2.2.3 Paper

Paper consumption is common in various sectors. Newspapers use print paper to publish daily news and information. Glossy paper provides a high-quality finish to printed materials. There are three main types of paper. Industrial use, cultural use, and food packaging are used. Industrial use involves using paper for various purposes. Printing and writing on paper, newspaper production, and even the printing of currency are all examples of cultural use. The different categories reflect the different applications and purposes of the paper. Paper is used in many aspects of our daily lives. it is important to consider sustainable practices and promote recycling. (Rahman et al,2014).

The paper consumption leads to it being a significant component of the solid waste. Roughly one third of the total municipal solid waste is accounted for by it. Paper is an appropriate material for burning due to its low nitrogen and sulfur content. This characteristic makes it a good choice for waste-to-energy conversion processes. It is possible to extract energy from paper waste through various technologies, such as gasification, thereby contributing to waste management and energy production at the same time. (Khongkrapan et al,2013).

### 2.2.4 Rubber

The presence of rubber compounds is from discarded tires, which accounts for a significant portion of both natural and synthetic rubber waste. According to the European Tire and Rubber Manufacturers, European Union countries generated 3, other sources of rubber waste include tires, shoe soles, gloves, and rubber products (Rubber Manufacturers,2016)

### 2.2.5 Textiles

Every new garment will eventually end up in the waste stream. Synthetic fibers such as nylon and nylon 2 are some of the materials in clothing and textile waste. The diverse range of fabrics and materials used in the textile and fashion industry contributes to the composition of textile waste. (Balcik-Canbolat et al,2017).

Plate I : Solid waste dump site

## 2.3 Types of Pyrolysis Reactors Used to Utilize Different Domestic Waste

The choice of reactor type is crucial due to the significant heat transfer required through the reactor wall to facilitate effective degradation of the materials. (Aishwarya et al,2016). The mechanisms involved in this process have been extensively investigated by researchers over the years. (Czajczyn´ska et al,2017).

## 2.4 Pyrolysis Products and their Possible Applications

Pyrolysis can be used to transform waste into an energy source. (Jouhara et al, 2017). The profitability of the process can be enhanced by using the pyrolysis products on a larger scale. The composition and characteristics of char make them appealing as potential raw materials for specific industrial sectors and various applications. Increased profitability and wider market appeal can be achieved by utilizing pyrolysis products in different industries. (Czajczyn´ska et al,2017).

## 2.5 Bioenergy Conversion Techniques

There is a focus on the production of liquids. Fast pyrolysis has several advantages, including high oil yields of up to 75% by weight and cost-effective technology. A dark brown liquid is what py-oil appears to be (Jahirul et al., 2012). The py-oil obtained from fast pyrolysis has a low calorific value and consists of various chemical components. Significant attention has been given to improving the properties of py-oil to make it a viable substitute for crude oil. Physical, chemical, and catalytic approaches have been explored for py-oil upgrading. Carbonization involves the thermal decomposition of wood in a furnace. making it a more viable option for various energy and chemical applications (Elleuch, 2013).

The carbonization furnace used in this process is a closed system that uses the off-gas produced during carbonization as fuel. The raw material is loaded into two metallic carbonization chambers at the top of the furnace. There are two insulated gas channels that connect the chambers to the combustor. The recycled carbonization gases are used in the combustor. The carbonization chambers are heated by the heat exchanger when the gases generated in the combustor pass through. The temperature is controlled inside the chambers. The operating cycle begins with a preheating step to raise the temperature. The

carbonization of the biomass occurs under nearly isothermal conditions when the temperature is increased until it reaches 600 degrees Celsius. The carbonization experiment runs for 4 hours. The reactor is cooled to room temperature.


Plate II : Furnace used for biomas carbonization.( Elleuch,2013).

2.6 Thermal Treatment Processes

A waste treatment process that involves high temperatures is called thermal treatment. It transformed with this high-temperature treatment. The purpose of thermal treatment is to facilitate the removal of waste components through the application of heat. Reducing the volume of waste, destroying harmful substances, and recovering energy from the waste stream are some of the things it can do. There are some common thermal treatment technologies. These methods use high temperatures to treat waste. (Aleluia and Ferrão, 2016). The advanced thermal treatment technologies offer efficient ways to manage waste. Ensuring that proper environmental safeguards and emissions control measures are in place to minimize the impact on air quality and the environment is important. (Dudek et al., 2018).

The advanced thermal treatment technologies offer efficient ways to manage waste. Ensuring that proper environmental safeguards and emissions control measures are in place to minimize the impact on air quality and the environment is important. Producing fuels like charcoal, coke, and producer gas has been done using gasification and pyrolysis. Coal and wood are used to make coke and charcoal. The producer gas is produced through coke gasification. These processes can transform carbonaceous materials into usable forms such as gases or solid fuels with specific properties and applications. (Bartocci et al., 2018).

### 2.6.1 Incineration

The waste is subjected to very high temperatures during the process of drying. The high temperature causes the waste to be burned. Bottom ash, gases, particles, and heat are included. The residual materials that remain after the fire are the bottom ash. The gases and particles can be treated to reduce emissions and the impact on the environment. The heat produced during the process can be used to generate electricity. (Wang et al., 2017).

The waste is subjected to very high temperatures during the process of drying. The high temperature causes the waste to be burned. Bottom ash, gases, particles, and heat are included. The residual materials that remain after the fire are the bottom ash. The gases and particles can be treated to reduce emissions and the impact on the environment. The heat produced during the process can be used to generate electricity. Incineration is an advanced and sophisticated method of waste treatment hierarchy as it can effectively reduce the volume of waste and generate energy simultaneously. (Vaida and Lelea, 2017). Icing is one of the most effective methods. It offers advantages in terms of preserving valuable landfill space and avoiding the negative environmental impacts associated with traditional landfilling. Incinerating waste reduces the amount of waste that needs to be thrown away. It helps to conserve land resources

and prolong the lifespan of existing landfill sites. The release of greenhouse gases and other harmful pollutants can be greatly reduced by the use of incineration. It is possible to mitigate the adverse environmental impacts associated with landfilling by converting waste into energy through controlled combustion. (Wang et al., 2017).

Studies have shown that the amount of waste can be reduced by up to 70%. The reduction in weight and volume is good for waste management. It helps to maximize the use of available space. The generation of harmful byproducts can be reduced by the incineration process. The conversion of waste into less bulky ash and gases is achieved by burning organic materials at high temperatures. They can be treated to minimize their environmental impact. Incense offers an efficient and effective means of waste reduction, improving waste management practices and minimizing the associated negative consequences. (Ma et al., 2016).

### 2.6.2 `Pyrolysis

Optimal conditions for maximizing liquid fuel production include higher temperatures ranging from 800 to 1000 C and very short residence times. These conditions are relevant when preparing a suitable feedstock for direct carbon fuel cells. The specific temperature and residence time requirements can be tailored to maximize the output.

Charcoal production has been a successful method for a long time. It evolved from simple batches used for making charcoal for cooking fires to more advanced industrial processes. The earliest forms of charcoal production were carried out in pits or mounds. Industrial charcoal production can be accomplished through both batches of ovens and continuous multiple hearth furnaces. The systems enable efficient and controlled carbonization. The

process of processing a specific amount of biomass can be done in batches or continuous multiple hearth furnaces. The methods have been improved for large-scale charcoal production. The long-standing success of charcoal production shows its effectiveness as a technique for converting wood into fuel, as well as contributing to the utilization of resources and providing valuable end products.

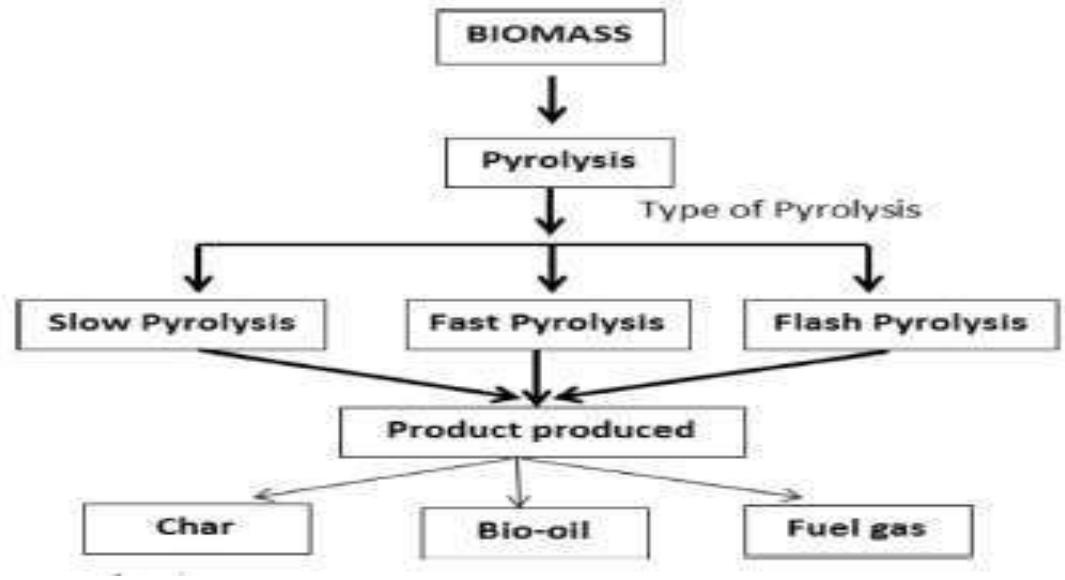


Figure 2.1: Different types of pyrolysis process (Moya et al., 2017)

The organic material undergoes thermal degradation when it is heated to the desired temperature. The absence of oxygen allows the material to break down into various substances, such as gases and liquids. The composition and properties of the resulting products can be influenced by the temperature range chosen. Pyrolysis can be used to convert wood, crop residues-rich components and the production of renewable fuels and chemicals. It ensures that the biomass undergoes thermal decomposition, which leads to the desired pyrolysis products. (Moya et al., 2017).

The concentration of energy can be improved through the transformation of the material through the process of pyrolysis. Valuable chemicals can be recovered during the process.

Gases, liquids, and bio-oils are some of the byproducts generated by the decomposition of organic materials. The production of chemicals with high market value is one of the applications where these compounds can be further processed and utilized. The history of the production of charcoal can be found in the history of pyrolysis, due to its ability to convert biomass into fuels of higher energy density and recover valuable chemicals. The technology is being explored for a wider range of applications, including waste management, renewable energy production, and the development of sustainable chemicals and fuels. (Yang et al., 2018).

The yields of products are influenced by two different reactions. The primary reactions involve the degradation of the solid material. In the absence of oxygen, the waste material is subjected to high temperatures. The breaking down of complex organic compounds is caused by the thermal degradation of the solid. The release of volatile gases, vapours, and tar-like substances are caused by the decomposition of the solid matrix. Secondary reactions occur when the primary volatiles are produced. These reactions occur at elevated temperatures and involve various chemical processes. Fuel production and the formation of volatile compounds can be contributed to by the secondary reactions. The balance between gas, liquid, and solid products can be influenced by temperature, residence time, and other factors. The knowledge of primary and secondary reactions helps in tailoring the process for specific feedstocks and desired product outcomes. (Zhan et al., 2018).

The operating conditions and experimental equipment used affect the extent of secondary reactions. Solid char, light gases, and heavy compounds are transformed into intermediate reactive products by Pyrolysis, which plays a crucial role in thermal processes. Pyrolysis has the potential to reduce dioxin pollution issues. Dioxins can be formed when certain

materials are burned. The absence or limited presence of oxygen reduces the formation of dioxins and other harmful pollutants by controlling the temperature, residence time, and gas composition, it is possible to maximize the production of desired products. This aspect makes pyrolysis an attractive option for waste treatment and energy recovery, as it offers the potential for environmentally friendly conversion. (Wu et al., 2017).

When exposed to heat or over time, the oily liquids derived from pyrolysis of municipal solid waste pose challenges for energy recovery due to their high oxygen content, corrosiveness, and instability. Direct use as a fuel source is restricted by these characteristics. Researchers are looking at different approaches to address these limitations. One approach involves refining and upgrading the pyrolysis liquids. The methods aim to remove impurities, reduce the oxygen content, and improve the stability and energy density of the liquids, making them more suitable for energy conversion technologies. The pyrolysis liquids can be used to make valuable chemicals or fuels. The potential for energy recovery can be maximized by converting these liquids into higher value products. The liquids can be processed into bio-oil, which can undergo further refining to produce transportation fuels or serve as a precursor in various chemical processes. Although the oily liquids obtained from MSW present challenges for direct energy recovery, ongoing research and development efforts are focused on improving their properties and finding alternative pathways for their efficient utilization in the energy sector (Zhe et al., 2018).

The cost and complexity of the process are increased by the internal waste generated from municipal solid waste. Further research and development is needed to make pyrolysis technologies more economically viable for large-scale implementation. It is important to

continue exploring innovative solutions and refining processes to overcome these challenges and make pyrolysis a more efficient, cost-effective, and sustainable waste treatment option for the future. (Rafati et al., 2016).

## 2.7 Pyrolysis of Organic Materials

Pyrolysis is a process that uses heat to convert waste into fuel. This heat causes the long chain molecule in the feedstock to break down. Non-carbon materials are volatilized as a result of cross-linking reactions. Potential applications include waste management, renewable energy production, and the production of valuable chemicals. (Adeniyi, 2014). The heating rate of the feedstock is gradually increased until it reaches a suitable temperature in the range of 600 to 850 degrees Celsius. Once the desired temperature is reached, it is maintained for a specific, the production of desired products can be achieved by maintaining the feedstock at the appropriate temperature. By controlling the heating rate and residence time, the process can be maximized to achieve desired outcomes, such as maximizing the production of valuable gases or liquids, or achieving specific product properties. The gradual increase in heating rate followed by maintaining the feedstock at the desired temperature for an extended residence time is a crucial step in the process of converting the feedstock into desired products. ( González,2009).

The generic equation for the pyrolysis of biomass is described below;

$$C_nH_mO \text{ (biomass)} \xrightarrow{\text{Heat}} \sum_{\text{liquid}} C_xH_yO_z + \sum_{\text{gas}} C_aH_bO_c + H_2O + C(\text{char}) \qquad (2.0)$$

Pyrolysis and gasification processes enable the production of many chemicals, such as ethylene, carbon, and other valuable substances. These processes allow the conversion of waste materials into useful products like coke. The transformation of solid materials into gases and vapours is one of the advantages of gasification. Reduced costs for handling,

transportation, and storage of the resulting gases are some of the benefits of this conversion. The produced gases can be utilized as a fuel present in the syngas generated from gasification processes serve multiple purposes. The energy content of these gases makes them valuable resources The benefits of gasification include efficient conversion of solid materials into gases, enhanced fuel flexibility, and the utilization of captured gases to mitigate greenhouse gas emissions. These processes help to make energy production and chemical manufacturing more sustainable. (Sharma et al,. 2014).

The overall energy balance and environmental consequences can be influenced by the efficiency of the process and the ability to capture and utilize the energy content of the syngas. Efforts are being made to address the fuel requirement. Exploring renewable energy sources is part of this. Research and development in areas like heat recovery, process integration, and advanced gasification technologies aim to minimize energy input while maximizing the production of valuable syngas. (Sharma et al,. 2014).

### 2.7.1 Classification of pyrolysis

Basically there are 3 types of pyrolysis and according to literature they have various combinations and conditions namely:

1. Slow Pyrolysis
2. Fast Pyrolysis
3. Intermediate Pyrolysis

#### 2.7.1.1 Slow Pyrolysis

When the main output is bio-char, there are specific characteristics associated with this approach. A gradual heating rate of less than 20C per minute is achieved by the pyrolysis process, which operates within a temperature range of 400 to 800C. The quantity of

products obtained depends on a number of factors. The primary products resulting from pyrolysis are bio-char and tar, which have an approximate yield of 30% and 35%, quantity of gases and oils can vary based on process conditions and the desired outcomes. (Braz, 2014).

2.7.1.2 Fast Pyrolysis

Fast pyrolysis has distinct features compared to slow pyrolysis. It is good for the production of bio-oil. There are some key characteristics of flash pyrolysis. Particles smaller than 2mm are used in the utilization of the feedstock. The fine particle size allows for rapid heating.

A shorter vapor residence time can be achieved with high heating rates.

2.7.1.3 Intermediate Pyrolysis

Long residence time pyrolysis is characterized by a longer duration for the reactions to occur. The extended residence time allows for the processing of challenging materials.

Additional time is required for complete decomposition and conversion into useful products. The longer residence time in this process ensures thorough thermal degradation of the feedstock, resulting in desired outcomes. Handling and managing the process are challenges it presents. Careful control is required to maximize the conversion efficiency when the duration is longer. This allows for the utilization of diverse organic waste streams in an efficient and sustainable manner.

2.8 Thermochemical Processes and Biomass Pre-treatment

Under controlled temperature and oxygen conditions, certain processes are used to convert the original biomass into more practical forms of energy carriers. The goal of these conversion processes is not to directly produce useful energy but rather to transform the

biomass into more manageable and versatile forms that can be further utilized for energy production. The breakdown and transformation of complex organic compounds can be accomplished by subjecting the biomass to controlled temperature and oxygen levels. The energy carriers can be stored, transported, and utilized more conveniently The advantage of transforming biomass into more suitable forms for subsequent energy generation is offered by the conversion processes mentioned (Sharma et al., 2014).

The use of more convenient energy carriers, such as those produced through carbonization, gasification, and catalytic liquefaction, offers several advantages. These processes provide energy-dense materials that are easier to transport and exhibit predictable combustion properties. The production of bio-oil, biochar, and gases can be achieved through Pyrolysis. Carbonization is a process that converts biomass into charcoal through high temperatures. The use of catalysts or a high hydrogen partial pressure is required for Catalytic liquefaction, which operates at low temperatures but high pressures. The process facilitates the transformation into liquid fuels. Depending on the requirements and desired output, each of these processes can be employed. These techniques are used to prepare the biomass for further conversion by enhancing its reactivity and breaking down complex compounds. 2.8.1 Advantages of the use of biomass as fuel

The carbon footprint of fossil fuels is higher than that of renewable fuels. Significant reductions in net carbon emissions can be achieved with proper management. There are several environmental and social benefits associated with the production and use of wood. It is considered a "carbon lean" fuel because it produces a smaller amount of carbon emissions than fossil fuels. It is a more sustainable energy option. There are various regions within Nigeria that can be used to source biomass. The need for long-distance

transportation is reduced by this availability. Local business opportunities are created and the rural economy is supported by the utilization of biomass as a fuel source. It can create jobs in rural areas where there are abundant resources. The economic incentive for the management of woodlands is provided by the use of biomass fuel. Ensuring a steady supply of wood is encouraged by sustainable practices. This promotes habitat preservation.

### 2.8.2 Gasification

High energy efficiency, flexibility in feedstock selection, and the ability to capture and utilize the resulting syngas are some of the advantages of gasification. It has the potential to be used for the production of clean and renewable energy from carbonaceous materials. (Lopes et al., 2018).

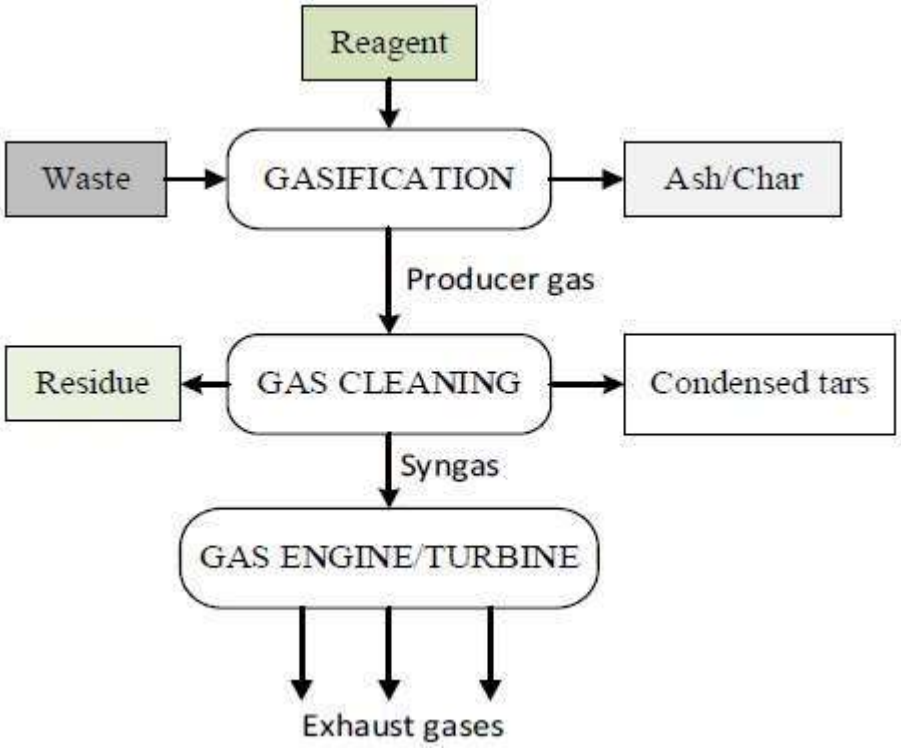


Figure 2.2: The gasification process (Lopes et al., 2018)

## 2.9 Fuel Cells

### 2.9.1 History of fuel cell

Fuel Cell (FC) was first discovered by Sir William Grove in 1839 called “Gaseous Voltaic Battery”. After several attempts to perfect the invention, Dr. Jacques develop the first Direct Carbon Fuel Cell (DCFC) using molten hydroxide as electrolyte in an attempt to generate electricity from coal in 1896 (Arenillas et al., 2013).

A variety of materials were used in the research. More than 1kilowatt of power was produced by 100 cells stacked together. The lifespan of the first DCFC was short due to the quick breakdown of the electrolyte. The component was seen as the primary battery. Carbon's chemical energy is transformed into electrical energy using a DCFC. A range of resources were used in the study. The original DCFC had a short lifespan. The main battery was supposed to be this one. Most of the previous studies on DCFC used molten carbonate as the electrolyte. The arrangement did not produce larger current densities. Due to the strong Funding for DCFC research was stopped when oil prices fell. (Dudek, 2018). There are no moving parts so they work silently. Fine particulate matter, nitrogenous, and sulphur compounds can be emitted at incredibly low levels to reduce their harmful impact on the environment. Some of the most hazardous substances are included in the internal combustion engine's emissions.

2.9.2 Basic working principle of fuel cell

Fuel cells have better theoretical efficiency than heat engines because their power output is not governed by the Carnot cycle. It provides a very low emission. Unlike batteries, thermal engines use fuel, fuel cells and battery cells to generate power. (Hoogers, 2003).

$$2H_2 + O_2 \rightarrow 2H_2O \qquad (2.1)$$

The electrical energy released is not the same as the heat energy. (Dicks, 2003).

A fuel cell has two electrodes and an ion conducting electrolyte, catalyst splits hydrogen or a fuel containing hydrogen into two different types of ion. Oxygen reacts with electrons and sometimes with substances like water or protons, as appropriate, at the cathode.

2.9.3 Why fuel cell

According to current developments, the most pressing energy and environmental challenges require new approaches to be solved. For the scenario of future energy, fuel cell technology offers a viable and sustainable solution. Despite the fact that fuel cells have been around for more than a century, current commercialization is preoccupied with improving their efficiency in response to a number of factors, including a growing awareness.( Jain, 2007).

Fuel cell systems are efficient with a power rate of over 100 kilowatts, unlike conventional power sources, is nearly as efficient as it is at full load. Fuel cells respond quickly to power demands. The capacity for load following is related to the decrease in production. Its loadfollowing capabilities are referred to as its capacity to rapidly decrease output. (Jain, 2007). Fuel cell systems are efficient with a power rate of over 100 kilowatts, unlike conventional power sources, is nearly as efficient as it is at full load. Fuel cells respond quickly to power demands. The capacity for load following is related to the decrease in production. Its loadfollowing capabilities are referred to as its capacity to rapidly decrease output.

2.10 Classification of Fuel Cell

The classification of fuel cells (FCs) is based on the electrolyte used. But it is noteworthy to say their functions are basically the same as shown in Table below For the operations at the anode, a fuel (hydrogen, carbon, etc.) is oxidized into electrons and proton, and at the

cathode, oxygen is reduced to oxide species. Depending on the electrolyte, either protons or oxide ions are transported through the ion conducting but electrically insulating electrolyte to combine with oxide or protons to generate water and electric power (Hoogers,

2003; Adeniyi, 2014).

The different types of fuel cells grouped based on the type of electrolyte used.

1. Polymer Electrolytic Membrane Fuel Cell (PEMFC)

    i. Solid Polymer Fuel Cell (SPFC) and

    ii. Proton Exchange Membrane Fuel cell (PEMFC)

2. Alkaline Fuel Cell (AFC)
3. Phosphoric acid Fuel Cell (PAFC)
4. Solid Oxide Fuel Cell (SOFC)
5. Molten Carbonate Fuel Cell (MCFC)
6. Direct Methanol Fuel Cell (DMFC)
7. Direct Carbon Fuel cell (DCFC)

Table 2.1: Developed fuel cells characteristics and applications

| Fuel | Electrolyte | Operating Temp ($^{O}$C) | Charge carrier | Fuel range/Application | Electric cell Type | Power efficiency |
|---|---|---|---|---|---|---|

| | | | | | |
|---|---|---|---|---|---|
| Proton exchange membrane FC(PEMFC) | Solid polymer | 50-100 | $H^+$ | Pure $H_2$ 35-40% tolerates $CO_2$ | Automotive CHP(5250KW) |
| Alkaline FC(AFC) | KOH | 60-120 | $OH^-$ | Pure $H_2$ 35-55% | <5KW, niche market space |
| Phosphoric acid FC(PAFC) | Phosphoric acid | ~220 | $H^+$ | Pure $H_2$ 40% tolerate $CO_2$,1% CO | Portable CHP (200KW) |
| Molten carbonate FC (MCFC) | Lithium Potassium Carbonate | ~650 | $CO_{32-}$ | $H_2$, CO, >50% $CH_4$ Other hydrocabon (tolerate $CO_2$) | 200KW-MW range CHP and stand alone |
| Solid oxide FC (SOFC) | Solid Oxide electrolyte yttria zirconia | ~1000 | $O_{2-}$ | $H_2$,CO, >50% CH4,O | 2KW-MW range CHP and stand alone |
| Direct carbon fuel cell (DCFC) | Molten salt / $O^{2-}$ conducting ceramic | ~500-1000 | | Other hydrocarbon (tolerate $CO_2$) | |
| $H_2$, CO, >80% CH4 | 25kw-120kw | | | | |

2.10.1 Alkaline fuel cells (AFC)

A 40% alkaline electrolyte is used in alkaline fuel cells. Fuel cells are high- performance because of how quickly chemical processes occur inside the cell. The space applications achieved efficiency of 60%. The fuel cell type has an issue with carbon dioxide poisoning it. When $CO_2$ and KOH mixed, the resistance will improve. Cleaning costs are involved. The amount of time before it needs to be replaced is influenced by the cell's susceptibility

to poisoning. The price will be raised further. Costs are less of a consideration for places like space or beneath the ocean. For more than 8,000 running hours, the AFC stacks can operate in a reliable manner.

$$\text{Anode Reaction: } 2H_2 + 4OH^- \rightarrow 4H_2O + 4e^- \quad (2.3)$$

$$\text{Cathode Reaction: } O_2 + 2H_2O + 4e^- \rightarrow 4OH^- \quad (2.4)$$

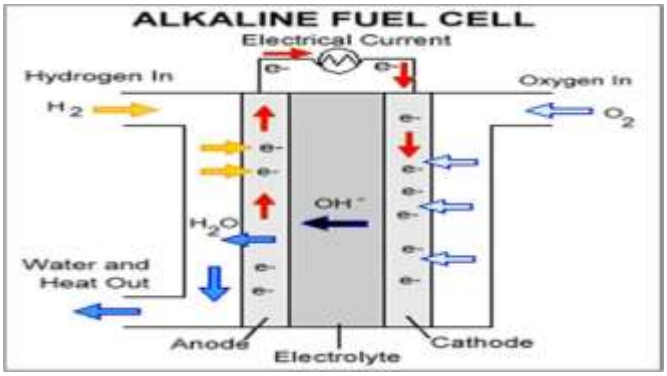


Figure 2.3: Configuration of a typical AFC cell (Cao et al., 2007).

2.10.2 Phosphoric acid fuel cells (PAFC)

This form of fuel cell powers many buildings. The acid can be held by the Teflon-bonded and porous carbon electrodes of the Silicon Carbide matrix. Impurities are not as bad by PAFCs. They have an efficiency of 85%, but only between 37 and 42% when producing just electricity. PAFCs are less powerful when compared to other fuel cells.

$$\text{Anode Reaction: } H_2 \rightarrow 2H + 2e^- \quad (2.5)$$

$$\text{Cathode Reaction: } \tfrac{1}{2}O_2 + 2H + 2e^- \rightarrow H_2O \quad (2.6)$$

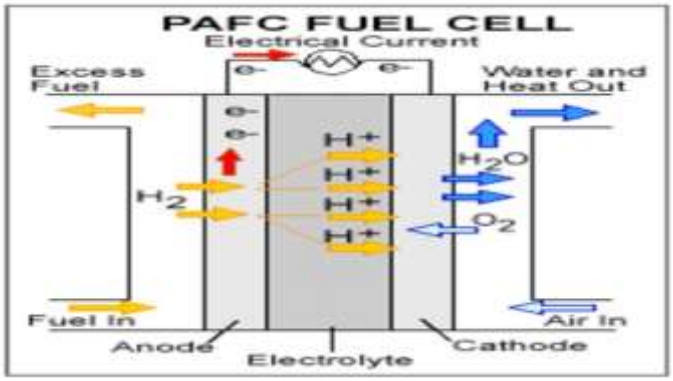

Figure 2.4: Configuration of a typical PAFC cell (Cao et al., 2007).

2.10.3 Polymer electrolyte membrane (PEM) fuel cells (PEMFC)

These cells are the best for smaller applications. Despite the fact that scientists are investigating catalysts that are more resistant to CO, this also raises costs.

$$\text{Anode Reaction: } H_2 \rightarrow 2H^+ + 2e^- \quad (2.7)$$

$$\text{Cathode Reaction: } \tfrac{1}{2}O_2 + 2H^+ + 2e^- \rightarrow H_2O \quad (2.8)$$

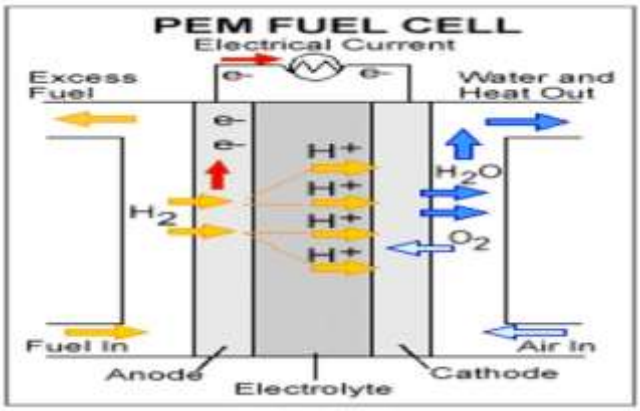


Figure 2.5: Configuration of a typical PEMFC cell (Cao et al., 2007).

2.10.4 Solid oxide fuel cells (SOFC)

SOFCs work at high temperatures. It will be done with efficiency of about 60%. The cells don't need to be built because the electrolyte is solid. High temperature operation lowers costs by eliminating the requirement for a precious-metal catalyst. They are resistant to sulfur and can be used as fuel. Coal-based gases can be used in SOFCs.

$$\text{Anode Reaction: } 2H_2 + 2O_2^- \rightarrow 2H_2O + 4e^- \quad (2.9)$$

$$\text{Cathode Reaction: } O_2 + 4e^- \rightarrow 2O_2^- \quad (2.10)$$

$$\text{Overall Cell Reaction: } 2H_2 + O_2 \rightarrow 2H_2O \quad (2.11)$$

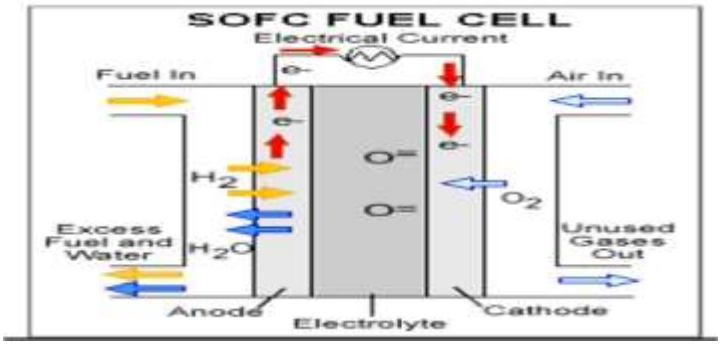


Figure 2.6: Configuration of a typical SOFC cell (Cao et al., 2007).

2.10.5 Molten carbonate fuel cells (MCFC)

The molten carbonate fuel cell makes use of molten carbonate salt as the electrolyte. It is mostly been fuelled with coal- derived fuel gases, methane or natural gas. The cells can work at up to 60% Efficiency. In molten carbonate fuel cells, negative ions travel through the electrolyte to the anode where they combine with hydrogen to generate water and electrons.

Anode Reaction: $CO_3^{2-} + H_2 \rightarrow H_2O + CO_2 + 2e^-$ (2.12)

Cathode Reaction: $CO_2 + ½O_2 + 2e^- \rightarrow CO_3^{2-}$ (2.13) Overall Cell Reaction: $H_2 + ½O_2 \rightarrow H_2O$ (2.14)

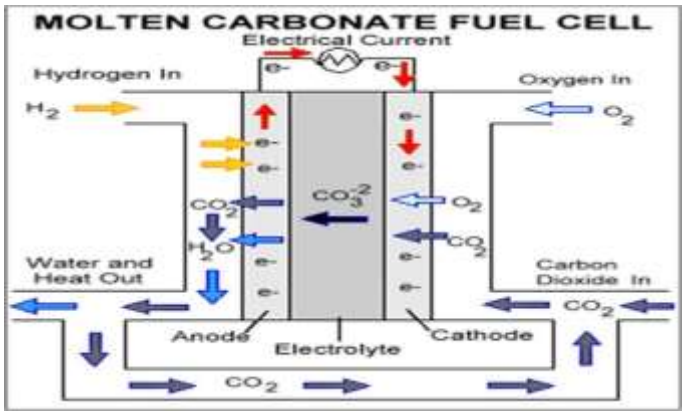

Figure 2.7: Configuration of a typical MCFC cell (Cao et al., 2007).

2.10.6 Direct methanol fuel cell (DMFC)

The performance of the DMFC is constrained by a number of material related problems, such as membranes that allow the free passage and low-activity catalyst materials. In the sections to follow, a more thorough examination of the anode reaction and unique catalyst materials will be covered. Up until recently, this has been the focus of the majority of investigations, because it is thought to be the most constrained part of the DMFC's performance.

Anode reaction: $CH_3OH + H_2O \rightarrow CO_2 + 6H^+ + 6e^-$ (2.15)

Cathode reaction: $^3/_2O_2 + 6H^+ + 6e^- \rightarrow 3H_2O$ (2.16)

Overall reaction: $CH_3OH + ^3/_2O_2 + H_2O \rightarrow CO_2 + 3H_2O$ (2.17)

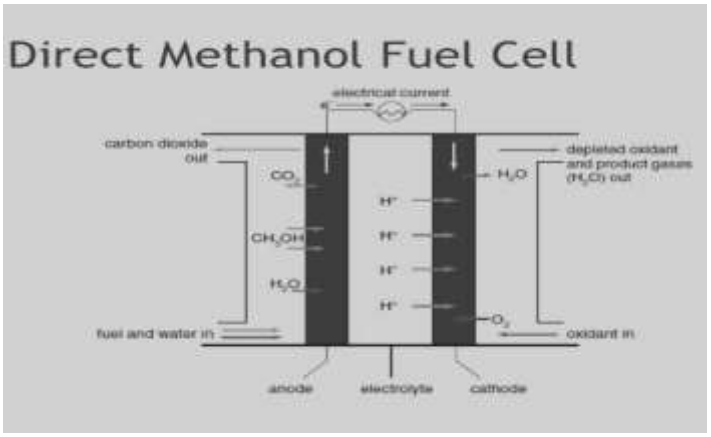


Figure 2.8: Configuration of a typical DMFC cell (Cao et al., 2007). Table 2.2: Classification of fuel cell based on electrolyte used

| Electrolyte (ion carrier) | Operating Temperature ($^oC$) | Electrode Reaction |
|---|---|---|
| Alkaline ($OH^-$) | ~100$^oC$ | Anode: $2H_2 + 4OH^- \rightarrow 4H_2O + 4e^-$<br>Cathode: $O_2 + 2H_2O + 4e^- \rightarrow 4OH^-$ |

| | | |
|---|---|---|
| Phosphoric Acid ($H^+$) | ~200°C | Anode: $H_2 \rightarrow 2H + 2e^-$<br>Cathode: $½O_2 + 2H + 2e^- \rightarrow H_2O$ |
| Proton Exchange membrane ($H^+$) | ~80°C | Anode: $H_2 \rightarrow 2H + 2e$-<br>Cathode: $½O_2 + 2H^+ + 2e^- \rightarrow H_2O$ |
| Molten Carbonate ($CO_3^-$) | ~650°C | Anode: : $CO_3^{2-} + H_2 \rightarrow H_2O + CO_2 + 2e^-$<br>Cathode: $CO_2 + ½O_2 + 2e^- \rightarrow CO_3^{2-}$ |
| Solid Oxide | ~ 1000°C | Anode: $2H_2 + 2O^{2-} \rightarrow 2H_2O + 4e^-$<br>Cathode: $O_2 + 4e^- \rightarrow 2O_2^-$ |

## 2.11 Direct Carbon Fuel Cell

The direct carbon fuel cell (DCFC) is a high temperature fuel cell that directly uses carbon as fuel supplied to the anode, which also has the ability to reduce the complexities of reforming hydrocarbon raw materials to fuels such as hydrogen. The DCFC offers high thermal efficiencies for electrical power generation compared to other fuel cell types using different fuels. The raw materials used for powering a DCFC are solid, carbon-rich fuels (Cao et al., 2007). The overall system efficiency of a DCFC, taking into account of secondary losses is in the range of 60-70 % (Giddey et al., 2012),

### 2.11.1 Features of a direct carbon fuel cell (DCFC)

1. A direct carbon fuel cell operates at high temperatures (500-900°C), it converts the chemical energy in solid carbon into electricity through its direct electrochemical oxidation. at this operating temperature range.
2. Fuel utilization can be nearly 100%. This is because of the separate phase between the fuel feed and the product gas.
3. The solid fuel feed system for delivery of fuel to reaction sites is quite complex compared to gaseous or liquid fuel fed fuel cell systems.

4. The theoretical efficiency of direct carbon fuel cell is also high, just about 100%. 5. The by-product is pure CO2 requiring no gas separation and can be directly segregated hence, avoiding cost and efficiency penalties

The Electrochemical reactions involved in the DCFC are shown in equations 2.29- 2.31.

$$\text{Anode: } C + 2O^- \rightarrow CO_2 + 4e^- \quad (2.18)$$

$$\text{Cathode: } O_2 + 4e^- \rightarrow 2O^- \quad (2.19)$$

$$\text{Overall: } C + O_2 \rightarrow CO_2 \quad E^o = 1.02V \quad (2.20)$$

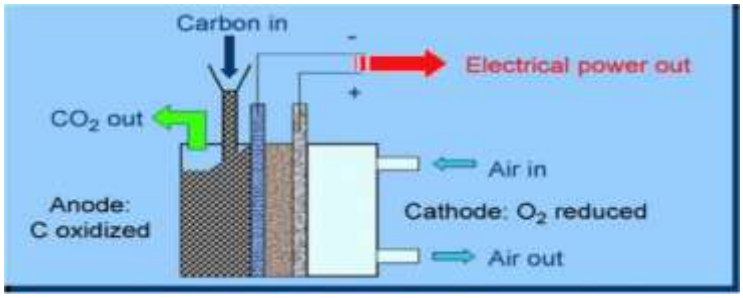


Figure 2.9: Configuration of a DCFC cell ( Wolk, 2007).

2.11.2 Classification of direct carbon fuel cell

Direct Carbon Fuel Cell are classified according to the type of electrolyte used . The majorly employed are:

I. DCFC with a molten carbonate electrolyte

II. DCFC with a molten hydroxide electrolyte

III. DCFC with an YSZ-based solid electrolyte

2.11.2.1 DCFC with a molten carbonate electrolyte

Molten carbonate electrolytes are very good for DCFCs, they are highly conductive, have good stability when $CO_2$ is present, and have an appropriate melting temperature for its application. The cell voltage is formed at the anode side and consumed at the cathode side, and there is an influence on the cell voltage by this partial pressure (Wolk et al., 2007). The

use of mixed molten carbonates ($Li_2CO_3/K_2CO_3$) for DCFC is recommended because of their high conductivity, good stability in the presence of $CO_2$ (carbon electro-oxidation product) and suitable melting temperature (Cao et al., 2007,Cherepy et al., 2005). $CO_2$ is formed at the anode side and consumed at the cathode side, therefore, its partial pressure has an influence on the cell voltage (Cao et al., 2007). Activation of the cathode catalyst was done by thermal treatment in air followed by lithiation to form a compact layer of nickel oxide (NiO). Anode and cathode were separated by several layers of Zirconia felt. The cell operates with carbon (anode side) and air/$CO_2$ mixture (cathode side). Oxygen in the air reacts to produce carbonate ions which oxidizes the carbon particles at the anode. This tilted design allowed the excess electrolyte to drain from the cell thus avoiding flooding of the cathode (Yarlagadda, 2011).

$$\text{Anode: } C + 2CO_3^{2-} \rightarrow 3CO_2 + 4e^- \quad (2.21)$$

$$\text{Cathode: } O_2 + 2CO_2 + 4e^- \rightarrow 2CO_3^{2-} \quad (2.22)$$

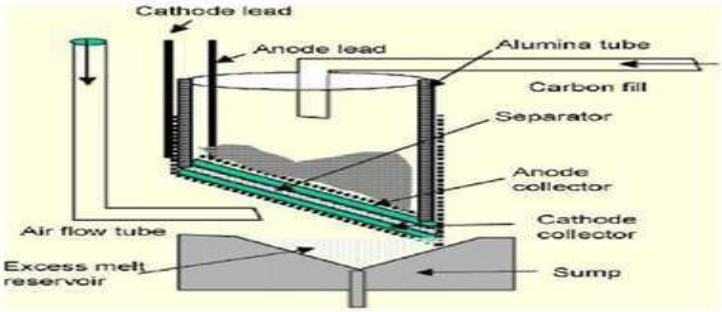


Figure 2.10: Tilted DCFC with a molten carbonate electrolyte (Cao et al,. 2010).

2.11.2.2 Advantages of molten carbonate in DCFC

Long-term stability in CO2 is one of the benefits of using molten carbonate as an electrolyte. (Kacprzak et al.,2016). It can oxidize carbon. It is not as strong as NaOH. The

operating temperature of carbonate-based systems is higher than that of molten hydroxidebased systems. Carbon can be used as both a current collector and a anode. (Deleebeck.,2014; Cooper et al., 2005).

2.11.3 DCFC with a molten hydroxide electrolyte

The molten hydroxide DCFC, uses molten hydroxide as electrolyte in DCFC,molten hydroxides have a number of advantages such as higher ionic conductivity, higher activity of the carbon electrochemical oxidation which means a higher carbon oxidation rate and lower over potential (Yarlagadda, 2011).

Electrochemical reactions involved with the molten hydroxide DCFC clearly illustrated below.

$$\text{Anode: } C + 4OH^- \rightarrow CO_2 + 2H_2O + 4e^- \quad (2.23)$$

$$\text{Cathode: } O_2 + 2H_2O + 4e^- \rightarrow 4OH^- \quad (2.24)$$

$$\text{Overall: } C + O_2 \rightarrow CO_2 \quad (2.25)$$

2.11.3.1 Advantages of molten hydroxide in DCFC There are benefits to using molten hydroxide electrolyte.

1. It has a strong ionic conductivity.

2.The higher the reactivity with carbon, the greater the anodic oxidation rate and the lower the potential losses.

3.The operating temperatures were low due to the low melting point. (Giddey et al., 2012).

2.11.4 DCFC with an YSZ-based solid electrolyte

This DCFC where the cell consists of a solid Yttria Stabilized Zirconia (YSZ) electrolyte layer along with a liquid electrolyte which comprises a mixture of lithium carbonate ($Li_2CO_3$), potassium carbonate ($K_2CO_3$) and sodium carbonate ($Na_2CO_3$) (Yarlagadda,

2011).

The electrochemical reaction that takes place in this system is as shown

$$\text{Anode: } C + 2O^- \rightarrow CO_2 + 4e^- \quad (2.26)$$

$$\text{Cathode: } O_2 + 4e^- \rightarrow 2O^- \quad (2.27)$$

$$\text{Overall: } C + O_2 \rightarrow CO_2 \quad (2.28)$$

2.12 Process of Fueling Fuel Cells.

Types of fuel used to fuel cells always varies for different types. Hydrogen use to be the fuel to power fuel cells, technological advancement has led to the use of biomass, coal, natural gas and municipal solid waste as suitable fuels for fuel cell system.

2.12.1 Hydrogen

It being water produced by hydrogen oxidation. Zero-emission vehicles powered by PEM fuel cells emit only water when they use hydrogen. Since hydrogen doesn't naturally exist as a gaseous fuel, it needs to be produced from a fuel source in order to be used.

Table 2.3: Hydrogen and other fuels properties for fuel cell systems.

| Properties | Hydrogen $H_2$ | Methane $CH_4$ | Ammonia $NH_3$ | Methanol $CH_3OH$ | Ethanol $C_2H_5OH$ | Gasoline $C_8H_{18}$ |
|---|---|---|---|---|---|---|
| Molecular weight | 2.016 | 16.04 | 17.03 | 32.04 | 46.07 | 114.2 |
| Freezing point ($^oC$) | -259.2 | -182.5 | -77.7 | -98.8 | -114.1 | -56.8 |
| Boiling point ($^oC$) | -252.77 | -161.5 | -33.4 | 64.7 | 78.3 | 125.7 |
| Net enthalpy of combustion @ 25$^oC$ (kJ $mol^{-1}$) | 241.8 | 802.5 | 316.3 | 638.5 | 1275.9 | 5512.0 |

| | | | | | | |
|---|---|---|---|---|---|---|
| Heat of vaporisation (kJ $kg^{-1}$) | 445.6 | 510 | 1371 | 1129 | 839.3 | 368.1 |
| Liquid density (kg $m^{-3}$) | 77 | 425 | 674 | 786 | 789 | 702 |
| Specific heat at STP ($Jmol^{-1}$ $K^{-1}$) | 28.8 | 34.1 | 36.4 | 76.6 | 112.4 | 188.9 |
| Flammability limits in air (%) | 4-77 | 4-16 | 15-28 | 6-36 | 4-19 | 1-6 |
| Autoignition temperature in air (oC) | 571 | 632 | 651 | 464 | 423 | 220 |

2.12.2 Natural gas

One of the easiest ways to extract carbon from natural gases is the thermal decomposition or cracking of natural gas. Methane can be broken down into carbon and hydrogen with less than 18 kcaVmo1 of heat of creation. If we apply the 80% thermal efficiency of cracking operations, we can estimate that 10. At operating pressures below 5m and temperatures between 800 and 1000C. (Cherepy et al., 2002).

In the thermal black process, methane is destroyed without the presence of air in tandem firebrick furnaces that are reheated. During the furnace black process, methane or furnace oil is partially burned in a rich flame, and carbon fines are collected as a by-product. Both of these techniques are extremely inefficient because energy is not conserved. The generated hydrogen is used as fuel. The processes can be made more efficient if hydrogen is used. The third and most recent method is the plasma black method, which cracks methane using an electric discharge. Carbon and hydrogen are recovered. The procedure is effective according to claims. Electric power usage lowers the overall fuel efficiency to below 50% if a non-fossil fuel source is used. The industrial black process uses affordable hydropower in Canada. (Cooper et al., 2008).

### 2.12.3 Petroleum

This are deposit found in sedimentary rock, a mixture of solid, liquid and gaseous hydrocarbon compounds. Fuels derived from petroleum account for one half of the world's total energy supply which are gasoline, diesel fuel, aviation fuel, kerosene etc. Various components of petroleum are separated into fractions by distillation (Larminie and Dicks, 2003; Adeniyi, 2014). For fuel cell these chemical composition are good which helps determine the type of fuel processing used for generating hydrogen. (Larminie and Dicks, 2003; Adeniyi, 2014).

### 2.12.4 Coal and coal gas

Coal an abundant complex chemical fossil fuel. Formed from the remains and indurations of many plant similar to those of peat. Coal are Classified based on the inherent plant material (coal type), degree of metamorphosis (coal rank), and also degree of impurities (coal grade). Processing of coal to produce liquids, gases and coke is mainly dependent on the properties of the raw coal material. Fuel cell can be powered by the gases produced from coal gasification or from coal powder (Larminie and Dicks, 2003).

### 2.12.5 Bio-fuels

These are fuel gotten from biomass and all natural organic material associated with living organisms, found on land and marine vegetable matter. There is a great desire for using biogases in fuel cell systems. Most biogases have low heating values and high level of carbon oxides and nitrogen. Fuel cells most especially the DCFC, MCFC and SOFC can handle very high concentration of carbon oxides (Larminie and Dicks, 2003). Bio liquids are also good for fuel cell application, methanol and ethanol are good examples. Methanol

is the proposed fuel for Fuel cell vehicles (FCVs). It is synthesised from syngas derived from biomass or natural gas. Ethanol gotten from direct fermentation of biomass. Alcohol could be reformed into hydrogen-rich gas (Larminie and Dicks, 2003).

## 2.13 Thermodynamic Analysis

### 2.13.1 First law of thermodynamics

The First Law of Thermodynamics states that the energy of a system is conserved. Energy is neither lost nor generated but is converted from one form to another.

$$Q - W = \Delta E \tag{2.29}$$

From Equation 2.29, Q is the amount of heat as input in the system, -W is the work done by the system, $\Delta E$ is the change in total energy which is dependent on the initial and the final state (Hoogers, 2003).

The fuel cell is an open system, it allows the flow of mass and energy through its boundaries. The total energy of the system is the sum of the changes in internal, U, kinetic, KE, and potential, PE, energies.


a) control mass b) control volume

A stationary control volume system under steady-flow conditions has its change in kinetic and potential energy as zero with other properties constant with time ($\Delta KE = \Delta PE = 0$) (Fuel Cell handbook, 2003). Thus the first law is expressed for a typcal fuel cell (Open system) in equation 2.30

$$Q - W = \Delta H \qquad (2.30)$$

2.13.2 Second law of thermodynamics

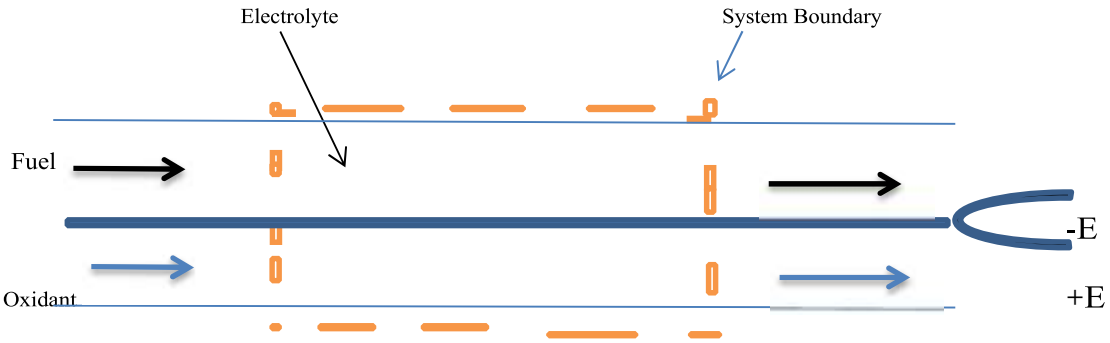


Figure 2.11: Mechanisms of thermodynamics of direct carbon fuel cell (Dicks, 2003) The Second Law of Thermodynamics defines the property entropy, which can be utilized as a measure of the disorder in a system. A process that does not produce entropy is known as a reversible process in the event that it very well may be performed and afterward come back to its initial state. In this way, in a reversible process, by the First Law, no net trade of heat or work happens in either the system or environment: both come back to their original states. An irreversible process, then again, generates entropy in view of, for instance, expansion with no restrictions, heat loss from friction, or heat exchange through a finite temperature difference. A process that involves heat exchange can be made reversible if the finite temperature gradient, is limited to an infinite difference (to the

detriment of the rate of heat exchange) (Hoogers, 2003). Entropy depends on this reversible heat exchange, and as a property, it is expressed as

$$\Delta S = \frac{\quad}{\quad} \qquad (2.31)$$

For a process that undergoes reversible heat transfer, $Q_{rev}$, at a constant temperature, $T_o$, entropy.

2.13.3 Heat engines

These four characteristics define accurately the operations of a heat engine (Hoogers, 2003):

i It Receives heat from a high-temperature source

ii Then Converts part of this heat to work

iii Rejects the remaining waste heat to a low-temperature sink

iv Operates on a thermodynamic cycle

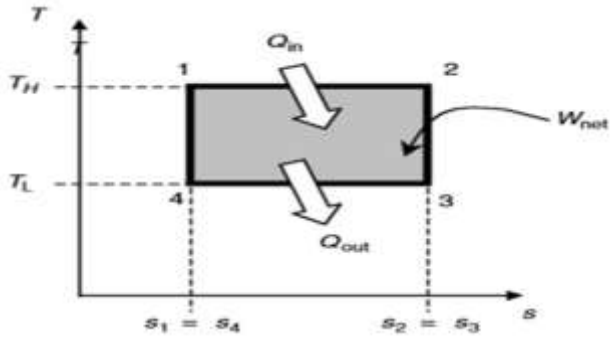


Figure 2.12: T-S diagram of carnot cycle (Larminie, 2003).

Heat engines transforms thermal energy, or heat, $Q_{in}$ into mechanical energy , or work $W_{out}$ they cannot do this task perfectly, so some of the input heat energy is not converted into work, but is dissipated as waste heat $Q_{out}$ into the environment.

$$Q_{in} = W_{out} + Q_{out} \qquad (2.32)$$

The thermal efficiency of a heat engine is the percentage of heat energy that is transformed into work thus it is determined by the amount of work converted from the amount of energy input into the system which is given as:

$$\eta_{th} = \qquad = 1 - \frac{\quad}{\quad} \tag{2.33}$$

The efficiency of the best heat engines is usually below 50 % and sometimes lower. Because of the a large fraction of the fuels produced worldwide go to powering heat engines, half of the useful energy produced worldwide is wasted in engine inefficiency hypothetically. This inefficiency can be attributed to three causes namely:

i. Carnot efficiency. ii.

Irreversibility.

iii. Mechanical friction and losses in the combustion process.

2.13.3.1 Carnot efficiency

The thermal efficiency of all heat engines is fundamentally constrained by the second law of thermodynamics. Nearly none of the heat input into an engine, even in an ideal, frictionless engine, can be converted into works, $T_H$ & $T_L$ carnot's theorem can be represented thus:

$$\eta_{th} \leq 1 - \frac{\quad}{\quad} \tag{2.34}$$

The carnot cycle efficiency is a limiting figure for an ideal engine cycle. This efficiency is a minimum that can't be exceeded because of the technologies that transform heat into mechanical energy. The maximum achievable efficiency of a steam plant is 73%. The different forms of energy are converted to electricity, fuel cell converts the electrochemical properties into electricity. The figure above explains clearly the operations in a fuel cell which include the conversion of inputs directly into some kind of output.

2.13.4 EMF and the energy of the hydrogen fuel cell

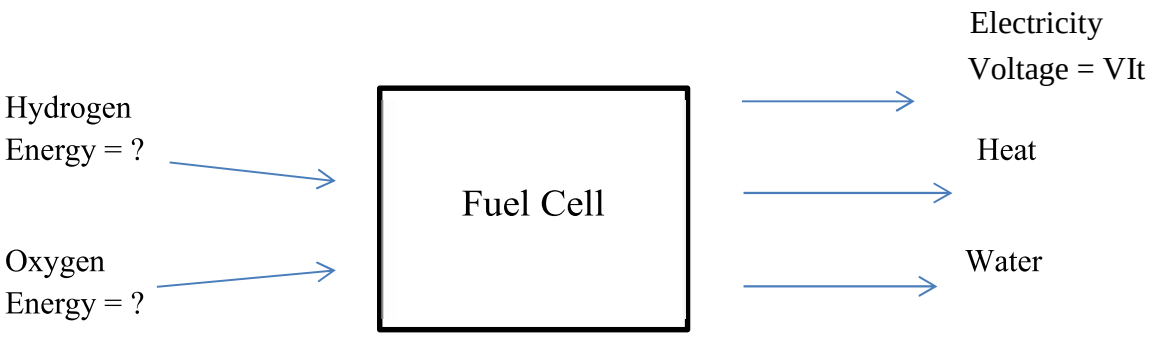


Unlike convention power generation systems where their differe Figure 2.13: Fuel cell inputs and outputs (Dicks, 2003)

A fuel cell converts various kinds of energy into electricity. The actions in a fuel cell are explained in detail by the above graphic. It is easy to calculate the electrical power and energy production. (Larminie and Dicks, 2003).

$$\text{Power} = VI \text{ and Energy} = VIt \qquad (2.35)$$

that are still relevant, exergy is the word that best fits the endeavour to use the concept of high-temperature. (Larminie and Dicks, 2003).

2.13.5 Gibbs free energy

Gibbs free energy is important in fuel cell. It is defined as the 'energy available to do external work, its independent of work done by changes in pressure and volume'. In a fuel cell, the 'external work' involves moving electrons round an external circuit any work done by a change in volume between the input and output is not harnessed by the fuel cell. Exergy is all the external work that can be extracted, including that due to volume and

pressure changes. Enthalpy can be simply defined as the Gibbs free energy and the energy connected with the entropy (Larminie and Dicks, 2003). In a fuel cell operating at constant pressure and temperature, the maximum electrical work (Wel) available is given by the change in Gibbs free energy (ΔG) of the electrochemical reaction:

$$Wel = \Delta G = - nFE \tag{2.36}$$

Where n is the number of electrons participating in the reaction, F is Faraday's constant (96,487 coulombs/g-mole electron), and E is the ideal potential of the cell.

The change in Gibbs free energy can also be written as:

$$\Delta G = \Delta H - T\Delta S \tag{2.37}$$

At constant temperature and pressure, ΔG = -395.3 KJ/mol ΔH = -393.95KJ/mol Where ΔH is the enthalpy change which is also the total thermal energy available and ΔS is the entropy change. TΔS represent the amount of heat produced by a fuel cell operating reversibly. Reactions occurring in a fuel cells that having negative entropy change generate heat (hydrogen oxidation), while those having positive entropy change (direct solid carbon oxidation) extract heat from their surroundings if the irreversible generation of heat is smaller than the reversible absorption of heat (Jain, 2009). Enthalpy can be simply defined as the Gibbs free energy and the energy connected with the entropy.

$$\text{Enthalpy } \Delta H = \Delta G + T\Delta S \tag{2.38}$$

Where ΔH is the Enthalpy

ΔG is the Gibbs free energy

TΔS is the Energy connected with Entropy

In a fuel cell, it is the change in Gibbs free energy of formation, $G_f$ , that gives the energy expelled. This change is the difference between the Gibbs free energy of the products and the Gibbs free energy of the inputs or reactants (Larminie and Dicks, 2003).

$$G_f = G_f \text{ of products} - G_f \text{ of reactants} \quad (2.39)$$

However, the Gibbs free energy of formation is not constant; it changes with temperature and state (liquid or gas). below shows $\Delta g_f$ for the basic hydrogen fuel cell reaction.

$$H_2 + O_2 \rightarrow H_2O \quad (2.40)$$

Gibbs free energy is converted into electrical energy. for the hydrogen fuel cell, two electrons pass round the external circuit for each water molecule produced and each molecule of hydrogen used. So, for one mole of hydrogen used, 2N electrons pass round the external circuit – where N is Avogadro's number. If −e is the charge on one electron, then the charge that flows is

$$-2Ne = -2F \text{ coulombs} \quad (2.41)$$

F being the Faraday constant, or the charge on one mole of electrons. If E is the voltage of the fuel cell, then the electrical work done moving this charge round the circuit is

$$\text{Electrical work done} = \text{charge} \times \text{voltage} = -2FE \text{ joules} \quad (2.42)$$

If the system is reversible (or has no losses), then this electrical work done will be equal to the Gibbs free energy released $\Delta g_f$. So

$$\Delta g_f = -2F \cdot E \text{ joules}$$

Thus

$$E = \qquad (2.43)$$

The above equation gives the electromotive force (EMF) or reversible open circuit voltage of the hydrogen fuel cell.

2.13.6 Cell efficiency

Pressure and heat can be used to turn chemical energy into electrical energy. One of the limitations of traditional energy sources is the Carnot cycle. Fuel cells are not constrained by the Carnot cycle because they produce energy through the reaction of the fuel. (Giddey et al., 2012).

For a fuel cell conversion device, the thermal efficiency is defined as the amount of useful energy produced relative to the change in enthalpy, $\Delta H$, between the product and feed streams.

$$\eta = \frac{\qquad}{\qquad} \qquad (2.44)$$

Conventionally, chemical (fuel) energy is first converted to heat, which is then converted to mechanical energy, and subsequently converted to electrical energy (Hoogers,2002).

In the ideal case of an electrochemical converter, such as a fuel cell, the change in Gibbs free energy, $\Delta G$, of the reaction is available as useful electric energy at the temperature of the conversion. The ideal efficiency of a fuel cell, operating reversibly is given as:

$$\eta_{ideal} = \frac{}{} \qquad (2.45)$$

The fuel cell technology is more efficient than the conventional heat engines. The efficiency of a system is regardless of its size. A small system can be as efficiency as a large one and this is important in an attempt to generate power in a combined heat and power system (Nurnberger et al,2010).

The DCFC has many benefits and is expanding. A DCFC system can be built without heat engines or reformers, which lowers the cost of shipping and reduces environmental pollution. The production of solid rich-carbon particles used as fuel in a DCFC requires less energy and resources than the manufacturing of hydrogen-rich fuels used electric efficiency for a DCFC with a fuel utilization factor close to one may be processes. In fuel cells, the losses associated with auxiliary subsystems are usually under 10%. The electric efficiency for a DCFC is between 70% and 67%.

2.13.7 Open circuit voltage (OCV)

The open circuit voltage is the greatest that can be achieved for a specific fuel cell. When there is no external load. A linear voltage decrease is seen at intermediate current densities when the non-instantaneous reaction kinetics results in a rapid voltage drop from OCV. Its concentration of the reactants will be lower at the cell's exits than it is at the entry. (Larminie and Dicks, 2003).

2.13.8 Voltage

Fuel cells oftenly generate about 0.6 volts to 0.9 volts DC per cell but the output voltage falls as the current is increased due to the internal impedance and losses within the cell, the opening or holes in the cell should be sealed to provide higher voltage.( Jai, 2010),

2.13.9 Current density

The current density can be calculated by dividing the current by the cross-sectional area of the fuel cell.

From Ohm's Law: V=IR (2.46)

Where V= Cell Voltage, I = Current and R = Resistance

Since current density = current per Area and Area =unity (1)

$$\frac{\quad}{\quad} \quad \frac{\quad}{\quad} = \qquad (2.47)$$

2.13.10 Power density

The power density delivered by a fuel cell is the product of the current density and the cell voltage at that current density divided by the active surface area of the cell. Because the size of the fuel cell is very important, other terms are also used to describe fuel cell performance. Specific power is referred to as the ratio of the power generated by a cell (or stack) to the mass of that cell (or stack) (Li et al.,2003).

$$\text{Power Density} = \frac{\quad}{\quad} \qquad (2.50)$$

And electrical power is calculated from:

If V =IR and P=IV, then P=I (IR)

Therefore, $P=IV= I^2R$ (since I and R is the only known) measured in watt/$cm^2$

It uses an electrochemical process to directly convert chemical energy to electricity.

2.13.11 Fuel cell irreversibility

The system's loss of work or energy is referred to as this, while other terms include over potential, and polarization. There are only ohmic losses that function as a resistance. ). they are namely ( Larminie and Dicks, 2003)

i. Activation losses ii. Ohmic losses (having current densities in the range of 50-900 mA/cm$^2$) iii. Mass transport or concentration losses (having current densities greater than

900mA/cm2)

iv. Kinectic losses (having current densities less than 50 mA/cm$^2$)

2.13.11.1 Activation Losses

The slowness of the reactions on the surface leads to activation losses. When driving the chemical reaction that transports electrons ( Larminie and Dicks, 2003)

.

2.13.11.2 Ohmic losses

During fuel cell operation, ion must pass through the electrolyte. The losses are caused by the ion flowing (Adeniyi, 2014).

$$V = IR \tag{2.51}$$

$$\Delta V_{ohm} = ir \tag{2.52}$$

in order to serve as the foundation over which the electrodes are constructed, or it needs to be wide enough to allow an electrolyte circulation flow. It must be thick enough to prevent any electrical connections between the electrodes and the electrolyte. (Larminie and Dicks, 2003).

2.13.11.3 Fuel Crossover and Internal Currents

Fuel crossover are term used for that small amount of wasted fuel that migrates through the electrolyte. In a practical fuel cell some fuel will diffuse from the anode through the electrolyte to the cathode, because of the catalyst, it will react directly with the oxygen, producing no current from the cell. The crossing over of one hydrogen molecule from

anode to cathode where it reacts, wasting two electrons, amounts to exactly the same as two electrons crossing from anode to cathode internally, rather than as an external current. The internal currents and the fuel crossover are essentially equivalent ( Larminie and Dicks 2003)

2.13.11.4 Concentration losses/Mass transport

Losses that result from the change in concentration of the reactants at the surface of the electrodes as the fuel is used (Adeniyi 2014). If at the anode of a fuel cell supplied with hydrogen and during cell operation there will be a slight drop in pressure, if the hydrogen is consumed as a result of a current being drawn from the cell. This pressure reduction results from the fact that there will be a flow of hydrogen down the supply ducts and tubes, and this flow will result in a pressure drop due to their fluid resistance. This reduction in pressure will depend on the electric current from the cell (and $H_2$ consumption) and the physical characteristics of the hydrogen supply system. Similarly, If the oxygen at the cathode of a fuel cell is supplied in the form of air, then it is self-evident that during fuel cell operation there will be a slight reduction in the concentration of the oxygen in the region of the electrode, as the oxygen is extracted. The extent of this change in concentration will depend on the current being taken from the fuel cell, and on physical factors relating to how well the air around the cathode can circulate, and how quickly the oxygen can be replenished. This change in concentration will cause a reduction in the partial pressure of the oxygen (Zecevic et al,2005). Conclusively a reduction in the gas pressure will lead to a reduction the cell voltage.

2.13.12 Effect of temperature in a DCMC fuel cell operation

The Gibbs free energy changes with temperature ( it decreases with elevated temperature) and at high temperature, the electrochemical reactions proceed more quickly, which

manifests in lower activation voltage losses. Also, noble metal catalysts are often not needed. The high temperature of the cell and the exit gases means that there is heat available from the cell at temperatures high enough to facilitate the extraction of carbon from other more readily available fuels, such as natural gas.

The high temperature exit gases and cooling fluids are a valuable source of heat for buildings, processes, and facilities near the fuel cell. In other words, such fuel cells make excellent 'combined heat and power (CHP) systems'.

The high operating temperature of MCFCs provides the opportunity for achieving higher overall system efficiencies and greater flexibility in the use of available fuels compared with the low temperature types. (Larminie, 2003).

### 2.13.13 Advantages and applications of fuel cell

The most important disadvantage of fuel cells is the same for all types, being the cost. Apart from that, there are diverse advantages, which emphasise more or less strongly for different types and generate different applications.

#### 2.13.13.1 Simplicity

The major part of a fuel cell are relatively simple with few that require to be moved from one place to another. This can help maintain the longevity and reliability of the system.

#### 2.13.13.2 Low flare gases

The world at large is faced with the problem of gas emission most especially $CO_2$ which causes greenhouse effect and global warming. The by-product of the fuel cell reaction, when hydrogen is the fuel is pure water, which means fuel cell can be essentially 'Zero emission' (Yue et al,2016). This is the main advantage when used in vehicles, as there is a requirement to reduce vehicle emissions.

2.13.13.3 Silence

Fuel cells are very quiet, even those with extensive extra fuel processing equipment. This is very important in both portable power applications and for local power generation in combined heat and power schemes (Larminie and Dicks, 2003).

# CHAPTER THREE

## 3.0 MATERIALS AND METHOD

Diagrams of some of the equipment and setup stands are included in this chapter. It gives an in-depth understanding of the calorific value evaluation process. The design and assembly of the DCFC equipment, as well as the preparation of the molten hydroxide electrolyte for fuel cell operation, are provided.

### 3.1 Equipment and Reagents

#### 3.1.1 Equipment

The list of equipment and processes employed in determining the performance of the solid waste in the DCFC which in turn was used to generate electricity are shown in Table 3.1.

Table 3.1: List of equipment

| S/No | Equipment | Manufacturer | Model |
|---|---|---|---|
| 1 | Oven | England | +2 |
| 2 | Furnace | England | SAR-590-G |
| 3 | Kjedahl digertor | England | GERHARDT |
| 4 | Micro kjedahl distiller | | |
| 6 | Refartech Retractor | England | TECATOR |
| 7 | Beaker | England | BNB-380-600 ml |

| | | | | | | | |
|---|---|---|---|---|---|---|---|
| 8 | Measuring Cylinder | England | C31860/9 | | | | |
| 9 | Reagent bottle | England | BTF-350-500 ml | | | | |
| 10 | Digestion tubes | Germany | 100ml | | | | |
| 11 | Petric dishes | England | PYRAX | | | | |
| 12 | Flask or Round bottom | England | FR150/2S, 150ml | | | | |
| 13 | Weighing boots | England | 14 | Cathode lamps | England | | |
| 15 | Volumetric flask | England | 16 | Extracting bottles | England | 75ml | |
| 17 | Calorimeter | England | CBA-300 | | | | |
| 18 | Crucibles | England | Ceramic | | | | |
| 19 | Mortar and pestles | England | MWA-300-090M, 125mm | | | | |
| 20 | Sieves | England | SIH-300-110Q, 10 mesh | | | | |
| 21 | JEOOLJSM Microscope | 5600LV | | | | | |
| 22 | Empyrean Diffractometer | Germany | DY 674 2010 | | | | |
| 23 | Spectrophometer | England | UV2100 | | | | |
| 24 | Heating Block | Locally fabricated | 25 | Resistor box | Locally fabricated | | |
| 26 | Multimeter | | | | | | |
| 27 | Weighing balance | 28 | Gas cylinders | 29 | Stop Watch | 30 | Gas pipes |

### 3.1.2 Reagents

The list of reagents used for the preparation of the carbon fuel and the electrolyte are shown in Table 3.2.

Table 3.2 : List of reagents

| S/No. | Reagent/Chemical | MANUFACTURER | Purity % |
|---|---|---|---|

| | | | |
|---|---|---|---|
| 1 | Sodium hydroxide | India | 98.9 |
| 2 | Potassium hydroxide | England | 98 |
| 3 | Bromocresol green | England | 99 |
| 4 | Ethanol | England | 99.7 |
| 5 | Diethyl ether | | |
| 6 | Sulphuric acid | England | 89.07 |
| 7 | Nitric acid | England | 96.7 |
| 8 | Hydrochloric acid | England | 97 |
| 9 | Ammonium hydroxide | England | 97 |
| 10 | Kjedhal Tablet | | |
| 11 | Ascobic acid | England | 99.7 |

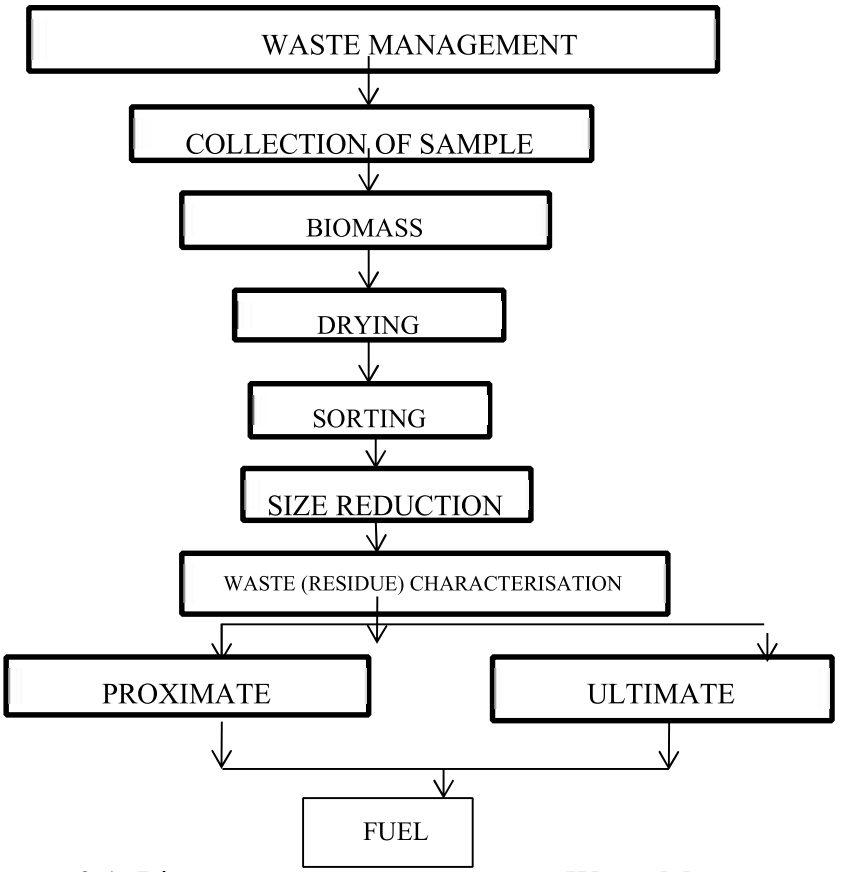


Figure: 3.1: Biomass Waste Management

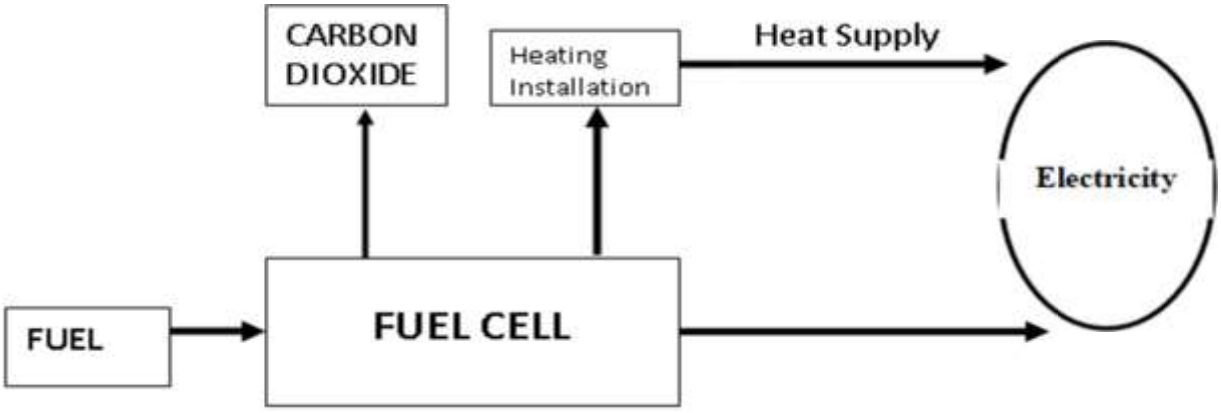


Figure 3.2: Direct Carbon Fuel Cell Operation

3.2 Material Preparation

Municipal solid waste was selected for this experiment. These Sample namely; was obtained from Trikania Kaduna, Kaduna state. The solid waste sorted in biodegradable and non-biodegradable.The biodegradable samples were sun dried for about a week and then sun dried to ensure homogeneity. Afterwards, size reduction was carried out by pounding with pestle and mortar . The pounded sample was further sieved with 500 μm (0.5mm) sieve. Putting of the sample in the sieve was done mechanically to aid effectiveness, uniformity and total recovery. The process was then repeated several times until the particles attained the desired sizes. There and then, it was sent to STEP-B Bosso campus FUTMinna, Niger state for pyrolysis and School of Agriculture Main campus, Gidan Kwano for characterization (Proximate and Ultimate).

3.2.1 Pyrolysis of solid waste samples

The samples were prepared and ready to be carbonized. The samples were dried in an oven for an hour at an operating temperature of 100 $^{o}$C. The dried sample was put into a hightemperature muffler furnace called the Carbolite RHF 600 after being placed in a crucible with nitrogen gas in order to purge the crucible containing the solid carbon from

oxygen. The furnace was heated to 500$^{o}$C for 30 minutes at a rising rate of 10$^{o}$C/min. After which the char was sieved using a 250 µm size mesh to obtain fine carbon particles.

Plate III :Pyrolyser

Plate IV: Sawdust

Plate V: Carbonized Sawdust

Plate VI: Sugarcane bagasse

Plate VII: Carbonized Sugarcane bagasse

Plate VIII: Orange peels

Plate IX: Carbonized Orange peel

### 3.2.2 Proximate analysis of biomass

The chemical composition of the biomass can only be determined through a close investigation. The four components of moisture content, fixed carbon, volatile matter, and ash are used to provide an analysis of the composition of the biomass. The fixed carbon is estimated by the difference.

3.2.2.1 Moisture content analysis

The amount of water in each sample was determined by the test analysis. A known-weight empty crucible was placed in a drying oven for 30 minutes to remove all traces of humidity. The new weight was recorded after cooling down in a desiccator. The sample was weighed down to 1g. The sample and crucible were placed in a drying oven for one hour. After reaching room temperature, the crucible and its contents were put in a desiccator to dry off. The observed weight after cooling was constant until it was less than 0

$$\text{.Moisture Content (\%)} = 100\ \frac{(W2- \quad)-(W3-W\ )}{(W2-W\ )}\ X\ 100 \qquad (3.1)$$

3.2.2.2 Ash content analysis

Following the previous weighing procedures, 1.0g of the dry test samples for each were measured, heated for 30 minutes at 750°C in a muffler furnace called the Carbolite RHF 1600, cooled to room temperature in a desiccator, and weighed. The process was repeated every hour until the weight remained steady. Using the following equation in grams (g),

$$\text{Ash Content (\%)} = \frac{(\text{Weight of ash})}{(\text{Initial weight of dried sample})}\ X\ 100 \qquad (3.2)$$

3.2.2.3 Volatiles content analysis

The sample's volatile matter content was calculated using the Meynell method. After weighing the empty crucible, The sample was heated for a further 5 minutes at 800C, Volatile Matter = Weight of residual dry sample before heating – weight of dry sample after heating

$$\text{Volatile Matter (\%)} = \frac{\qquad\qquad\qquad\qquad\qquad\qquad}{\qquad\qquad\qquad\qquad\qquad\qquad}\ X\ 100 \qquad (3.3)$$

3.2.2.4 Fixed carbon analysis

The fixed carbon analysis calculates how much biomass is still present after moisture, volatiles, and ash have been eliminated. The following relation was used to calculate the samples' fixed carbon content:

Fixed carbon content (%) = 100 – (moisture content + volatile matter + Ash content) (3.4)

3.2.3 Ultimate analysis

The fuel samples' components were found by an analyser in a platinum crucible. The sample was burned at a higher temperature in the atmosphere of oxygen, converting the carbon to carbon dioxide, the hydrogen to water, the sulphur to sulfuric dioxide, and the nitrogen to nitrogen two. An IR detector was used to detect the first three chemicals, while a thermal conductivity detector was used to measure $N_2$.

3.2.3.1 Carbon and hydrogen contents

The Big-Pregle Method was used to calculate the amounts of carbon and hydrogen. A gram of the sample was placed in a tube and burned to absorb carbon dioxide and magnesium to estimate the amount of carbon and hydrogen. The amount of water and carbon dioxide was calculated using the difference in weight before and after water absorption. The Hydrogen and Carbon (%) were evaluated thus as:

$$\%C = \frac{(\ .\ \ )}{\_\_\_\_\_} \times 100\% \quad (3.5)$$

While for Hydrogen content we have

$$\%H = \frac{(\ .\ \ )}{\_\_\_\_\_} \times 100\% \quad (3.6)$$

### 3.2.4 Calorific value (CV) determination

The calorific value is the amount of heat emitted by a specific biomass during complete combustion at standard pressure and reference temperature. The amount of heat released increases with the calorific content. The sample was analysed using a bomb calorimeter. The equation used to calculate the calorific value is given as:

$$\text{Calorific Value} = \frac{(\qquad)(\qquad)}{\qquad\qquad\qquad\qquad\qquad\qquad} \tag{3.6}$$

## 3.3 X-Ray Diffraction (XRD) Analysis

The sample is being examined with an X-ray beam. The atoms in a mineral are arranged according to the d-spacing, which is the precise spacing between the crystal lattices' stakes. When an X-ray beam passes through a sample of carbon, it produces peaks that are typical of each type of diffracted light along a set of planes, and the way these peaks are diffracted is indicative of how the atoms are arranged in the mineral. The powdered samples were sieved. A wide angle press was used to push the powder into an aluminum sample holder and rim after grouping the sample fraction of less than 2 micron carbon. Phillips P.W. 1011 goriometer connected to a recorder. The scanning took place between 2' and 40'. The time constant is 1' 20 cm/min. The diffractograms were interpreted using the reference conversion table to 20 to d-values.


Plate X : Rigaku D/Max-lllC X-ray diffractometer

## 3.4 SEM Analysis

The JOEL-JSM 7600F scanning electron microscope was used to capture the images. The samples were deposited on a sample holder with a carbon foil. The samples are covered with a metallic coating.

Plate XI : JOEL-JSM 7600F Scanning Electron Microscope

## 3.5 Preparation of Carbonate Electrolyte using a Mesh Wire

The electrolyte was prepared using molten hydroxide of Sodium and Potassium salt

(Adeniyi 2014). 9.5g of NaOH and 15.5g of KOH (i.e. 38 mol% of NaOH and 62 mol% of KOH) were measured and mixed together and later transferred to a stainless steel (Copper et al., 2008). The stainless steel was then place on a heating source, where it was been prepared. The mixture was immediately stirred continuously to ensure homogeneous mixture. Molten started at a temperature of $10^0$C and at $50^0$C, the molten carbonate has completely formed 25mm Aluminium wire mesh was saturated with the melted molten carbonate and upon cooling, the molten carbonate stick to the aluminum wire mesh and it was used as the electrolyte

Plate XII: Electrolyte preparation

Plate XIII: Electrolyte

3.6 Preparation of Carbon Fuel Particles

The carbon fuel particles used in the reaction were combined with the mixed hydroxide salt (15wt% of Biomass, 46.6wt% NaOH and 53.4wt% KOH). The fuel for the DCFC was created by combining the two salts with 4.5g biomass carbon particle to form the fuel for the DCFC (Adeniyi, 2014).

Plate XIV: Carbon Fuel mixed with hydroxide salts

3.7 Design and Assembling of the DCFC

A 20mm ceramic tube was used to make the anode and cathode. This helps with heat retention and temperature control. The aluminium mesh wire was 25mm in diameter and saturated at 60 $^{0}$C. The ceramic tubes were connected to the copper wires with crystal beads used as current collectors. The hot plate was the heat source. (Adeniyi,2014; Copper,2008).

Plate XV: Fuel cell

Plate XVI: Electrode for Conduction

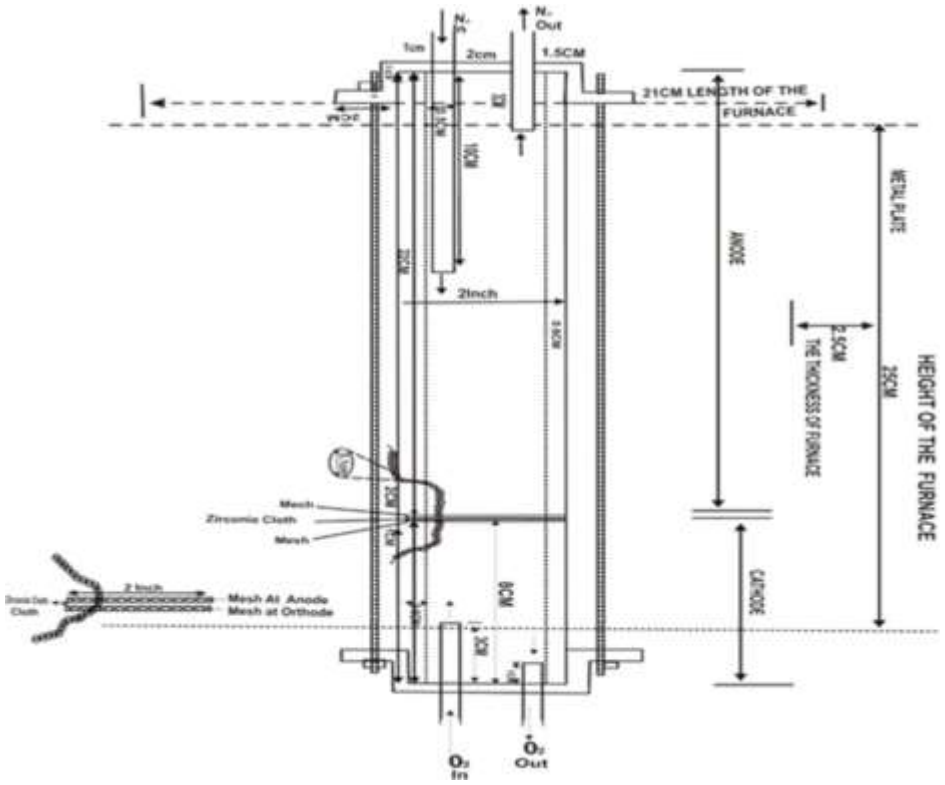


Figure 3.3: Design of the DCFC (Adeniyi,2014)

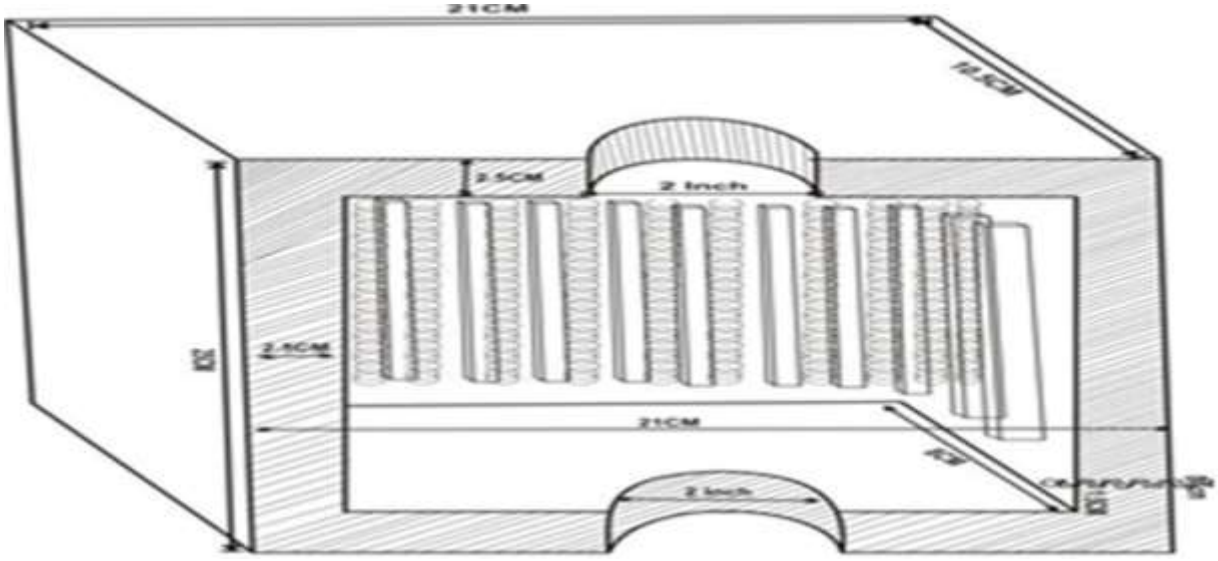

Figure 3.4: Design of furnace

Plate XVII : MHDCFC Operation

# CHAPTER FOUR

## 4.0 RESULTS AND DISCUSSION

The Water Resources and Fishery Technology Laboratory located at the University of Technology Minna. The Thermal Treatment Laboratory of the Chemical Engineering Complex of the Federal University of Technology, Minna investigated the fuel performance of the Molten Hydroxide Direct Carbon Fuel Cell.

### 4.1 Thermo-Gravimetric Analysis

The result of the Thermo-Gravimetric analysis involves the Proximate Analysis and it is represented in Table 4.1.

Table 4.1: Proximate analysis of municipal solid waste (MSW)

| Sample Description | Moisture Content (wt%) | Ash Content (wt%) | Volatile Matter (wt%) | Fixed Carbon (wt%) |
|---|---|---|---|---|
| Saw Dust | 2.17 | 5.23 | 71.83 | 20.77 |
| Sugarcane bagasse | 3.60 | 2.10 | 67.00 | 27.30 |
| Orange Peel | 1.56 | 3.24 | 72.60 | 22.60 |
| MSW | 1.36 | 3.57 | 65.10 | 29.97 |

Table 4.2: Ultimate analysis of municipal solid waste (MSW)

| Sample Description | C (wt%) | H (wt%) | O (wt%) | N (wt%) | S (wt%) |
|---|---|---|---|---|---|
| Saw Dust | 50.91 | 3.43 | 44.24 | 0.26 | 0.16 |
| Sugarcane bagasse | 48.73 | 4.98 | 45.20 | 0.83 | 0,22 |
| Orange Peel | 40.20 | 4.80 | 35.50 | 0.38 | 0.21 |

| | | | | | |
|---|---|---|---|---|---|
| MSW | 58.40 | 6.60 | 34.00 | 0.72 | 0.28 |

Table 4.1 provides the results of the thermogravimetric (proximate ) analysis performed on the samples indicating the properties of the fuel source which is an important check for the suitable fuel for use in the direct carbon fuel cell DCFC. The resulting sawdust has a moisture content of 2.17 wt%, an ash content of 5.23 wt%, and a volatile matter content of 71.83 wt%, respectively. The obtained sugarcane bagasse sample has the following matching moisture, ash, and volatile matter contents: 3.60 wt%, 2.10 wt%, and 67.00 wt% .Orange peel percentages were 1.56wt%, 3.24wt%, and 72.60wt%.

The MSW's equivalent moisture, ash, and volatile matter contents were 1.36 wt%, 3.57 wt %, and 65.10 wt% respectively. According to Table 4.2, the MSW sample had a high carbon content of 58.40 wt%, which is higher than the carbon contents of sawdust, orange peel, and sugarcane bagasse. It is a better fuel for the DCFC due to the MSW sample's high carbon concentration and low moisture content.

### 4.1.1 Calorific value

The calorific value is important in the design of a DCFC because it establishes the amount of heat produced when a unit quantity of fuel is burned. The calorific values of the proposed fuel obtained are:

Table: 4.3: Calorific value of the carbon samples

| S/No | Sample Description | Calorific Value (MJ/Kg) | LHV (MJ/Kg) | HHV (MJ/Kg) |
|---|---|---|---|---|
| 1 | Sawdust | 7.0 | 5.66 | 6.79 |
| 2 | Sugarcane bagasse | 6.7 | 8.27 | 9.78 |
| 3 | Orange peel | 5.8 | 6.30 | 7.63 |

| | | | | |
|---|---|---|---|---|
| 4 | MSW | 7.9 | 9.54 | 11.00 |

## 4.2 XRD Analysis Result

The method of analyzing the phase in solid materials is called XRD. Material reactivity is influenced by its phase composition and can be measured using XRD. The total composition is divided into two parts. The area under the sharply resolved peaks and the remaining area under the curve above ground are the intensities of diffracted beam. it was investigated using the X-ray diffraction analysis. This was done after the carbonized sample was obtained. The result is presented in Figure 4.1 to 4.4. The X-ray diffractometer system and the value points were obtained using different methods. The basis for comparison for the carbon samples to be used in the fuel cell can be found in the pattern of the goriometer. and it has been agreed by several researcher.

### 4.2.1 XRD for sawdust

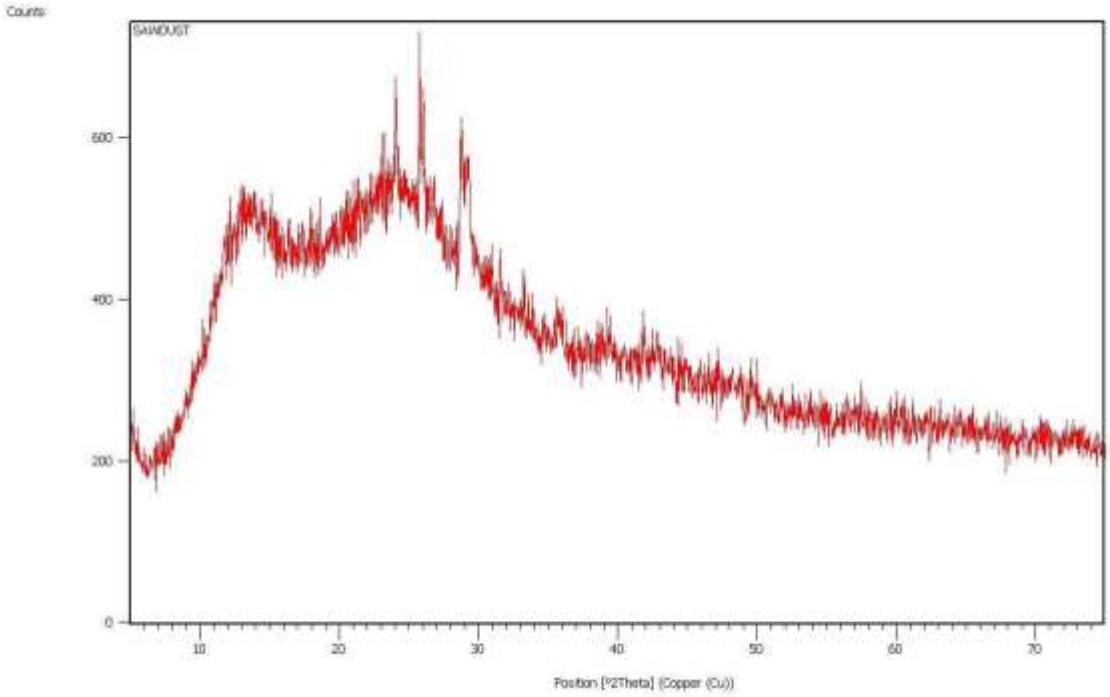


Figure 4.1: X-ray Diffraction Pattern for Sawdust Carbon

Figure 4.1, the X-ray pattern, shows how a broad diffraction feature manifests in the 2theta range of, say, 10-60$^{o}$ for sawdust. For carbon materials, the peak at 2Θ = 20-30$^{o}$ can be attributed to (002) reflection, while the one at 2Θ = 40-50$^{o}$ can be attributed to (100) reflection. The tallest peak in the picture has a relative intensity of 100% compared to the 2.9850Å obtained for miscanthus carbon (Adeniyi, 2014). A corresponding d-spacing of 3.45867Å, and an angle of 25.7588$^{o}$ (2Θ-axis). In turn, this exhibits a high value that denotes a high degree of unit cell size and reactive sites. The outcome reveals a copper content structure that is disorganized.

4.2.2 XRD for Sugarcane Bagasse

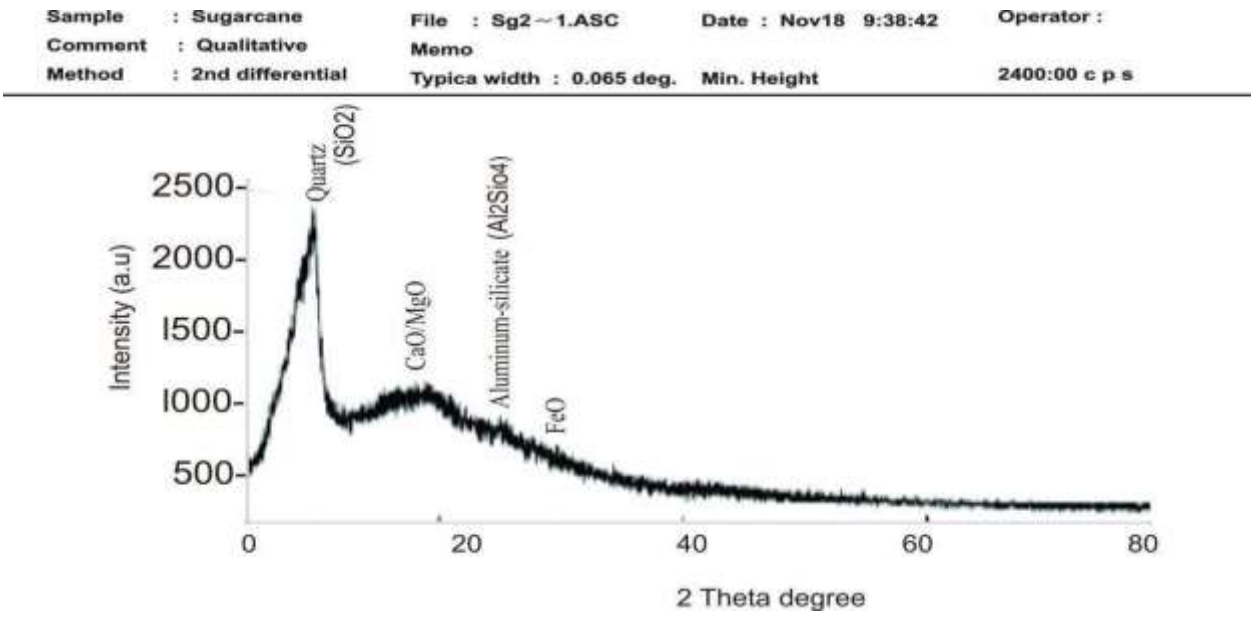


Figure 4.2: X-ray Diffraction Pattern for Sugarcane Bagasse Carbon

4.2.3 XRD for orange peel

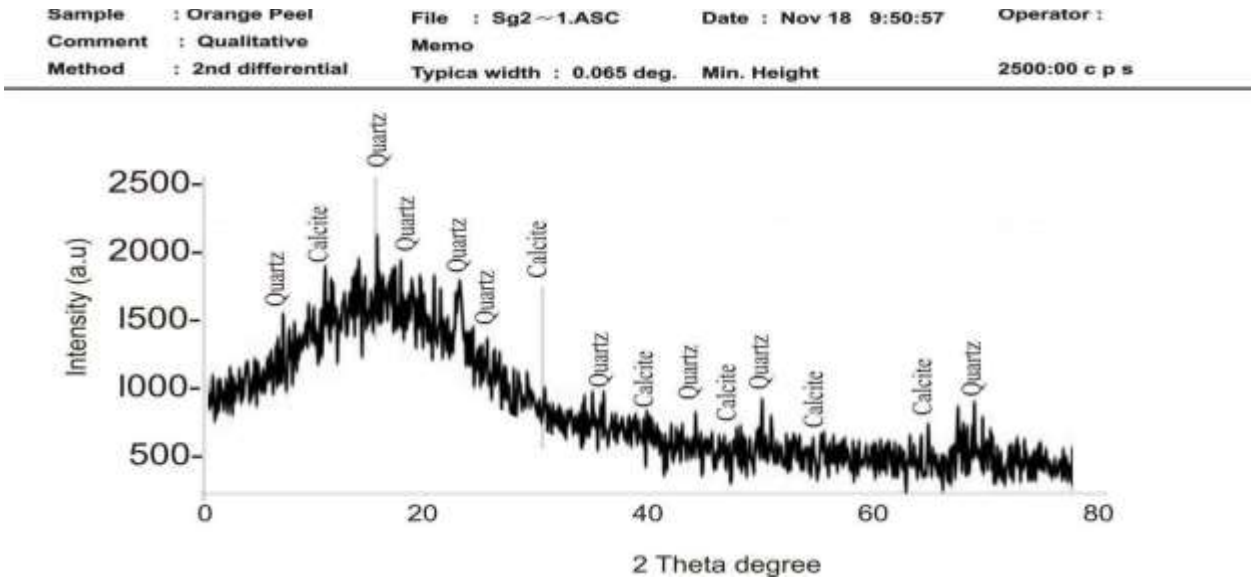


Figure 4.3: X-ray Diffraction Pattern for Orange Peel Carbon

According to Figures 4.2 and 4.3, the maximum peak in Figure 4.2 has a relative intensity of 100% and is located at angles of 26.637º and 26.24º (2Ɵ-axis) for orange peel carbon fuel and sugarcane bagasse, respectively. The corresponding d-spacing is 3.34Å. The large unit cell size and potential reactive sites within the carbon atom are indicated by this. The outcome demonstrates the level of disordered graphite content, which is a crucial component for carbon oxidation, and the strong peaks highlight the presence of silica, oxygen, The peak at 26.637º correspond to quartz crystalline $SiO_2$( Kacprzak, 2017) and the other peaks are for the impurities present.

4.2.4 XRD for municipal solid waste (MSW)

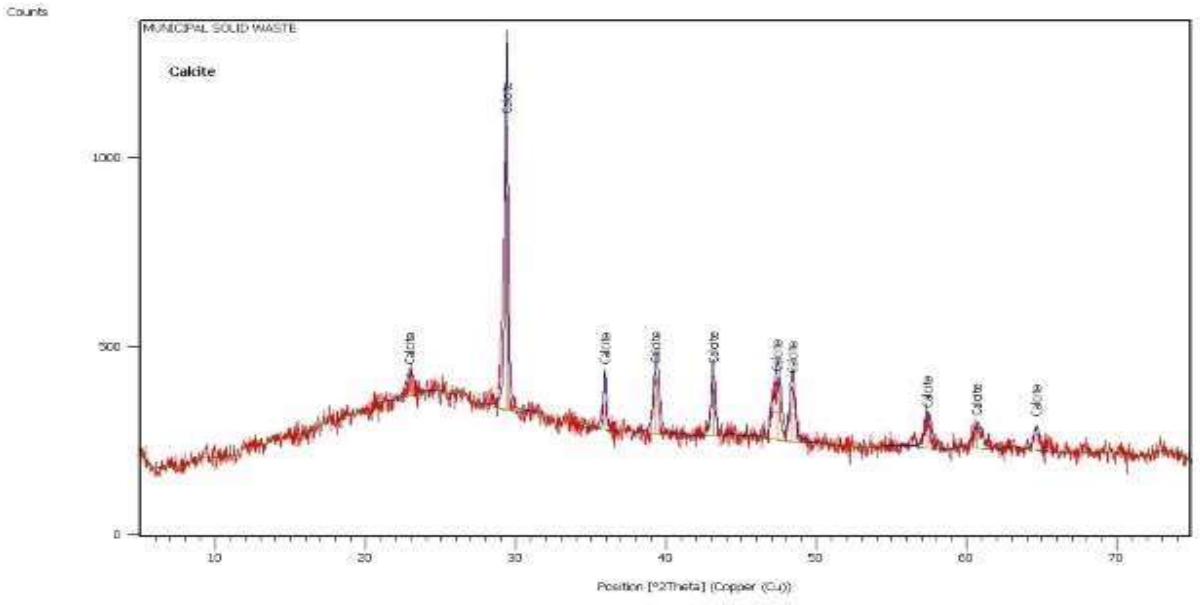

Figure 4.4: X-ray Diffraction Pattern for MSW Carbon

XRD data for MSW is shown in figure 4.4. The crystallographic parameters are the R-3C and 167 space group number of the rhombohedral calcite crystal system. Four distinct peaks can be seen in the data at (2Ɵ) values of 24º, 29.5º, and 58.5º. Peak 58.5º is in the amorphous region, whereas the others are in the crystal region.

## 4.3 SEM/EDX Analysis

At the surface of the solid sample, the SEM produces a variety of signals using a focussed stream of high energy electrons. The signals that result from electron sample interaction provide details about the sample, such as its crystalline structure, chemical content, and texture. The elemental makeup of the fuel samples is visible on the EDX.

### 4.3.1 The morphological analysis of carbonized sawdust

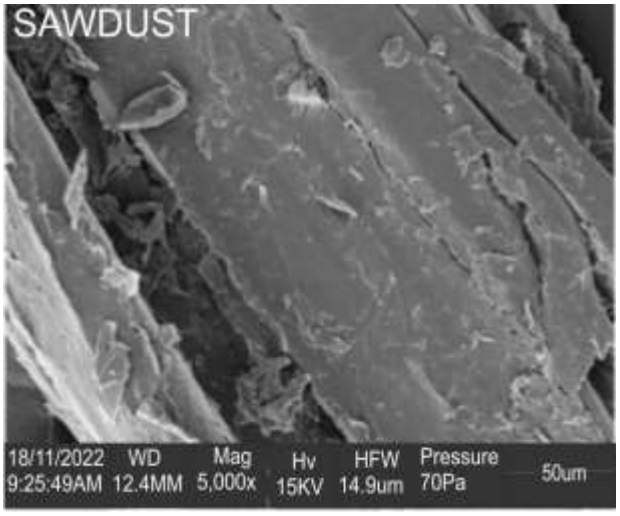


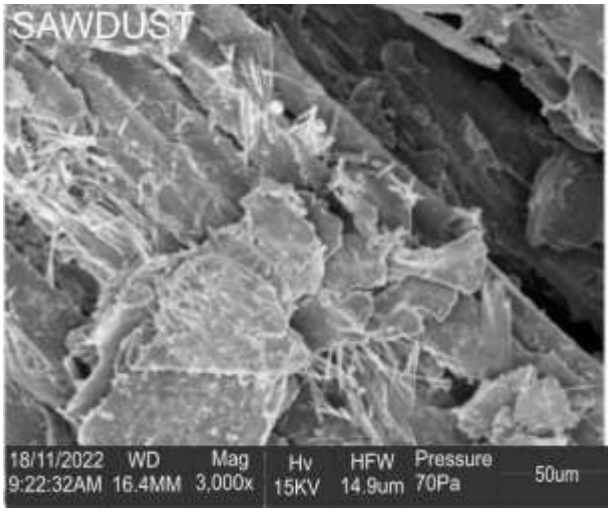

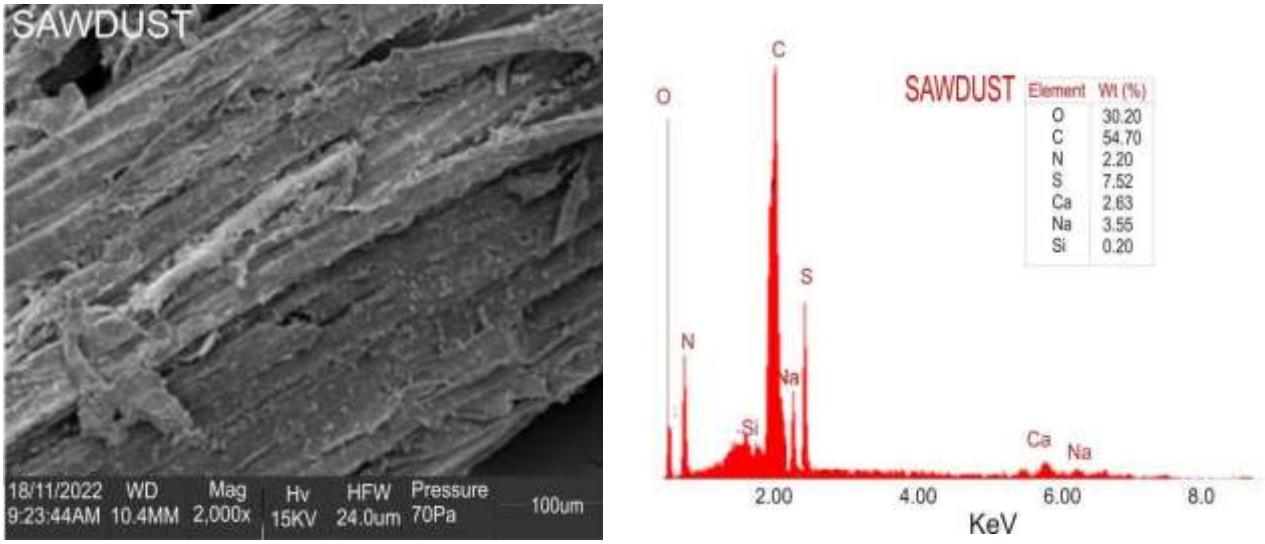


Figure 4.5: SEM/EDX of Sawdust Carbon at $5000_x$,$3000_x$ and $2000_x$ Magnification

The morphological structure of carbonized sawdust at 450 $^oC$ under magnifications of 5000, 3000, and 2000 is shown in Figure 4.5. The SEM micrograph shows that sawdust has a nonuniform but well-developed pore structure and is particularly rich in small particles. These characteristics might be a result of surface area since as porosity rises, so does surface area. The fuel sample's elemental makeup is displayed by the EDX. The weight percentages of C, O, N, S, Ca, Na, and Si in the sawdust are 54.70%, 30.20%,

2.20%, 7.52%, 2.63%, 3.55%, and 0.20% respectively.

4.3.2 The morphological analysis of carbonized sugarcane bagasse

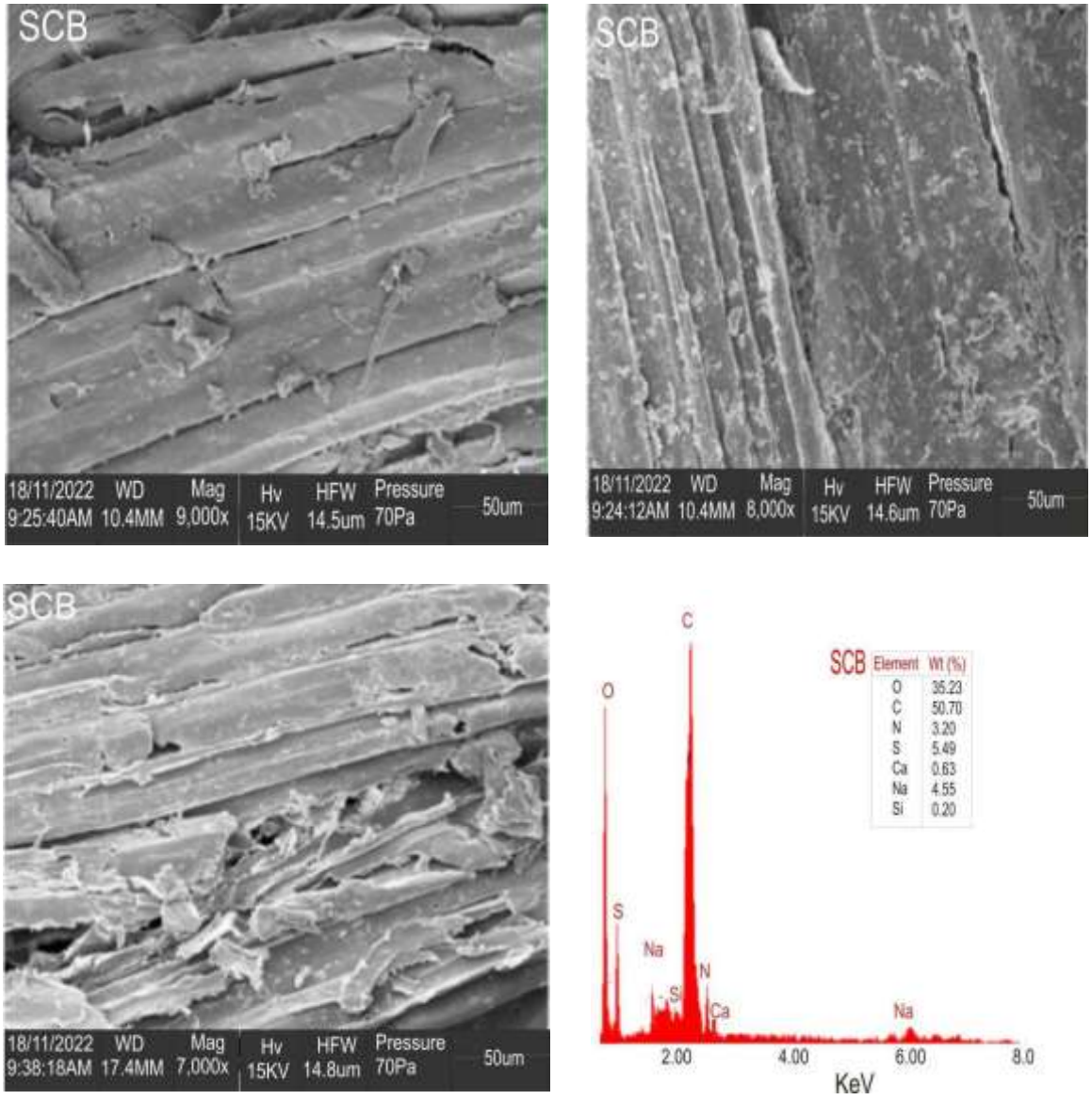


Figure 4.6: SEM/EDX of Sugarcane Bagasse Carbon at $9000_x$,$8000_x$ and $7000_x$ Magnification.

The morphological structure of carbonized sugarcane bagasse at 500°C with magnifications of 9000, 8000, and 7000 times is shown in Figure 4.6. Instead of disconnected particles with an uneven and rough surface, the SEM micrograph of sugarcane bagasse reveals the existence of smaller particles that seem to be a well-bonded aggregate. Too much magnification and an incorrect accelerating voltage setting may be to

blame for the roughness. The components of sugarcane bagasse are C, O, N, S, Ca, Na, and Si, with weight percentages of 50.70%, 35.23%, 3.20%, 5.49%, 0.63%, 4.55%, and 0.20%, respectively.

4.3.3 The morphological analysis of carbonized orange peel.

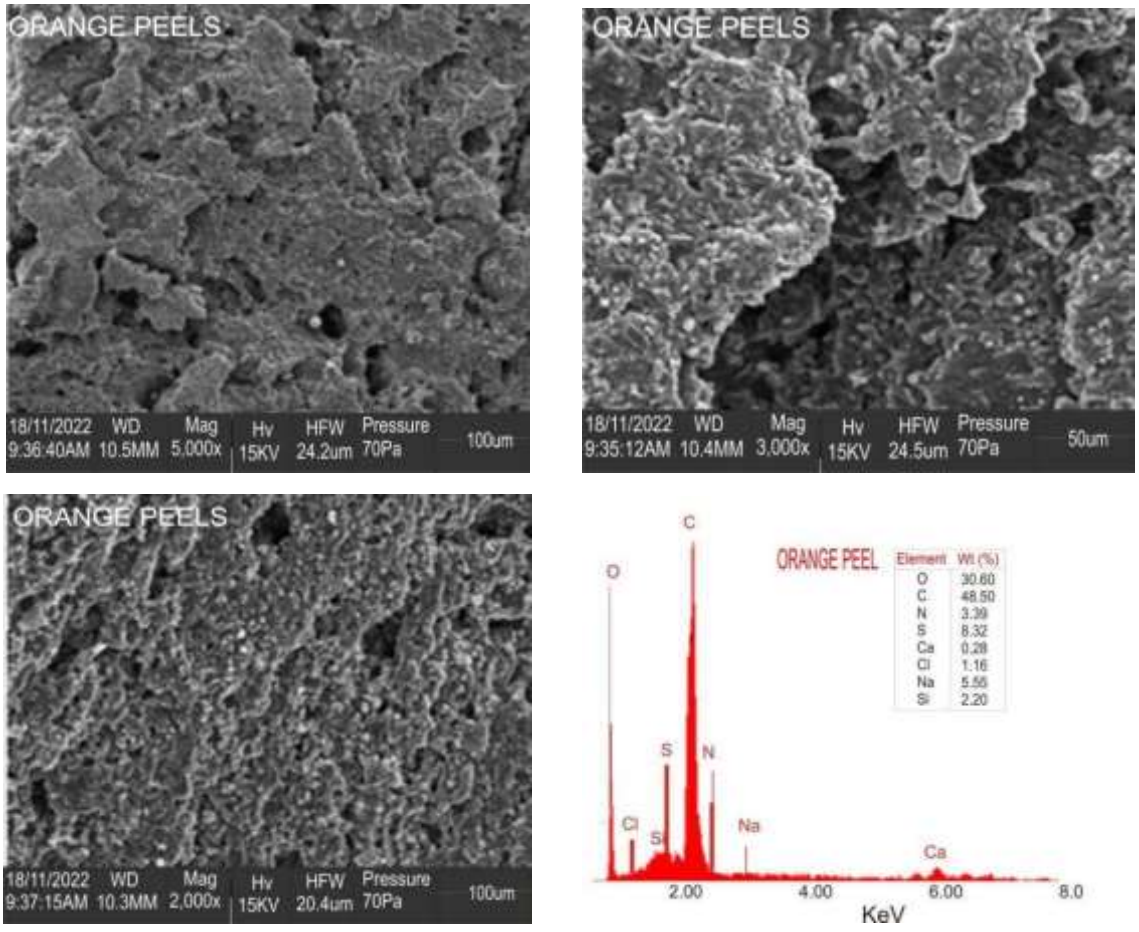


Figure 4.7 SEM/EDX of Orange Peel Carbon at $5000_x$,$3000_x$ and $2000_x$ Magnification.

The morphological structure of carbonized orange peel at 500 $^oC$ under magnifications of 5000, 3000, and 2000 is shown in Figure 4.7.According to the SEM micrograph, orange peel is extremely rich in small, irregularly shaped particles with little to no pore development. These characteristics might be a result of surface area since as porosity rises,

so does surface area. The fuel sample's elemental makeup is displayed by the EDX. The weight percentages of C, O, N, S, Ca, Na, and Si in the sawdust are respectively 48.5%, 30.60%, 3.39%, 8.32%, 0.28%, 5.56%, and 2.20%.

4.3.4 The morphological analysis of carbonized municipal solid waste (MSW).

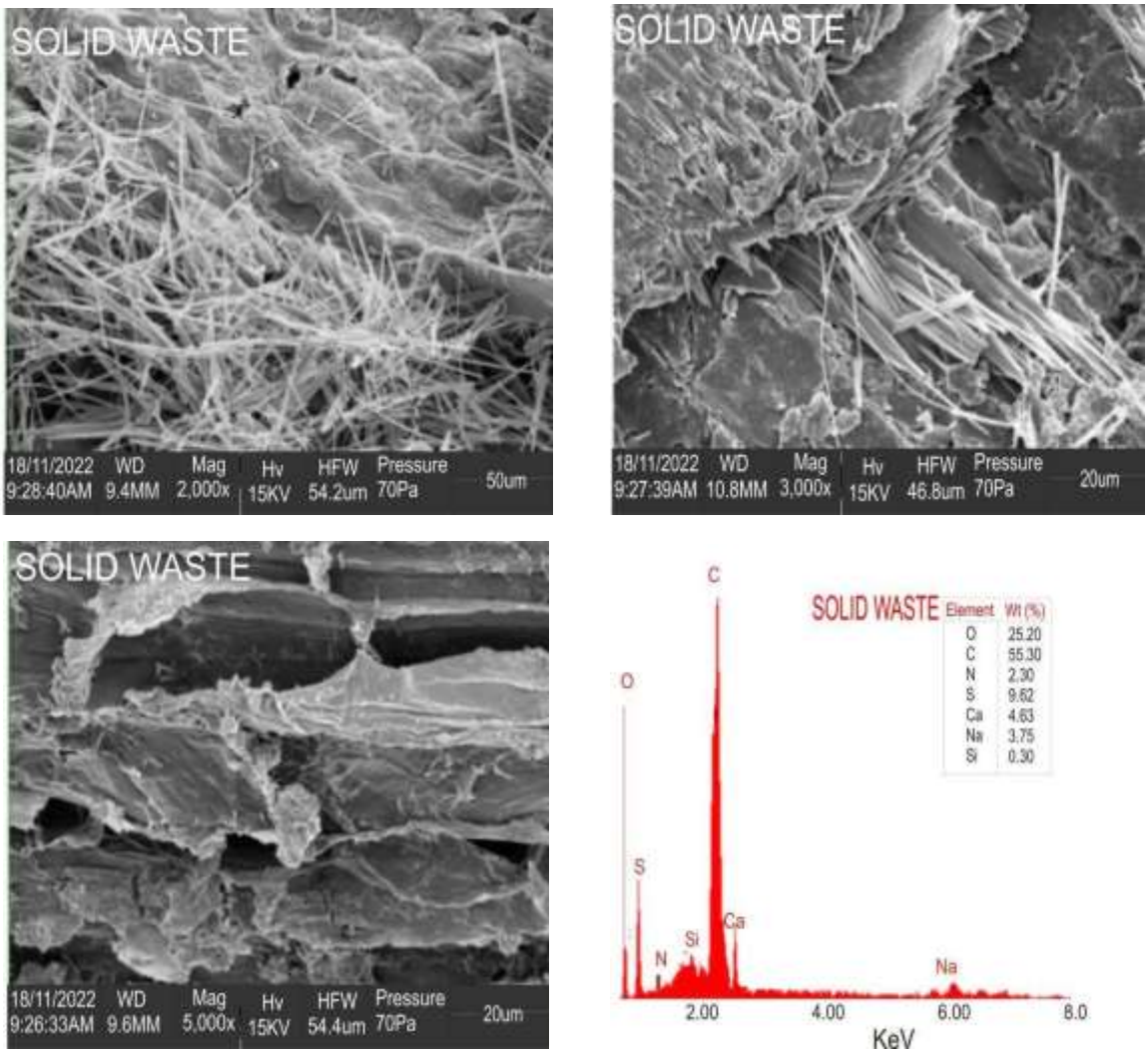


Figure 4.8 SEM/EDX of MSW carbon at $5000_x$,$3000_x$ and $2000_x$ Magnification.

The morphological structure of carbonized sawdust at 500oC under magnifications of 5000, 3000, and 2000 is shown in Figure 4.8. The SEM micrograph shows that MSW has a highly developed pore structure and is exceptionally rich in tiny particles. These characteristics might be a result of surface area since as porosity rises, so does surface area.

The fuel sample's elemental makeup is displayed by the EDX. The weight percentages of C, O, N, S, Ca, Na, and Si in the sawdust are respectively 55.30%, 25.20%, 2.30, 9.62%, 4.63%, 3.75%, and 0.30%.

## 4.4 Voltage from MHDCFC Using Various Fuel

For the purpose of this research analysis, the fuels that was used are listed below and their voltage readings are analysed.

(i) Saw dust

(ii) Sugarcane bagase

(iii) Orange peel

(iv) MSW (Sawdust, Orange peel and Sugarcane bagasse)

### 4.4.1 Voltage from MHDCFC using sawdust as fuel

The Molten Hydroxide Direct Carbon Fuel Cell (MHDCFC) experiment was conducted at temperatures ranging from 50°C to 350°C, 150 $cm^3$/min for oxygen and 200 $cm^3$/min for nitrogen, respectively. However, the large increase that was observed from 50$^o$C to 200$^o$C can be linked to electron mobility that aids in the transmission of electricity. As the temperature increased from 50 to 200$^o$C, it shows that there was an increase in voltage and the cell resistance decreased. Another explanation is that the salt melted quickly at 200$^o$C, producing the greatest voltage of 0.44 V, and that when temperature rises further, the voltage falls due to activation loss. At this temperature, the cell's carbon fuel is used more quickly and the hydroxide is effectively decomposed. Low OCV (0.44 V) may be caused by extremely high volatile matter (71.83 wt%) and ash content (5.23 wt%) levels.

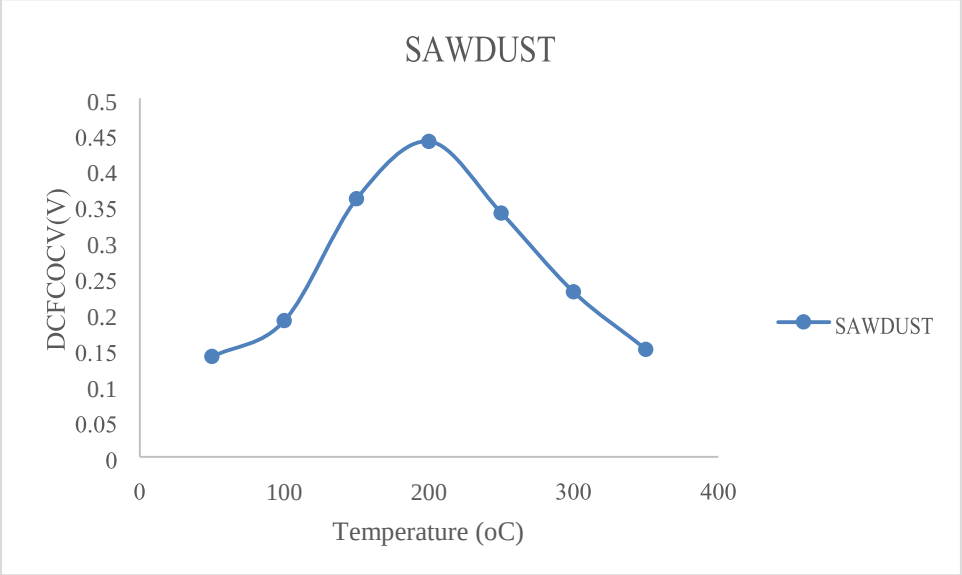


Figure 4.9: MHDCFC OCV at varying Temperature using Sawdust Carbon

### 4.4.2 Voltage from MHDCFC using sugarcane bagasse as fuel

With a peak voltage reading of 0.39 V and gas flow rates of 150 $cm^3$/min for $O_2$ and 200 $cm^3$/min for $N_2$, respectively, Figure 4.10 illustrates the OCV obtained utilizing carbon derived from sugarcane bagasse as fuel from 50$^oC$ gradually to an operating temperature of 200$^oC$. At temperatures exceeding 200 $^oC$, the voltage started to decrease until it reached 0.11 V at 350 $^oC$ operating temperature. there was an immediate rise in voltage. However, as the temperature exceeded 200 $^oC$, the voltage started to fall because of activation polarization, which is caused by mass transportation and hydroxide breakdown.

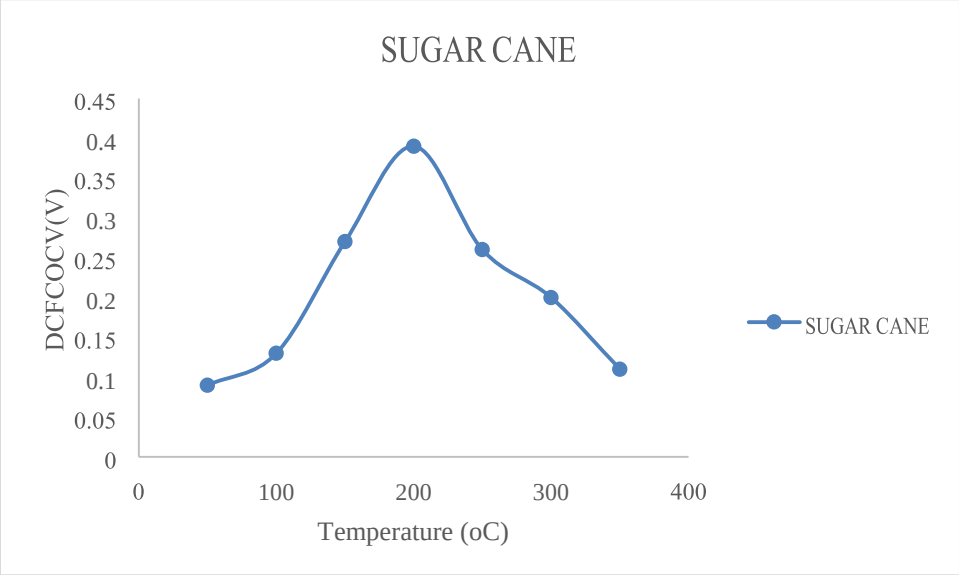


Figure 4.10: MHDCFC OCV at varying Temperature using Sugarcane Bagasse Carbon

### 4.4.3 Voltage from MHDCFC using Orange peel as fuel

With a peak voltage reading of 0.37 V and gas flow rates of 150 $cm^3$/min for $O_2$ and 200 $cm^3$/min for $N_2$, respectively, Figure 4.11 depicts the OCV achieved utilizing carbon derived from orange peel as fuel from 50$^oC$ repeatedly to a working temperature of 200$^oC$. The voltage increased as the temperature rose and the cell resistance decreased, but beyond 200 $^oC$ the voltage started to fall due to activation polarization, which is brought on by mass transportation and the breakdown of hydroxide carbon fuel.

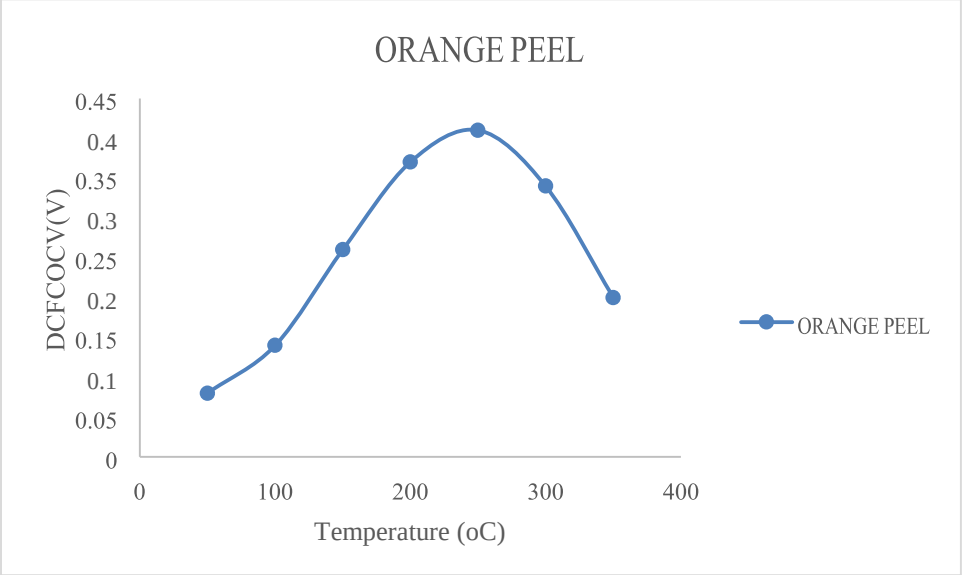


Figure 4.11: MHDCFC OCV at varying Temperature using Orange Peel Carbon 4.4.4 Voltage from MHDCFC using municipal solid waste as fuel

The MHDCFC operation of the mixture of sawdust-derived carbon black, sugarcane bagasse, and discarded orange peel with the hydroxide salt as fuel reveals the voltage profile at various temperatures in Figure 4.12. The outcome shown in Figure 4.12 is superior to that shown in Figures 4.9, 4.10, and 4.11. With a high value voltage reading of 0.65 V at 250$^{o}$C and a steady rise in temperature, this demonstrates an increased OCV for the cell. The voltage achieved will vary little decrease with a slight rise in the cell's temperature. In the MHDCFC, the combination of the three biomasses as fuel resulted in a greater OCV rating than the fuel's individual carbon.

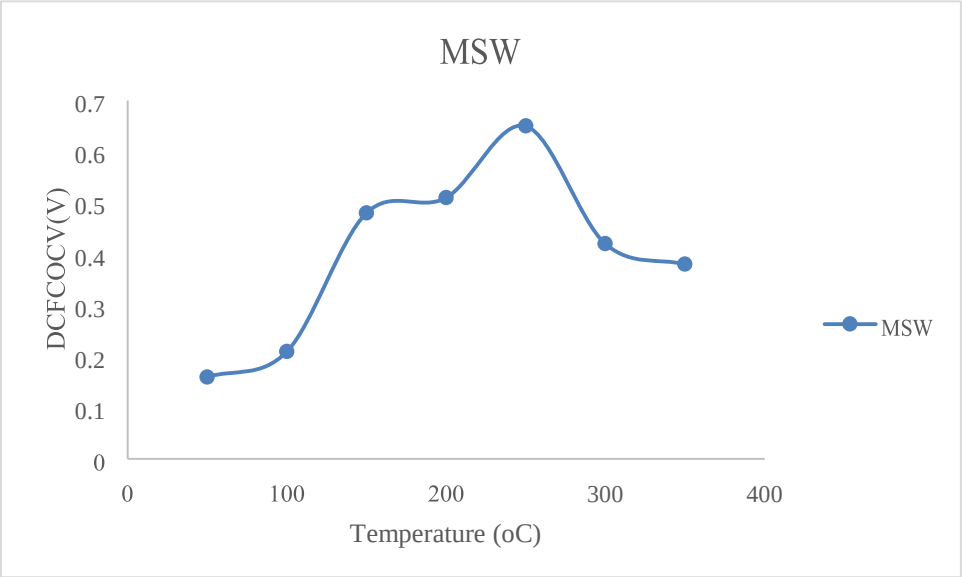


Figure 4.12: MHDCFC OCV at varying Temperature using MSW Carbon

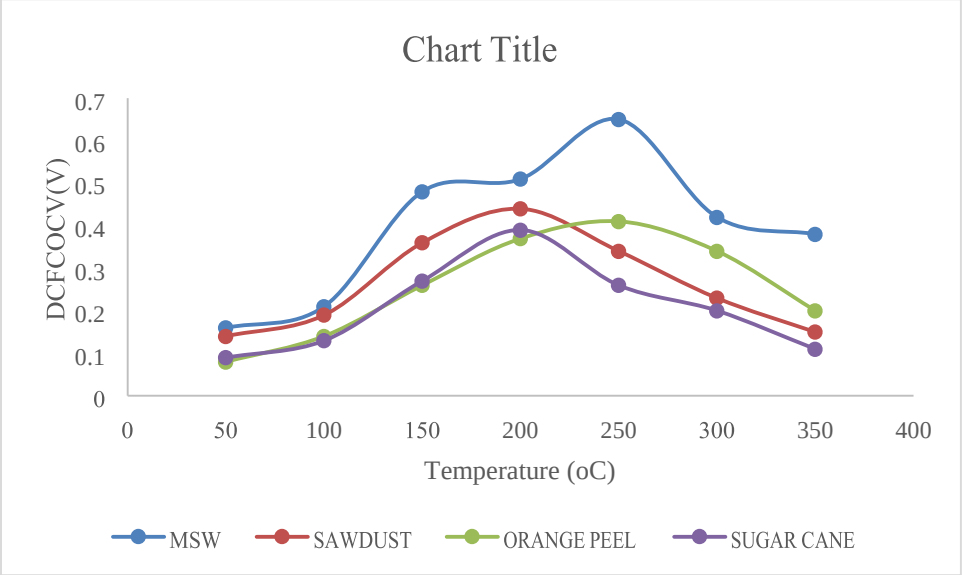


Figure 4.13: OCV Profile of the Three Bio-mass Carbon Fuel at Different Temperature

The voltage (OCV) obtained utilizing the three biomasses as fuel for the MHDCFC operation is shown in Figure 4.13. The maximum voltage was produced by the MSW (Sawdust, Orange peel, and Sugarcane Bagasse), and the lowest was produced by orange peel waste (0.0.37 V). Sawdust had the second-highest voltage value of 0.44 V, followed by sugarcane bagasse at 0.39 V. The carbon samples were made with a mixture of two

hydroxide salts (potassium and sodium), the salts were saturated using a wire mesh, and the salts were employed as the electrolyte during the fuel cell operation. It is simple to infer that when the temperature rises, the voltage rises and the internal resistance falls. The acquired carbon samples, including MSW, exhibit nearly identical patterns of voltage production. ( Adeniyi 2014), the melting of the hydroxide salt, carbonate breakdown, and ionic conduction in the phase of the molten hydroxide caused a noticeable increase in the open circuit voltage at a temperature range between 50 and 200 $^{o}$C, the fuel cell performance was found to be improved at 200 $^{o}$C.. (Adeniyi, 2012; Cherepy et al., 2005).

### 4.4.5 DCFC performance using sawdust waste as fuel

At various temperatures and with changing resistor loads, the electrochemical performance was assessed. The results of the MHDCFC using sawdust carbon particle fuel, With a current density of 7.6 mA/cm$^2$, the highest voltage reading (0.19 V) at 100 $^{o}$C was attained. A voltage of 0.36 V and a current density of 14.4 mA/cm$^2$ were measured at 150 °C. 17.6 mA/cm$^2$, 0.44 V was produced for 200$^{o}$C. Maximum current density was 26.0 mA/cm$^2$ at 250 $^{o}$C, and voltage was 0.65 V. Because the peak voltages were all measured with a 1 resistor load supplied to the cell, there was a tiny decrease in the individual voltage at every temperature. The voltage dropped and the current density followed as the resistor load grew. In the current investigation, the midpoint of the current density-voltage curve declined because of activation resistance, which also causes activation polarization losses or even voltage drop in the cell. This is as a result of how slowly the reactions occurred on the electrode surface, and the ions over the electrolyte is known as ohmic losses or voltage drop, which is caused by the ohmic resistance. The ohmic resistance of the fuel cell causes the curves to continue to decline linearly. Mass transportation and concentration losses are

to blame for this. (Larminie and Dicks,2003; Cherepy et al., 2005; Hoogers, 2003). According to Figure 4.5, the fuel sample contains 54.70 weight percent carbon, 30.20 weight percent oxygen, 2.63 weight percent calcium, and 0.20 weight percent silicon. After these elements were oxidized, the MHDCFC's performance improved, but it was still significantly less due to the fuel's low proportion of key constituent elements. (C, O, Ca and Si).

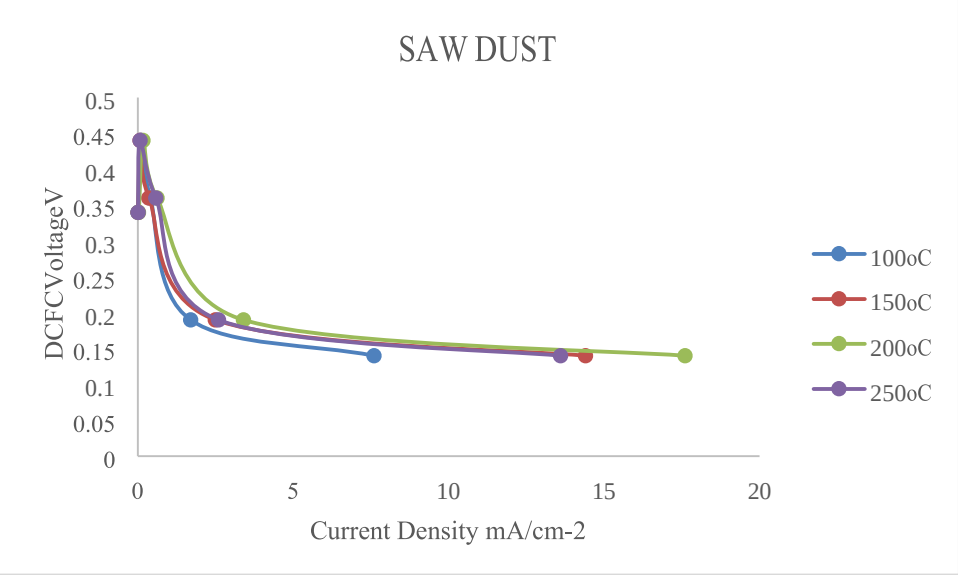


Figure 4.14: Graph of DCFC Voltage against Current Density for Sawdust

It can be seen from Figure 4.15 that power density and current density both rise with temperature. At 100 $^{o}$C, the maximum power density was 1.44 mW/cm$^2$, while the maximum current density was 14.4 mA/cm$^2$, while the maximum power density was 5.2 mW/cm$^2$ and the maximum efficiency was 25% at 150 $^{o}$C. Maximum current density at 200 °C is 17.6 mA/cm$^2$, while maximum power density is 7.7 mW/cm$^2$. The power density was subsequently observed to decrease with increasing current density, and it was discovered that the change in temperature profile had a significant impact on these values.

Maximum current density at 250 °C was 13.6 mA/cm$^2$, and power density was 4.6 mW/cm$^2$, which is lower than the 127 mW/cm$^2$ (Elleuch et al 2013) for almond shell. The range of resistor loads employed for the various fuels could be the cause of the variation.

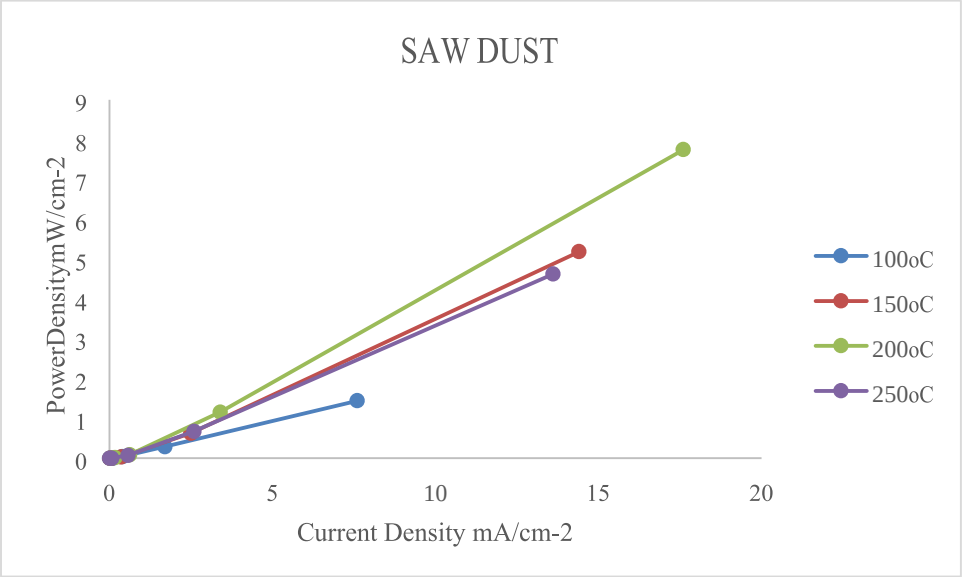


Figure 4.15: Graph of Power density against Current density for Sawdust The evaluation of the molten hydroxide direct carbon fuel cell for the four temperature profiles is summarized in Figure 4.16. The temperature for the current and power density is represented by 100C and 100P, and the same holds true for the remaining temperatures. (Adeniyi 2012),

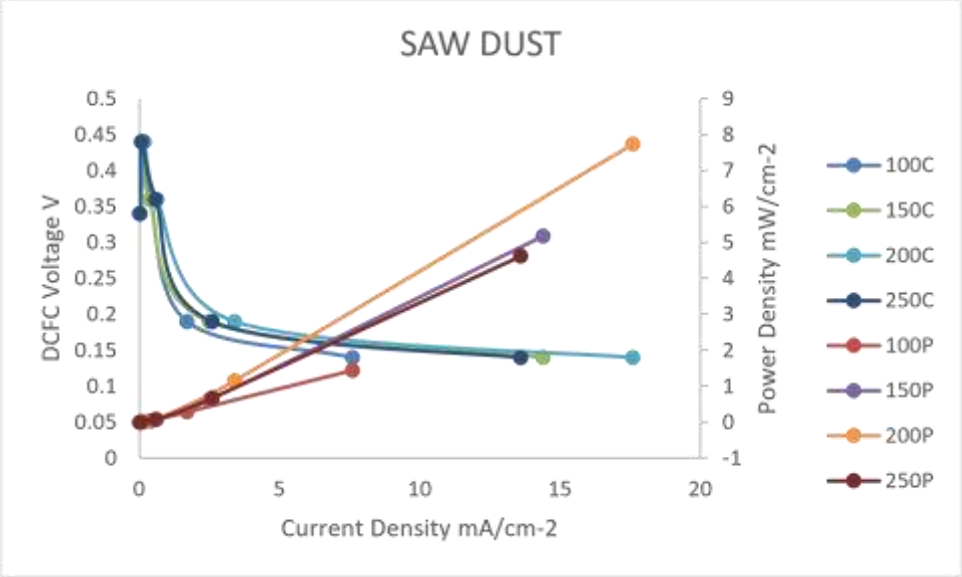


Figure 4.16: Overall Graph of Voltage against Current density and Power density for Sawdust

### 4.4.6 DCFC performance using orange peel waste as fuel

The findings of the MHDCFC for the fuel of orange peel carbon particle densities. With a current density of 5.6 mA/cm$^2$, the highest voltage reading (0.14 V) at 100 $^o$C was attained. A voltage of 0.26 V and a current density of 10.4 mA/cm$^2$ are present at 150 °C. With a current density of 14.8 mA/cm$^2$, 0.37 V was produced for 200$^o$C. At 250 $^o$C, there was a voltage of 0.41 V and a maximum current density of 16.4 mA/cm$^2$. Due to the fact that the peak voltages were all measured with a 1 resistor load connected to the cell, there was a little decrease in the individual voltage at every temperature. The voltage dropped as the resistor load grew, and the current density followed. In the current investigation, the midpoint of the current density-voltage curve declined because of activation resistance, which also causes activation polarization losses or even voltage drop in the cell. This is as a result of how slowly the reactions occurred on the electrode surface. The process of enabling the chemical reaction that moves electrons to and from the electrode results in the loss of some of the voltage generated. Ohmic losses or voltage drop, which are the

resistance to the flow of electrons through the material of the electrodes and the various interconnections and the ions through the electrolyte, are caused by the ohmic resistance. The curves continue to decrease linearly due to the ohmic resistance of the fuel cell. (Hoogers, 2003). The fuel sample in Figure 4.7 contains 48.50 wt% carbon, 30.60 wt% oxygen, 0.2 wt% calcium, and 2.2 wt% silicon. After these elements were oxidized, the fuel's performance improved, but it was still very subpar compared to the performance of the sawdust sample fuel.

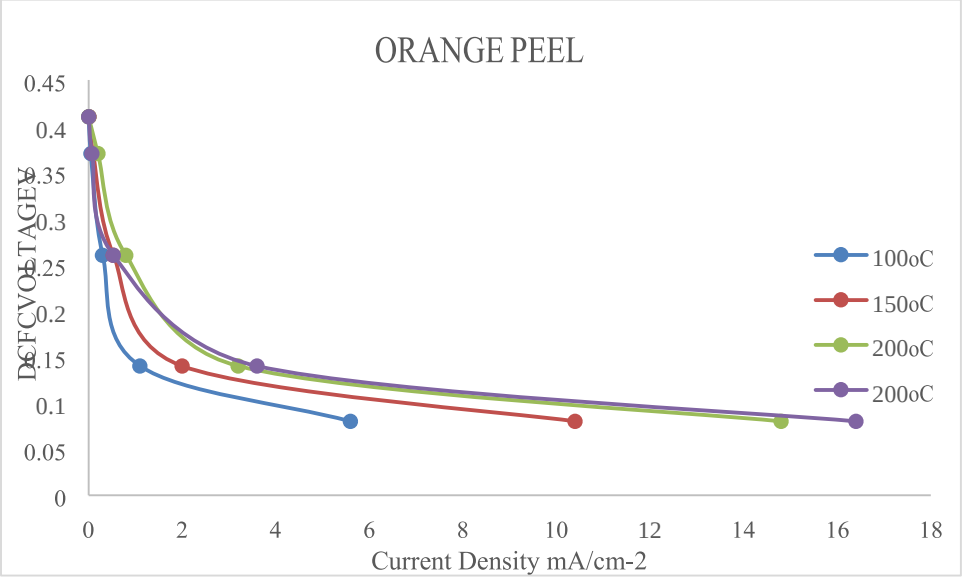


Figure 4.17: Graph of DCFC Voltage against Current density for Orange Peel It can be seen from Figure 4.18 that power density and current density both rise with temperature. Maximum power density was 0.784 mW/cm$^2$ at 100 °C, maximum current density was 10.4 mA/cm$^2$ at 150 °C, maximum current density was 14.8 mA/cm$^2$ at 200 °C, and maximum efficiency was 18%. Maximum power density was 2.704 mW/cm$^2$ at 100 °C, maximum efficiency was 5.60 mA/cm$^2$, and maximum efficiency was 10%. The power density decreased as the current density increased, and it was then discovered that the temperature profile shift had a significant impact on these numbers. With a power

density of 2.296 mW/cm$^2$, the maximum current density measured at 250 $^oC$ was higher than the 127 mW/cm$^2$ recorded for almond shell (Elleuch et al. 2013). The range of resistor loads employed for the various fuels could be the cause of the variation.

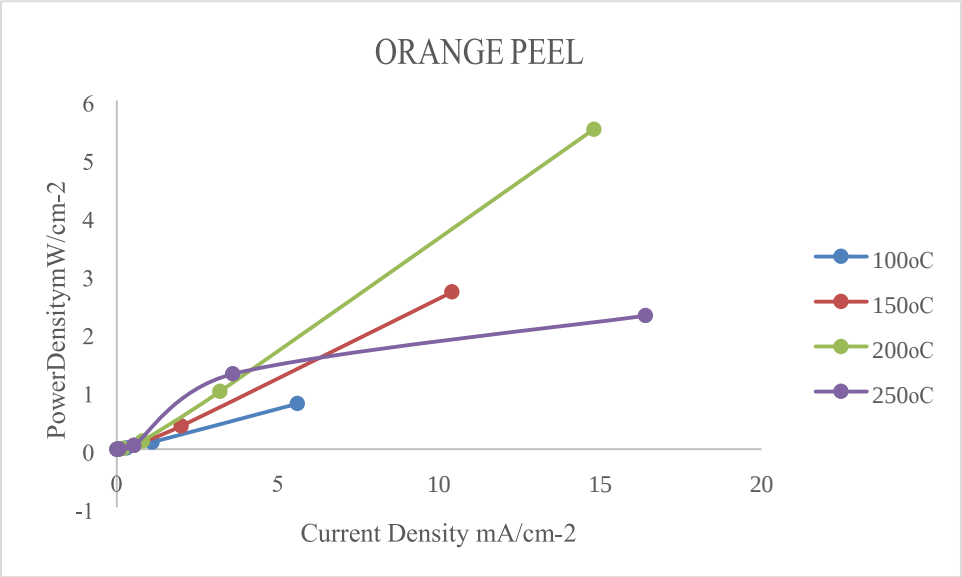


Figure 4.18: Graph of Power density against Current density for Orange Peel

The overall evaluation of molten hydroxide direct carbon fuel cells for the four temperature profiles is summarized in Figure 4.19. The temperature for the current and power density is represented by 100C and 100P, and the same holds true for the remaining temperatures. (Adeniyi 2014), the temperature and resistance have a significant impact on the performance of MHDCFCs.

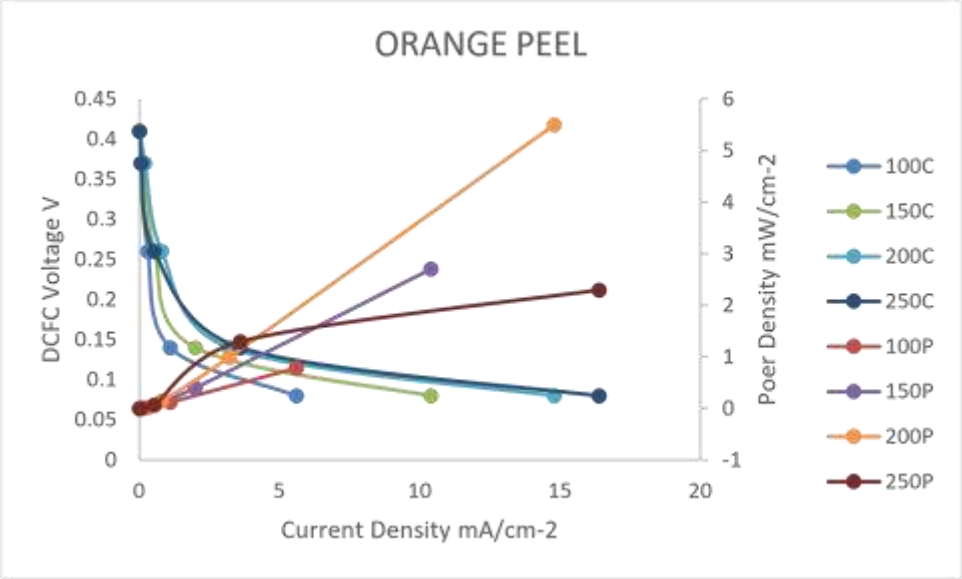


Figure 4.19: Overall Graph of Voltage against Current density and Power density for Orange Peel

### 4.4.7 DCFC performance using sugarcane bagasse waste as fuel

The results of the MHDCFC for the fuel made of sugarcane bagasse carbon particles are shown in Figure 4.20 as voltage versus current densities. With a current density of 5.2 mA/cm$^2$, the highest voltage reading (0.13 V) at 100 $^o$C was attained. A voltage of 0.27 V and a current density of 2.916 mA/cm$^2$ are present at 150 °C, 15.6 mA/cm$^2$, 0.39 V was produced for 200$^o$C. At 250 $^o$C, there was a voltage of 0.26 V and a maximum current density of 10.4 mA/cm$^2$. Due to the fact that the peak voltages were all measured with a 1 resistor load connected to the cell, there was a little decrease in the individual voltage at every temperature. The voltage dropped as the resistor load grew. In the current investigation, the midpoint of the current density-voltage curve declined because of activation resistance, which also causes activation polarization losses or even voltage drop in the cell. This is as a result of how slowly the reactions occurred on the electrode surface. The process of enabling the chemical reaction that moves electrons to and from the electrode results in the loss of some of the voltage generated. According to Figure 4.6, the

fuel sample contains 50.70 wt% carbon, 35.23 wt% oxygen, 0.63 wt% calcium, and 0.20 wt% silicon. When these elements are oxidized, the performance of the MHDCFC is improved, but it is still very subpar compared to the performance of the coal sample fuel. (C, O, Ca and Si).

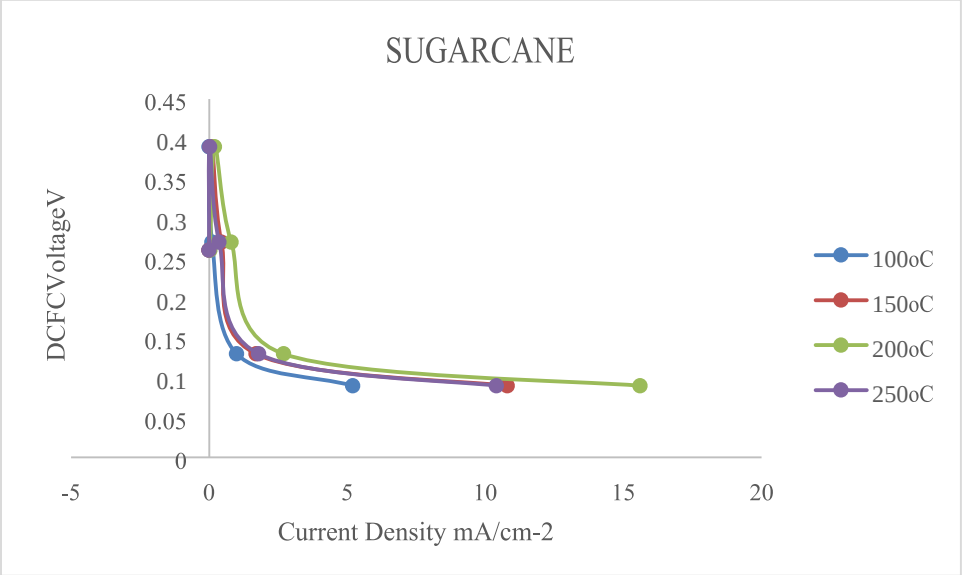


Figure 4.20: Graph of DCFC Voltage against Current density for Sugarcane Bagasse

It can be seen from Figure 4.21 that power density and current density both rise with temperature. At 100 °C, the maximum power density was 0.676 mW/cm$^2$, while the maximum current density was 10.8 mA/cm$^2$, while the maximum power density was 2.916 mW/cm$^2$, and the maximum efficiency was 40%. At 150 °C, the maximum current density was 15.6 mA/cm$^2$, while the maximum power density was 6.084 mW/cm$^2$, and the maximum efficiency was 27%. The power density was subsequently observed to decrease with increasing current density, and it was discovered that the change in temperature profile had a significant impact on these values. Maximum current density at 250 °C and power density were 10.4 mA/cm$^2$, to 2.704 mW/cm$^2$, up from the 127 mW/cm$^2$ value for almond shell (Elleuch et al.2013). The range of resistor loads employed for the various fuels could

be the cause of the variation.

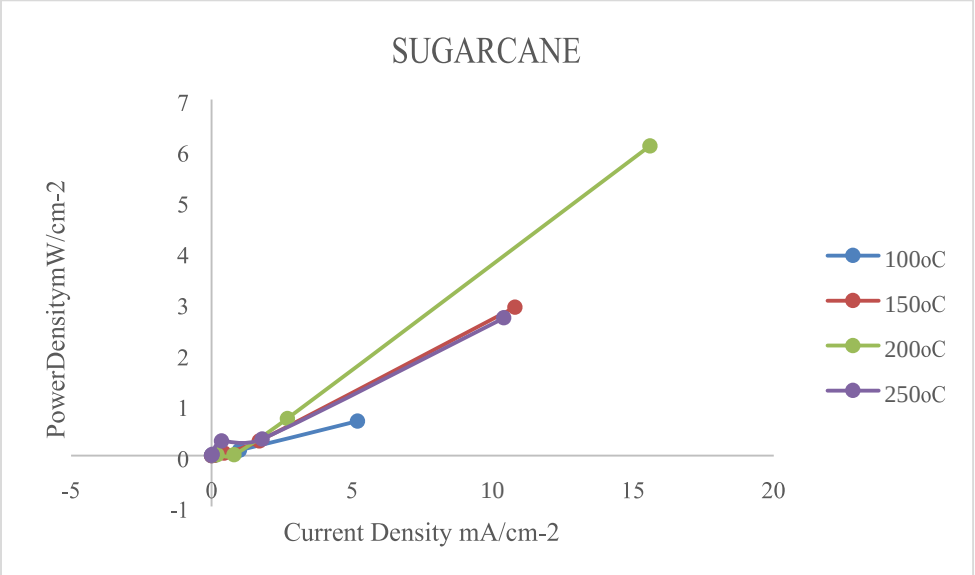


Figure 4.21: Graph of Power density against Current density for Sugarcane Bagasse

The overall evaluation of molten hydroxide direct carbon fuel cells for the four temperature profiles is summarized in Figure 4.22. The temperature for the current and power density is represented by 100C and 100P, and the same holds for the remaining temperatures. The temperature and the resistance has considerable effect on the MHDCFC performance.

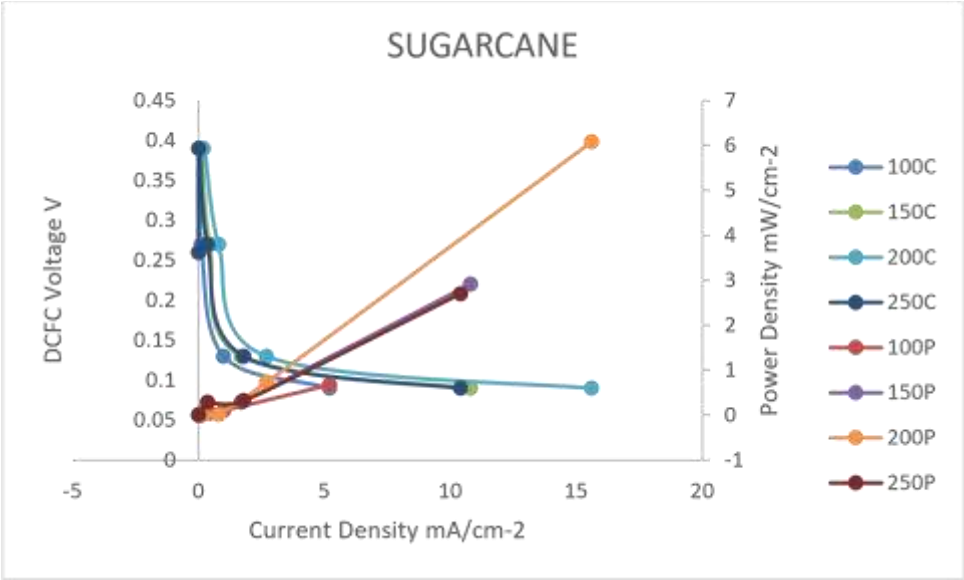

Figure 4.22: Overall graph of Voltage against Current density and Power density for Sugarcane Bagasse

### 4.4.8 DCFC performance using municipal solid waste as fuel

Figure 4.23 displays the findings of the MHDCFC for the carbon particle fuel made from municipal solid waste voltage against current densities. At 100 $^{o}$C, a current density of 8.4 mA/cm$^2$ resulted in the greatest voltage reading (0.21V). A voltage of 0.48 V and a current density of 19.2 mA/cm$^2$ were measured at 150 °C. With a current density of 20.4 mA/cm$^2$ for 200$^{o}$C, 0.51 V was produced. Maximum current density was 26.0 mA/cm2 at 250 oC, and voltage was 0.65 V. Due to the fact that the peak voltages were all measured with a 1 resistor load connected to the cell, there was a little decrease in the individual voltage at every temperature. The voltage dropped and the current density followed as the resistor load grew. In the current investigation, the midpoint of the current density-voltage curve declined because of activation resistance, which also causes activation polarization losses or even voltage drop in the cell. This is as a result of how slowly the reactions occurred on the electrode surface. The process of enabling the chemical reaction that moves electrons to and from the electrode results in the loss of some of the voltage generated, and the ions over the electrolyte is known as ohmic losses or voltage drop, which is caused by the ohmic resistance. Because of the ohmic resistance, the curves continue to decline linearly of the fuel cell. The fuel sample in Figure 4.8 contains 55.30 wt% carbon, 25.20 wt% oxygen, 4.63 wt% calcium, and 0.30 wt% silicon. After these elements were oxidized, the fuel's performance improved, but it was still very subpar compared to the performance of the coal sample fuel. (C, O, Ca and Si).


Figure 4.23: Graph of DCFC Voltage against Current density for MSW

It can be seen from Figure 4.24 that power density and current density both rise with temperature. At 100°C, the maximum power density was 1.764 mW/cm$^2$ while the maximum current density was 19.20 mA/cm$^2$ while the maximum power density was 9.22 mW/cm$^2$ and the efficiency was 33%. At 150°C and 200°C, the maximum current density was 20.4 mA/cm$^2$ while the maximum power density was 10.404 mW/cm$^2$ and the efficiency was 35%. The power density decreased as the current density increased, and it was then discovered that the temperature profile shift had a significant impact on these numbers.. The value of the maximum current density was 26 mA/cm$^2$ at 250$^o$C with a power density to 16.9 mW/cm$^2$ as compared with 127 mW/cm$^2$ reported for almond shell (Elleuch et al., 2013). The difference could be as a result of the range of resistor load used for the different fuels.

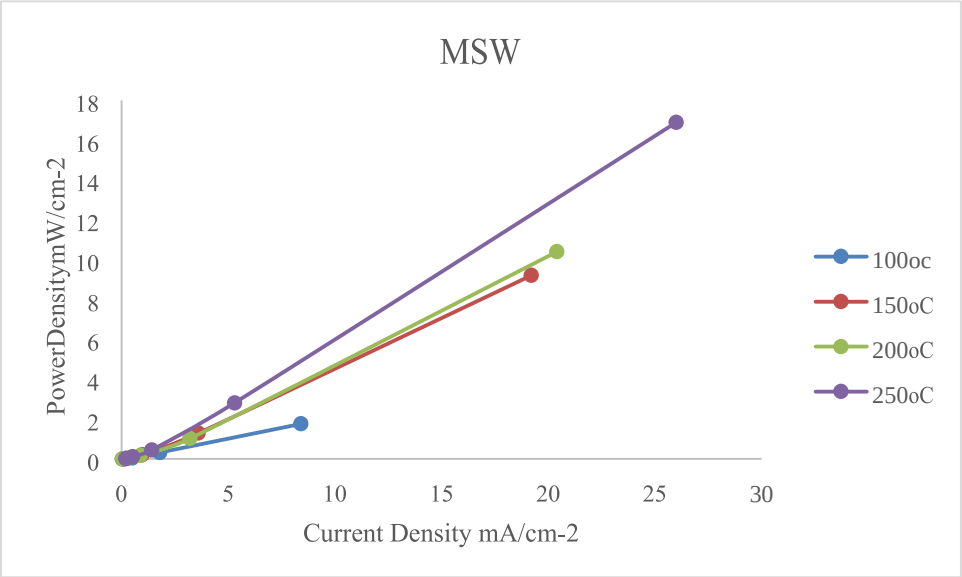


Figure 4.24: Graph of Power density against Current density for MSW The overall evaluation of the four temperature profiles for molten carbonate direct carbon fuel cells is summarized in Figure 4.25. The temperature for the current and power density is represented by 100C and 100P, and the same holds for the remaining temperatures. The temperature and the resistance has considerable effect on the MHDCFC performance.

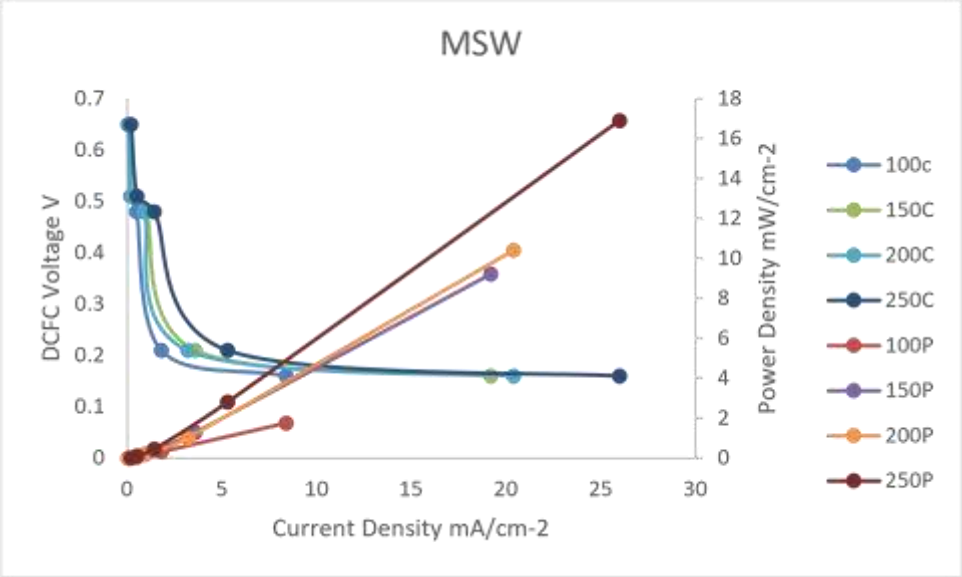


Figure 4.25: Overall graph of Voltage against Current density and Power density for MSW

4.5 Fuel Cell Efficiency

For ideal operation, the following values

$$E = \frac{\Delta hf}{4F} = 1.47 \text{ V if using the HHV}$$

Or

$$= 0.45 \text{ V if using the LHV}$$

This is in reference to a fuel cell that makes use of carbon fuel

$$\text{Cell efficiency} = \frac{Vc}{0.45} \times 100\% \text{ (with the reference to LHV)}$$

$$\text{Cell efficiency, } \eta th = \frac{Vc}{1.47} \text{ (with reference to HHV).}$$

### 4.5.1 Efficiency plot

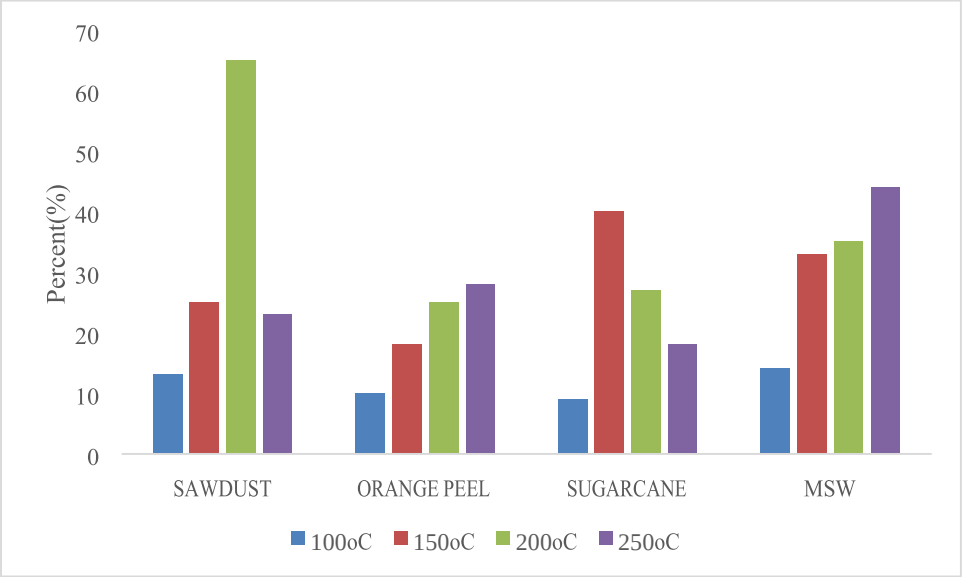


Figure 4.26: Overall Peak Efficiency of the Fuel samples (Sawdust, Orange peel, Sugarcane bagasse and MSW) at different Temperatures

The efficiency of the carbon fuel in the MHDCFC at various temperatures is clearly displayed in Figure 4.26. The efficiency rises steadily as the temperature rises for the various carbon fuel samples. The sawdust fuel had the lowest recorded fuel efficiency at 100°C (13%), and at 150°C, 200°C, and 250°C (23%, 65%, and 23%, respectively), the efficiency improved substantially. The high level of disorderliness in the XRD pattern

exhibited in Figure 4.1, along with obstructions from some contaminants. lowest fuel efficiency for the orange peel carbon fuel was obtained at 100°C and increased significantly to 18%, 25%, and 28% at 150°C, 200°C, and 250°C. The fuel sample's crystalline nature and some impurities in Figure 4.7 can be blamed for the efficiency. The lowest fuel efficiency for sugarcane bagasse fuel was 9% at 100 °C, and at 150 °C, 200 °C, and 250 °C, the efficiency likewise increased comparatively to 40%, 27%, and 18%, respectively. The efficiency can be attributed to the fuel sample's crystalline nature and some impurities in Figure 4.6. With a minimum and maximum efficiency of 14% and 44% at $100^0$C and $200^O$C, respectively, the electrochemical performance of the combined fuel, which is the MSW, turned out to be superior than the fuel from sawdust, orange peel, and sugarcane bagasse. The molten hydroxide starts to melt at a temperature between 200 and $250^0$C, allowing for mass transportation of the ions to and from the electrode. The ohmic resistance had an impact on the flow, but it was overwhelmed at these temperatures (200 to $250^0$C).

# CHAPTER FIVE

## 5.0 CONCLUSION AND RECOMMENDATION

## 5.1 Conclusion

The various waste samples were carbonized, and both proximate and ultimate analyses were completed. Every carbonized sample used as fuel in the MHDCFC underwent SEM/ EDX and XRD examination.

The electrochemical performance of sawdust waste, orange peel, sugarcane bagasse, and the combined fuel as MSW were investigated in molten hydroxide direct carbon fuel cells. The MSW fuel performed better than sawdust, orange peel, and sugarcane bagasse did. The open circuit voltage of MSW is 0.65V, which is greater than the open circuit voltages of sawdust waste (0.44V), orange peel waste (0.41V), and sugarcane bagasse (0.37V). The MSW's ideal peak power density was measured at 16.9 $mW/cm^2$, and its ideal maximum current density was 26.0 mA/cm2 with 1 resistance. The MSW carbon fuel had a 44% efficiency, which improved

The mixed carbon fuels comprise large-sized particles with the maximum peak of $26.637^o$ and matching d-spacing of 3.42Å, similar to sawdust. It was shown that higher current densities resulted from finer particle shape. This effort will stop environmental deterioration and support the sustainability of renewable energy sources.

## 5.2 Recommendation

1. Using the MHDCFC, MCDCFC, and SODCFC, performance of a variety of biomass materials should be investigated.
2. Zirconia cloth should be used as the electrolyte since it improves high voltage readings and ensures that the DCFC cell operates effectively.
3. An automated pilot plant should be designed to produce solid carbon fuel from MSW.

MSW Energy Production Plant Sustainability for Social, Energy, and Economic Benefit.

## 5.3 Contribution to Knowledge

The study found that municipal solid waste (saw dust, orange peel, sugarcane bagasse) electrochemical performance investigated using a binary direct carbon fuel cell (DCFC).The output gave voltage, current density and power density of 0.65V, 26.0mA/$cm^2$, 16.90mW/$cm^2$ at $250^0$C with minimum and maximum efficiency of 14% and 44% at $100^0$C and $200^0$C. Which indicates a suitable biomass carbon fuel used for energy generation in the DCFC, which is renewable, reduces environmental degradation and pollution, which is said to be eco-friendly.

## REFERENCES

Adeniyi, O. D., & Ewan, B. C. (2012). Electrochemical conversion of switchgrass and poplar in molten carbonate direct carbon fuel cell. International Journal of Ambient Energy, 33(4), 204-208.

Adeniyi, O. D., Ewan, B. C., Adeniyi, M. I., & Abdulkadir, M. (2014). The behaviour of biomass char in two direct carbon fuel cell designs. Journal of Energy Challenges & Mechanics (JECM), 1(4), 6.

Aleluia, J., & Ferrão, P. (2016). Characterization of urban waste management practices in developing Asian countries: A new analytical framework based on waste characteristics and urban dimension. Waste Management, 58, 415-429.

Arenillas, A., Menéndez, J.A., Marnellos, G.E., Konsolakis, M., Kyriakou, V., Kammer, K., Jiang, C., Chien, A. & Irvine, J.T.S. (2013). Direct coal fuel cells (DCFC).The ultimate approach for a sustainable coal energy generation. Bol. Grupo Español Carbón, 29, 8-11.

Axon, S. (2017). "Keeping the ball rolling": Addressing the enablers of, and barriers to, sustainable lifestyles. Journal of Environmental Psychology, 52, 11-25.

Ayllón,M.,Aznar,M., Sánchez,J.L. Gea,G.& Arauzo,J.(2006) Inflfluence of temperature and heating rate on the fixed bed pyrolysis of meat and bone meal, Chemical Engineering Journal, 121, 85–96.

Balcik-Canbolat,C., Ozbey,B.,Dizge,N. & Keskinler,B. (2017). Pyrolysis of commingled waste textile fibers in a batch reactor: analysis of the pyrolysis gases and solid product. International Journal of Green Energy, 14, 289–294,

Bartocci, P., Zampilli, M., Bidini, G., & Fantozzi, F. (2018). Hydrogen-rich gas production through steam gasification of charcoal pellet. Applied Thermal Engineering, 132, 817-823.

Bishoge, O. K., Huang, X., Zhang, L., Ma, H., & Danyo, C. (2019). The adaptation of Waste to Energy Technologies: towards the conversion of Municipal Solid Waste into a renewable energy resource. Environmental Reviews, 1, 1-22

Boldrin, A., Christensen, T.H. (2010). Seasonal generation and composition of garden waste in Aarhus (Denmark), Waste Management. 30, 551–557,

Braz, C. E. M., & Crnkovic, P. C. G. M. (2014). Physical-chemical characterization of biomass samples for application iin pyrolysis process. Chemical Engineering Transactions, 523-528.

Cao, D., Sun, Y., Wang, G. (2007). Direct carbon fuel cell: Fundamentals and recent developments. Journal of Power Sources, 167(2), 250-257.

Cherepy, N.J., Krueger, R., Fiet, K.J., Jankowski, A.F. & Cooper, J.F. (2005). Direct conversion of carbon fuels in a molten carbonate fuel cell. Journal of the Electrochemical Society, 152(1) A80-A87.

Cooper, J.F., & Berner, K. (2005). The carbon/air fuel cell, conversion of coal-derived carbons" in: The Carbon fuel Cell Seminar, Palm Spring, CA, Nov. 14th, UCRLPRES-216953, 1-16.

Cooper, J.F., & Cherepy, N. (2008). Carbon fuel particles used in direct carbon conversion fuel cells. US Patent Publication, No. US 2008/0274382 A1.

Czajczy Ska, D., Anguilano, L., Ghazal, H., Krzy, R., Reynolds, A. J., & Jouhara, H. (2017). Potential of pyrolysis processes in the waste management sector. Thermal Science and Engineering Progress, 3, 171-197.

Czajczyn´ ska D. , Anguilano L., Ghazal H., Krzyzyn ´ ska R., Reynolds A. J , Spencer N. & Jouhara H.(2017). Potential of pyrolysis processes in the waste management sector..Journal of Themal Science and Engineering,3, 171-197.

Deleebeeck, L., & Hansen, K. K. (2014). Hybrid direct carbon fuel cells and their reaction mechanisms—a review. Journal of Solid State Electrochemistry, 18(4), 861-882.

Dicks, A.L. (2006). The role of carbon in fuel cells. Journal of Power Sources, 156, 128141.

Dudek, M., Adamczyk, B., Sitarz, M., Sliwa, M., Lach, R., Skrzykiewicz, M., Raźniak, A., Ziąbka, M., Zuwala, J. & Grzywacz (2018). The usefulness of walnut shells as waste biomass fuels in direct carbon solid oxide fuel cells, Biomass and Bioenergy, 119, 144–154.

Elleuch, A., Boussetta, A., Yu, J., Halouani, K., & Li, Y. (2013). Experimental investigation of direct carbon fuel cell fueled by almond shell biochar: part I. Physico-chemical characterization of the biochar fuel and cell performance examination. International Journal of Hydrology Energy, 38(36), 16590e16604.

Elleuch, A., Halouani, K., & Li, Y. (2015). Investigation of chemical and electrochemical reactions mechanisms in a direct carbon fuel cell using olive wood charcoal as sustainable fuel. Journal of Power Sources, 281, 350-361.

Giddey, S., Badawal, S.P.S., Kulkarni, A. & Munnings, C. (2012). A Comprehensive Review of Direct Carbon Fuel Cell Technology. Progress in Energy and Combustion Science, 38, 360 – 399.

Giddey, S., Badwal, S. P. S., Kulkarni, A., & Munnings, C. (2012). A comprehensive review of direct carbon fuel cell technology. Progress in Energy and Combustion Science, 38(3), 360-399.

González,J.F., Román,S., Encinar,J.M.& Martínez,G.(2009). Pyrolysis of various biomass residues and char utilization for the production of activated carbons, Journal of Analytical and Applied Pyrolysis, 85, 134–141.

Grycová,B., Koutník,I., & Pryszcz,A.(2016) Pyrolysis process for the treatment of food waste, Bioresour.Technology. 218 , 1203–1207.

Hamad, T. A., Agll, A. A., Hamad, Y. M., & Sheffield, J. W. (2014). Solid waste as renewable source of energy: current and future possibility in Libya. Case Studies in Thermal Engineering, 4, 144-152.

Hoogers, G. (2002). Fuel cell technology handbook. CRC press.

Hoogers, G. (2003). Fuel Cell Technology Handbook. CRC Press LLC, Florida.

Jahirul, M., Rasul, M., Chowdhury, A., & Ashwath, N. (2012). Biofuels production through biomass pyrolysis —a technological review. Energies, 5, 4952-5001.

Jain, S.L., Lakeman, J.B., Pointon, K.D. & Irvine, J.T.S. (2007). A novel direct carbon fuel cell concept. Fuel Cell Science & Technology. 4, 280-282.

Jain, S.L., Lakeman, J.B., Pointon, K.D., Marshall, R. & Irvine, J.T.S. 2009). Electrochemical performance of a hybrid direct carbon fuel cell powered by pyrolysed MDF. Energy Environ. Sci. 2,687-693.

Jia, L., Tian, Y., Liu, Q., Xia, C., Yu, J., Wang, Z., Zhao, Y., & Li, Y., (2010). A direct carbon fuel cell with (molten carbonate)/(doped ceria) composite electrolyte. J. Power Sources, 195:5581-5586.

Jouhara,H., Nannou,T.K., Anguilano,L., Ghazal,H., & Spencer,N.(2017). Heat pipe based municipal waste treatment unit for home energy recovery, Energy .

Kacprzak, A., Kobyłecki, R. & Bis, Z. (2017). The effect of coal thermal pretreatment on the electrochemical performance of molten hydroxide direct carbon fuel cell. Journal of Power Technologies 97 (5) (2017) 382–387.

Kacprzak, A., Kobyłecki, R., Włodarczyk, R., & Bis, Z. (2016). Efficiency of nonoptimized direct carbon fuel cell with molten alkaline electrolyte fueled by carbonized biomass. Journal of Power Sources, 321, 233-240.

Khongkrapan,P., Thanompongchart,P., Tippayawong,N. & Kiatsiriroat,T. (2013). Fuel gas and char from pyrolysis of waste paper in a microwave plasma reactor. International Journal of Energy Environment. 4, 969–974.

Larminie, J. & Dicks, A. (2003). Fuel cell systems explained. 2nd edition, John Wiley & Sons Ltd., England. Li, X., Zhu, Z.H., de Marco, R., Bradley, J. & Dicks, A. (2010). Evaluation of Raw Coals as Fuels for Direct Carbon Fuel Cells. Journal of Power Sources, 195 (13):4051 – 4058.

Larminie, J., Dicks, A., & McDonald, M. S. (2003). Fuel cell systems explained (Vol. 2, pp. 207-225). Chichester, UK: J. Wiley.

Lopes, E. J., Queiroz, N., Yamamoto, C. I., Ramos, P., & Neto, D. C. (2018). Evaluating the emissions from the gasification processing of municipal solid waste followed by combustion. Waste Management, 73, 504-510.

López,A., de Marco,I., Caballero,B.M., Laresgoiti,M.F., Adrados,A., & Torres,A.(2011) Pyrolysis of municipal plastic wastes II. Influence of raw material composition under catalytic conditions. Waste Management. 31, 1973–1983.

Rahman, M.O., Hussain, A., & Basri,H.(2014). A critical review on waste paper sorting techniques. International Journal of Environmental Science Technology. 11 , 551–564.

Moya, D., Aldás, C., López, G., & Kaparaju, P. (2017). Municipal solid waste as a valuable renewable energy resource: A worldwide opportunity of energy recovery by using Waste-To-Energy Technologies. Energy Procedia, 134, 286-295.

Munnings, C., Kulkarni, A., Giddey, S., & Badwal, S.P.S. (2014). Biomass to power conversion in a direct carbon fuel cell. International Journal of Hydrogen Energy,39,12377-12385.

Nürnberger, S., Bußar, R., Desclaux, P., Franke, B., Rzepka, M., & Stimming, U. (2010). Direct carbon conversion in a SOFC-system with a non-porous anode. Energy & Environmental Science, 3(1), 150-153.

Omari A.M.(2015).Characterization of Municipal Solid Waste for Energy Recovery. Journal of Multidisciplinary Engineering Science and Technology.2,230-235. ISSN:3159-0040

Omisore, A. G. (2018). Attaining sustainable development goals in sub-Saharan Africa; The need to address environmental challenges. Environmental Development, 25, 138-145.

Pichtel, J. (2014). Waste Management Practices. Municipal, Hazardous, and Industrial, Second Edition. Boca Raton:Taylor and Francis Group.

Rafati, L., Rahmani Boldaji, M., Khodadadi, M., Atafar, Z., Ehrampoush, M. H., Mojtaba Momtaz, S., & Mokhtari, M. (2016). Waste to Energy: Challenges and Opportunities in Iran. Journal of Environmental Health and Sustainable Development, 1(3), 175-184.

Rubber Manufacturers Association.(2016). 2015 US Scrap Tire Management Summary. Washington DC, USA

Sambo A. S., Garba B., Zarma I. H., & Gaji M. M. (2006). Electricity Generation and the Present Challenges in the Nigerian Power Sector. Energy Commission of Nigeria, Abuja-Nigeria

Sharma, P. R., & Varma, A. J. (2014). Thermal stability of cellulose and their nanoparticles: effect of incremental increases in carboxyl and aldehyde groups. Carbohydrate polymers, 114, 339-343.

Vaida, D., & Lelea, D. (2017). Municipal Solid Waste Incineration: recovery or disposal. Case study of city Timisoara, Romania. Procedia Engineering, 181, 378-384.

Wang, Y., Yan, Y., Chen, G., Zuo, J., Yan, B., & Yin, P. (2017). Effectiveness of wasteto energy approaches in China: from the perspective of greenhouse gas emission reduction. Journal of Cleaner Production, 163, 99-105.

Wolk, R. H., Lux, S., Gelber, S., & Holcomb, F. H. (2007). Direct carbon fuel cells: Converting waste to electricity (No. ERDC/CERL-TR-07-32). Engineer research and development center champaign il construction engineering research lab.

Wu, D., Zhang, A., Xiao, L., Ba, Y., Ren, H., & Liu, L. (2017). Pyrolysis characteristics of Municipal Solid Waste in oxygen-free circumstance. Energy Procedia, 105, 1255-1262.

Yang, Y., Heaven, S., Venetsaneas, N., Banks, C. J., & Bridgwater, A. V. (2018). Slow pyrolysis of organic fraction of municipal solid waste (OFMSW): Characterisation of products and screening of the aqueous liquid product for anaerobic digestion. Applied Energy, 213, 158-168.

Yarlagadda, V. R. (2011). Conductivity measurements of molten metal oxide electrolytes and their evaluation in a direct carbon fuel cell (DCFC).

Yue, X., Arenillas, A., & Irvine, J. T. (2016). Application of infiltrated LSCM–GDC oxide anode in direct carbon/coal fuel cells. Faraday discussions, 190, 269-289.

Zecevic, S., Patton, E. M., & Parhami, P. (2005). Direct electrochemical power generation from carbon in fuel cells with molten hydroxide electrolyte. Chemical Engineering Communications, 192(12), 1655-1670.

Zhan, H., Zhuang, X., Song, Y., Yin, X., Cao, J., Shen, Z., & Wu, C. (2018). Step pyrolysis of N-rich industrial biowastes: Regulatory mechanism of NO x precursor formation via exploring decisive reaction pathways. Chemical Engineering Journal, 344, 320331.

Zhe, X., Syed-Hassan, S. S. A., Xu, J., Song, H., Su, S., Zhang, S., & Xiang, J. (2018). "Evolution of coke structures during the pyrolysis of bio-oil at various temperatures and heating rates." Journal of Analytical and Applied Pyrolysis, 134, 336-342.

# APPENDIX

Higher Heating Values

HHV (MJ/dry kg) = 0.4571 (%C on dry basis) – 2.70

MSW ( Sawdust, Orange peel and Sugarcane bagasse waste)

HHV (MJ/dry kg) = 0.4571 (%C on dry basis) – 2.70

$HHV_{msw}$= 0.4571 (29.97) – 2.70

HHV=13.699 - 2.70

HHV= 10.9993 (MJ/dry kg)

HHV for Sawdust

$HHV_{sawdust}$ = 0.4571 (20.77) – 2.70

HHV=9.494 - 2.70

HHV= 6.79 (MJ/kg)

HHV for Orange peel

$HHV_{orange\ peel}$= 0.4571 (22.60) – 2.70

HHV=10.331 - 2.70

HHV= 7.6305 (MJ/kg)

HHV for Sugarcane bagasse

$HHV_{sugarcane\ bagasse}$ = 0.4571 (27.30) – 2.70

HHV=12.4788 - 2.70

HHV= 9.7788 (MJ/kg)

Lower Heating Values

LHV= HHV -0.212*H - 0.0245*M – 0.008*O

LHV for MSW ( Sawdust, Orange peel and Sugarcane bagasse waste)

LHV= 10.9993 – 0.212 (6.60) – 0.0245 (1.36) -0.008 (34.0)

LHV= 9.5396 (MJ/kg)

LHV for Sawdust

LHV= 6.7940 – 0.212 (3.43) – 0.0245 (2.17) -0.008 (44.24)

LHV= 5.6597 (MJ/kg)

LHV for Orange peel

LHV= 7.6305– 0.212 (4.8) – 0.0245 (1.56) -0.008 (35.4)

LHV= 6.2915 (MJ/kg)

LHV for Sugarcane bagasse

LHV= 9.7788 – 0.212 (4.98) – 0.0245 (3.60) -0.008 (45.20)

LHV= 8.2732 (MJ/kg)

Table A: Operating Voltages of the carbon samples

| Temperature ($^oC$) | OCV for MSW (V) | OCV for Sawdust (V) | OCV for Orange peel (V) | OCV for Sugarcane bagasse (V) |
|---|---|---|---|---|
| 50 | 0.16 | 0.14 | 0.08 | 0.09 |
| 100 | 0.21 | 0.19 | 0.14 | 0.13 |
| 150 | 0.48 | 0.36 | 0.26 | 0.27 |
| 200 | 0.51 | 0.44 | 0.37 | 0.39 |
| 250 | 0.65 | 0.34 | 0.41 | 0.26 |
| 300 | 0.42 | 0.23 | 0.34 | 0.20 |
| 350 | 0.38 | 0.15 | 0.20 | 0.11 |

MHDCFC Electrochemical Performance and Cell Efficiency

Table B1: MHDCFC Electrochemical Performance @ 100$^o$C MSW

| Resistors (Ω) | Voltage (V) | Current (I) | Current Density ($mA/cm^2$) | Power (W) | Power Density ($mW/cm^2$) | Efficiency (%) |
|---|---|---|---|---|---|---|
| 1 | 0.21 | 0.210 | 8.400 | 0.0441 | 1.764 | 14 |
| 2 | 0.18 | 0.090 | 3.600 | 0.0162 | 0.324 | 12 |
| 3 | 0.11 | 0.037 | 0.970 | 0.0041 | 0.054 | 8 |
| 4 | 0.07 | 0.018 | 0.250 | 0.0012 | 0.012 | 5 |

| | | | | | | |
|---|---|---|---|---|---|---|
| 5 | 0.03 | 0.006 | 0.096 | 0.0002 | 0.001 | 2 |

Table B2: MHDCFC Electrochemical Performance @ 150$^{o}$C MSW

| Resistors (Ω) | Voltage (V) | Current (I) | Current Density (mA/cm$^2$) | Power (W) | Power Density (mW/cm$^2$) | Efficiency (%) |
|---|---|---|---|---|---|---|
| 1 | 0.48 | 0.480 | 19.20 | 0.2304 | 9.216 | 33 |
| 2 | 0.36 | 0.180 | 3.600 | 0.0648 | 1.296 | 12 |
| 3 | 0.22 | 0.073 | 0.970 | 0.0161 | 0.214 | 15 |
| 4 | 0.10 | 0.024 | 0.250 | 0.0025 | 0.025 | 7 |
| 5 | 0.06 | 0.012 | 0.096 | 0.0007 | 0.006 | 9 |

Table B3: MHDCFC Electrochemical Performance @ 200 °C MSW

| Resistors (Ω) | Voltage (V) | Current (I) | Current Density ($mA/cm^2$) | Power (W) | Power Density ($mW/cm^2$) | Efficiency (%) |
|---|---|---|---|---|---|---|
| 1 | 0.51 | 0.510 | 20.4 | 0.2601 | 10.404 | 35 |
| 2 | 0.32 | 0.160 | 3.2 | 0.0512 | 1.024 | 22 |
| 3 | 0.20 | 0.067 | 0.89 | 0.0134 | 0.179 | 14 |
| 4 | 0.09 | 0.022 | 0.225 | 0.0020 | 0.0203 | 6 |
| 5 | 0.09 | 0.004 | 0.032 | 0.0001 | 0.00064 | 1.4 |

Table B4: MHDCFC Electrochemical Performance @ 250°C MSW

| Resistors (Ω) | Voltage (V) | Current (I) | Current Density ($mA/cm^2$) | Power (W) | Power Density ($mW/cm^2$) | Efficiency (%) |
|---|---|---|---|---|---|---|
| 1 | 0.65 | 0.65 | 26.0 | 0.4225 | 16.90 | 44 |
| 2 | 0.53 | 0.265 | 5.30 | 0.1405 | 2.81 | 36 |
| 3 | 0.32 | 0.1067 | 1.423 | 0.0341 | 0.46 | 22 |
| 4 | 0.21 | 0.0525 | 0.525 | 0.0110 | 0.11 | 14 |
| 5 | 0.11 | 0.022 | 0.20 | 0.0024 | 0.02 | 8 |

Table B5: MHDCFC Electrochemical Performance @ 100°C Sawdust

| Resistors (Ω) | Voltage (V) | Current (I) | Current Density ($mA/cm^2$) | Power (W) | Power Density ($mW/cm^2$) | Efficiency (%) |
|---|---|---|---|---|---|---|
| 1 | 0.19 | 0.19 | 7.6 | 0.0361 | 1.444 | 13 |
| 2 | 0.7 | 0.085 | 1.7 | 0.0145 | 0.289 | 12 |
| 3 | 0.09 | 0.03 | 0.4 | 0.0027 | 0.036 | 6 |
| 4 | 0.04 | 0.01 | 0.1 | 0.0004 | 0.0004 | 3 |
| 5 | 0.001 | 0.0002 | 0.0016 | 0.0000002 | 0.0000016 | 0.1 |

o

Table B6: MHDCFC Electrochemical Performance @ 150 C Sawdust

| Resistors (Ω) | Voltage (V) | Current (I) | Current Density ($mA/cm^2$) | Power (W) | Power Density ($mW/cm^2$) | Efficiency (%) |
|---|---|---|---|---|---|---|
| 1 | 0.36 | 0.36 | 14.4 | 0.1296 | 5.184 | 25 |
| 2 | 0.25 | 0.125 | 2.5 | 0.0313 | 0.625 | 17 |
| 3 | 0.08 | 0.027 | 0.36 | 0.0022 | 0.029 | 5 |
| 4 | 0.03 | 0.0075 | 0.075 | 0.0002 | 0.002 | 2 |
| 5 | 0.01 | 0.0002 | 0.016 | 0.00002 | 0.0002 | 0.7 |

Table B7: MH

ɔCFC Electrɔchemical Performance @ 200ºC Sawdust

| Resistors (Ω) | Voltage (V) | Current (I) | Current Density ($mA/cm^2$) | Power (W) | Power Density ($mW/cm^2$) | Efficiency (%) |
|---|---|---|---|---|---|---|
| 1 | 0.44 | 0.44 | 17.6 | 0.1936 | 7.744 | 65 |
| 2 | 0.34 | 0.17 | 3.4 | 0.0578 | 1.156 | 23 |
| 3 | 0.14 | 0.047 | 0.622 | 0.0065 | 0.087 | 10 |
| 4 | 0.07 | 0.018 | 0.175 | 0.0012 | 0.012 | 5 |
| 5 | 0.02 | 0.004 | 0.032 | 0.0001 | 0.001 | 1.4 |

Table B8: MH

ɔCFC Electrɔchemical Performance @ 250ºC Sawdust

| Resistors (Ω) | Voltage (V) | Current (I) | Current Density ($mA/cm^2$) | Power (W) | Power Density ($mW/cm^2$) | Efficiency (%) |
|---|---|---|---|---|---|---|

| | | | | o | | |
|---|---|---|---|---|---|---|
| 1 | 0.34 | 0.34 | 13.6 | 0.1156 | 4.624 | 23 |
| 2 | 0.26 | 0.13 | 2.6 | 0.0338 | 0.676 | 18 |
| 3 | 0.13 | 0.0433 | 0.578 | 0.0056 | 0.075 | 9 |
| 4 | 0.03 | 0.0075 | 0.075 | 0.00023 | 0.0023 | 2 |
| 5 | 0.01 | 0.002 | 0.016 | 0.00002 | 0.0002 | 0.7 |

Table B9: MHDCFC Electrochemical Performance @ 100 C Orange peel

| Resistors (Ω) | Voltage (V) | Current (I) | Current Density ($mA/cm^2$) | Power (W) | Power Density ($mW/cm^2$) | Efficiency (%) |
|---|---|---|---|---|---|---|
| 1 | 0.14 | 0.14 | 5.6 | 0.0196 | 0.784 | 10 |
| 2 | 0.11 | 0.055 | 1.1 | 0.0061 | 0.121 | 8 |
| 3 | 0.07 | 0.0233 | 0.31 | 0.0016 | 0.022 | 5 |
| 4 | 0.02 | 0.005 | 0.05 | 0.0001 | 0.001 | 1.4 |
| 5 | 0.002 | 0.0004 | 0.0032 | 0.0000008 | 0.64 | 0.14 |

Table B10: M

HDCFC Electrochemica Performance @ 150ºC )range peel

| Resistors (Ω) | Voltage (V) | Current (I) | Current Density ($mA/cm^2$) | Power (W) | Power Density ($mW/cm^2$) | Efficiency (%) |
|---|---|---|---|---|---|---|
| 1 | 0.26 | 0.26 | 10.4 | 0.068 | 2.704 | 18 |
| 2 | 0.20 | 0.10 | 2.0 | 0.02 | 0.4 | 14 |
| 3 | 0.12 | 0.04 | 0.533 | 0.0048 | 0.064 | 8 |
| 4 | 0.04 | 0.01 | 0.1 | 0.0004 | 0.003 | 3 |
| 5 | 0.007 | 0.0014 | 0.0112 | 0.00001 | 0.0001 | 0.5 |

o

Table B11: M
HDCFC Elec rochemical Performance @ 200°C Orange peel

| Resistors (Ω) | Voltage (V) | Current (I) | Current Density ($mA/cm^2$) | Power (W) | Power Density ($mW/cm^2$) | Efficiency (%) |
|---|---|---|---|---|---|---|
| 1 | 0.37 | 0.37 | 14.8 | 0.1369 | 5.476 | 25 |
| 2 | 0.31 | 0.16 | 3.2 | 0.0496 | 0.992 | 21 |
| 3 | 0.18 | 0.06 | 0.8 | 0.0108 | 0.144 | 12 |
| 4 | 0.08 | 0.02 | 0.2 | 0.0016 | 0.016 | 5.4 |
| 5 | 0.001 | 0.0002 | 0.0016 | 0.0000002 | 0.16 | 0.1 |

Table B12: MHDCFC Electrochemical Performance @ 250$^{o}$C Orange peel

| Resistors (Ω) | Voltage (V) | Current (I) | Current Density (mA/cm$^2$) | Power (W) | Power Density (mW/cm$^2$) | Efficiency (%) |
|---|---|---|---|---|---|---|
| 1 | 0.41 | 0.41 | 16.4 | 0.0574 | 2.296 | 28 |
| 2 | 0.36 | 0.18 | 3.6 | 0.0648 | 1.296 | 25 |
| 3 | 0.12 | 0.04 | 0.533 | 0.0048 | 0.064 | 8 |
| 4 | 0.03 | 0.0075 | 0.075 | 0.000225 | 0.00225 | 2 |
| 5 | 0.004 | 0.0008 | 0.0064 | 0.000032 | 0.000026 | 0.3 |

Table B13: MHDCFC Electrochemical Performance @ 100$^{o}$C Sugarcane bagasse

| Resistors (Ω) | Voltage (V) | Current (I) | Current Density (mA/cm$^2$) | Power (W) | Power Density (mW/cm$^2$) | Efficiency (%) |
|---|---|---|---|---|---|---|
| 1 | 0.13 | 0.13 | 5.2 | 0.0169 | 0.676 | 9 |
| 2 | 0.10 | 0.05 | 1.0 | 0.005 | 0.106 | 7 |
| 3 | 0.04 | 0.008 | 0.107 | 0.00032 | 0.0043 | 3 |
| 4 | 0.01 | 0.0025 | 0.0000003 | 0.000025 | 0.00025 | 0.7 |
| 5 | 0.002 | 0.0004 | 0.032 | 0.0000008 | 0.64 | 0.14 |

Table B14: MDCFC Electrochemical Performance @ 150$^{o}$C Sugarcane bagasse

| Resistors (Ω) | Voltage (V) | Current (I) | Current Density (mA/cm$^2$) | Power (W) | Power Density (mW/cm$^2$) | Efficiency (%) |
|---|---|---|---|---|---|---|
| 1 | 0.27 | 0.27 | 10.8 | 0.0729 | 2.916 | 40 |
| 2 | 0.17 | 0.085 | 1.7 | 0.0145 | 0.289 | 12 |
| 3 | 0.10 | 0.033 | 0.444 | 0.0033 | 0.0444 | 7 |
| 4 | 0.04 | 0.01 | 0.1 | 0.0004 | 0.004 | 3 |
| 5 | 0.003 | 0.0006 | 0.0048 | 0.000002 | 0.000014 | 0.2 |

Table B15: MHDCFC Electrochemical Performance @ 200$^{o}$C Sugarcane bagasse

| Resistors (Ω) | Voltage (V) | Current (I) | Current Density (mA/cm$^2$) | Power (W) | Power Density (mW/cm$^2$) | Efficiency (%) |
|---|---|---|---|---|---|---|
| 1 | 0.39 | 0.39 | 15.6 | 0.1521 | 6.084 | 27 |
| 2 | 0.27 | 0.14 | 2.7 | 0.0365 | 0.729 | 18 |
| 3 | 0.18 | 0.06 | 0.8 | 0.0108 | 0.014 | 12 |
| 4 | 0.08 | 0.02 | 0.2 | 0.0016 | 0.016 | 5 |
| 5 | 0.02 | 0.004 | 0.032 | 0.0001 | 0.001 | 1.4 |

Table B16: MHDCFC Electrochemical Performance @ 250$^{o}$C Sugarcane bagasse

| Resistors (Ω) | Voltage (V) | Current (I) | Current Density (mA/cm$^2$) | Power (W) | Power Density (mW/cm$^2$) | Efficiency (%) |
|---|---|---|---|---|---|---|
| 1 | 0.26 | 0.26 | 10.4 | 0.0676 | 2.704 | 18 |
| 2 | 0.18 | 0.09 | 1.8 | 0.0162 | 0.324 | 12 |
| 3 | 0.08 | 0.027 | 3.6 | 0.0022 | 0.288 | 5 |
| 4 | 0.009 | 0.0023 | 2.25 | 0.00002 | 0.0203 | 0.6 |
| 5 | 0.001 | 0.0002 | 0.0016 | 0.0000002 | 0.6 | 0.1 |